MicroRNAs-enriched exosomes as a new therapy for Parkinson's disease

Marta Raquel Carrola Esteves

Tese para obtenção do Grau de Doutor em
Biomedicina
(3º ciclo de estudos)

Orientador: Prof. Doutora Liliana Inácio Bernardino
Coorientador: Prof. Doutor Lino Silva Ferreira

Júri:
Professor Doutor Ilídio Joaquim Sobreira Correia
Doutor António José Braga Osório Gomes Salgado
Professora Doutora Inês Maria Pombinho de Araújo
Doutor Miguel Maria da Fonseca Miranda Ferreira Lino
Professora Doutora Graça Maria Fernandes Baltazar
Professora Doutora Liliana Inácio Bernardino

Covilhã, 5 de julho de 2023

Declaração de Integridade

Eu, Marta Raquel Carrola Esteves, que abaixo assino, estudante com o número de inscrição D2034 de Biomedicina da Faculdade de Ciências da Saúde, declaro ter desenvolvido o presente trabalho e elaborado o presente texto em total consonância com o **Código de Integridades da Universidade da Beira Interior**.

Mais concretamente afirmo não ter incorrido em qualquer das variedades de Fraude Académica, e que aqui declaro conhecer, que em particular atendi à exigida referenciação de frases, extratos, imagens e outras formas de trabalho intelectual, e assumindo assim na íntegra as responsabilidades da autoria.

Universidade da Beira Interior, Covilhã 2023 /07 /31

Assinado por: **Marta Raquel Carrola Esteves**
Num. de Identificação: 13602948
Data: 2023.07.31 11:57:00+01'00'

The experimental work presented in this thesis was carried out in the Brain Repair Group of the Health Sciences Research Centre at Faculty of Health Sciences, University of Beira Interior (CICS-UBI) under the scientific supervision of Professor Dr. Liliana Bernardino. Part of the work was performed in the Biomaterials and Stem Cell-Based Therapeutics Laboratory at the Center of Neurosciences and Cell Biology (CNC), University of Coimbra, under the scientific co-supervision of Professor Dr. Lino Ferreira. This work was financially supported by the "Fundação para a Ciência e a Tecnologia (FCT)" through the ICON project (Interdisciplinary Challenges On Neurodegeneration; CENTRO-01-0145-FEDER-000013) and under doctoral grants SFRH/BD/121822/2016 and COVID/BD/151782/2021, partially supported by projects 007630 UID/QUI/00313/2019 and POCI-01-0145-FEDER-029919, co-funded by COMPETE2020-UE and CENTRO-01-0145-FEDER-000014 through "Programa Operacional Regional do Centro" CENTRO 2020 and by the Interreg program, specifically the project "2IQBIONEURO: Impulso de una red de I + i en química biológica para diagnóstico y tratamiento de enfermedades neurológicas" (Ref: 1654) and NEUROATLANTIC entitled "An Atlantic innovation platform on diagnosis and treatment of neurological diseases and aging" (Ref: EAPA_791/2018). Image acquisition was performed in the Microscopy facility of CICS-UBI, a node of PPBI-Portuguese Platform of BioImaging (POCI-01-0145-FEDER-022122).

Agradecimentos

Concluída mais uma etapa da minha vida profissional não poderia deixar de manifestar o meu enorme agradecimento a todos aqueles que me acompanharam ao longo destes anos e contribuíram para a concretização deste trabalho.

Começo por agradecer à Professora Doutora Liliana Bernardino, a orientação desta tese. Foram 6 anos de partilha de conhecimento científico e críticas construtivas que se tornaram fundamentais no meu crescimento profissional. Não posso deixar também de agradecer toda a compreensão, apoio e motivação, principalmente nos momentos mais difíceis e desafiadores e também toda a confiança que me depositou no laboratório. Obrigada também pelos momentos "outside the CICS" que proporcionaram momentos de descontração bastante agradáveis e divertidos e na minha opinião importantes para a união do grupo. Tenho muito orgulho em tê-la como orientadora!

Ao Doutor Lino Ferreira agradeço a sua coorientação, partilha de conhecimento científico, amabilidade e apoio que em muito contribuíram para o sucesso deste trabalho.

Agradeço também aos Doutores Hugo Fernandes e Ricardo Abreu a disponibilidade no isolamento e enriquecimento das vesiculas extracelulares que foram indispensáveis na realização deste trabalho.

Agradeço às Doutoras Ana Clara Cristóvão, Raquel Ferreira, Cláudia Saraiva e ao Doutor Tiago Santos por todos os ensinamentos, por toda a ajuda e pelas críticas construtivas.

Aos meus colegas de grupo, atuais e aos que por ele passaram nos últimos 6 anos, em especial à Mariana Fiadeiro, Jéssica Nunes, Tânia Silva e Ana Vale, que sempre se prontificaram a ajudar, a partilhar conhecimentos e proporcionaram momentos de descontração no laboratório. Obrigada! Um especial agradecimento à Catarina Almeida e à Marta Pereira, que me acompanharam quase desde o início desta caminhada: Obrigada por me ajudarem na realização de algumas experiências, pelo incentivo e apoio, pelos bons momentos proporcionados sem esquecer os tempos da "salinha" que foram qualquer coisa =), mas acima de tudo pelo companheirismo e amizade. Foram sem dúvida fundamentais para a concretização deste trabalho.

Agradeço a todos os colegas do CICS-UBI que ao longo dos anos me ajudaram, quer pelo esclarecimento de dúvidas quer pela partilha de conhecimentos. Um agradecimento especial à Sandra Rocha e ao André Furtado pelo companheirismo, amizade, gargalhadas, pelas pausas para o café e pela paciência para os meus "desabafos".

Agradeço à Professora Doutora Graça Baltazar e ao seu grupo que sempre mostraram disponibilidade para me ajudar nos momentos em que precisei.

A todas as pessoas do CICS-UBI, em especial à Catarina Ferreira, Sofia Duarte, Dona Margarida e Maria José Pinto que sempre se mostraram disponíveis com a maior simpatia nos momentos em que precisei. Obrigada!

Agradeço à FCT o financiamento (SFRH/BD/121822/2016 e COVID/BD/151782/2021) e ao CICS-UBI por fornecer os equipamentos e as instalações necessárias para o desenvolvimento desta tese.

Aos meus amigos por me permitirem "desligar" do laboratório e me ajudarem a manter a minha sanidade mental =) Muito obrigada!

Por último quero agradecer ao Mateus, companheiro de quase uma vida, e aos meus pais por terem sido sempre o meu pilar, sempre me incentivarem e nunca me deixarem desistir desta caminhada que foi tantas vezes atribulada. Obrigada por tudo!

Resumo alargado

A doença de Parkinson (DP) é uma doença neurodegenerativa caracterizada principalmente por sintomas e complicações motoras. Dados epidemiológicos indicam que a prevalência da DP na população aumenta de cerca de 1% aos 60 anos para 4% aos 80 anos, sendo considerada uma das doenças neurodegenerativas mais prevalente. Ao nível fisiopatológico, esta doença é caracterizada pela degeneração progressiva e acentuada de neurónios dopaminérgicos na *substantia nigra* (SN) *pars compacta*. Esta subpopulação neuronal dopaminérgica é responsável pela produção de dopamina, neurotransmissor envolvido na coordenação motora. A presença de corpos de Lewy nos neurónios dopaminérgicos, agregados citoplasmáticos constituídos principalmente pela proteína alfa (α)-sinucleína, é uma característica patológica da doença. Na DP, a redução nos níveis de dopamina no cérebro leva ao aparecimento dos primeiros sintomas motores que incluem tremor, rigidez e dificuldades de locomoção e de sintomas não-motores que incluem fadiga, distúrbios do sono e alterações cognitivas. Devido à natureza complexa e multifatorial desta doença, os mecanismos subjacentes à sua patogénese permanecem por elucidar, e por isso ainda não existem tratamentos eficazes que parem ou desacelerem a sua progressão, embora tratamentos como o procedimento cirúrgico de estimulação cerebral profunda (DBS) permitam aliviar os sintomas motores de alguns pacientes.

Os microRNA (miRNA) são pequenos ácidos ribonucleicos não codificantes que desempenham um papel importante em diversos processos fisiológicos e patológicos através da regulação da expressão génica após a transcrição. Em particular, os níveis de miR-124, um miRNA expresso abundantemente no cérebro, encontram-se diminuídos em amostras humanas de cérebros *post mortem* e no plasma de pacientes com a DP e em modelos experimentais *in vitro* e *in vivo* da DP. Neste sentido, aumentar os níveis intracelulares de miR-124 no cérebro surge como uma estratégia terapêutica atrativa para a DP. Ao longo dos últimos anos têm sido descritos os efeitos neuroprotetores, neurogénicos e anti-inflamatórios do miR-124 em modelos experimentais da DP. Contudo, desconhece-se o efeito do miR-124 na acumulação e agregação da proteína α-sinucleína, uma das principais características patológicas da DP.

Neste seguimento, um dos principais objetivos desta tese de doutoramento foi avaliar o efeito do miR-124-3p na expressão e sinalização associada à proteína α-sinucleína num modelo animal da DP induzido pela administração de paraquat (PQ). No primeiro

trabalho apresentado nesta tese, verificou-se que a administração intraperitoneal de PQ aumenta os níveis proteicos da α-sinucleína e da α-sinucleína fosforilada na serina 129, forma modificada envolvida na agregação da α-sinucleína e presente em maior quantidade nos corpos de Lewy. Os resultados obtidos demonstraram que a administração intranigral do miR-124-3p diminui os níveis proteicos totais da α-sinucleína e da α-sinucleína fosforilada na serina 129 na SN de ratos tratados com PQ. Evidências prévias sugerem que a enzima NADPH oxidase 1 (Nox1), responsável pela produção de espécies reativas de oxigénio, favorece a acumulação e agregação da α-sinucleína. Neste sentido, verificou-se que o tratamento com o miR-124-3p promoveu uma diminuição dos níveis proteicos da Nox1 e do seu regulador, a GTPase Rac1, que se encontram aumentados na SN de ratos tratados com o PQ. Adicionalmente, verificou-se que os níveis reduzidos de Pitx3 na SN, fator de transcrição responsável pela regulação da expressão da enzima tirosina hidroxilase e por manter o fenótipo dopaminérgico, provocados pela administração de PQ, aumentaram após a administração de miR-124-3p. Este estudo demonstra pela primeira vez o papel do miR-124-3p na regulação da toxicidade da α-sinucleína possivelmente através da modulação da via de sinalização Nox-1/Rac1 e na regulação da expressão de Pitx3, importante para a sobrevivência e manutenção dos neurónios dopaminérgicos. Em suma, estes resultados evidenciam a potencial aplicação terapêutica de miR-124 na DP e α-sinucleinopatias relacionadas.

Embora os miRNA estejam a ser propostos como possíveis alvos terapêuticos em várias doenças, existem limitações associadas à sua capacidade de internalização nas células ou alcançar os tecidos lesados devido às suas características moleculares (molécula hidrofílica com carga negativa). Neste sentido, várias têm sido as abordagens descritas capazes de potenciar a sua entrega intracelular através de veículos de entrega. Recentemente, a utilização de veículos biológicos, nomeadamente pequenas vesiculas extracelulares (pVE) ou exossomas, como também são comumente designadas, tem atraído a atenção da comunidade científica devido à sua natureza biológica e capacidade eficiente de se incorporarem em células e tecidos. Neste seguimento, o segundo objetivo principal desta tese de doutoramento foi utilizar pVE isoladas de células mononucleares derivadas do sangue do cordão umbilical humano como veículo biológico para a entrega intracelular do miR-124 e avaliar a eficiência das pVE moduladas na neurogénese da zona subventricular e na neuroprotecção de neurónios dopaminérgicos. O segundo trabalho de investigação mostrou que as pVE são capazes de internalizar e entregar eficientemente o miR-124-3p nas células estaminais neurais da zona subventricular e em células dopaminérgicas da linha celular N27, *in vitro*. O tratamento de células estaminais neurais da zona subventricular com pEV moduladas com miR-124-3p (miR-124-3p pVE)

induziu a diferenciação neuronal e protegeu as células dopaminérgicas N27 contra a toxicidade induzida pela toxina 6-hidroxidopamina (6-OHDA). *In vivo*, as pEV injetadas no ventrículo lateral de murganhos foram detetadas na zona subventricular, que reveste os ventrículos laterais, e em seções cerebrais de estriado e SN, as regiões do cérebro mais afetadas pela doença. Verificou-se que a administração intracerebroventricular de miR-124-3p pVE não aumentou o número de novos neurónios no corpo estriado de murganhos lesados com a 6-OHDA. Contudo, a formulação foi capaz de proteger os neurónios dopaminérgicos na SN e as fibras estriatais, melhorando significativamente os déficits motores dos murganhos lesados com a 6-OHDA.

Em conclusão, os resultados obtidos durante o desenvolvimento desta tese fornecem numa primeira fase, novos dados sobre o papel neuroprotetor do miR-124-3p num contexto da DP, especificamente na modulação da proteína α-sinucleína. Numa segunda fase, os resultados suportam a utilização das pVE como agentes biológicos de entrega de miR-124-3p e o seu enriquecimento com miR-124-3p como uma estratégia promissora capaz de parar ou retardar a morte neuronal dopaminérgica na DP.

Palavras-chave

miR-124; alfa-sinucleína; pequenas vesículas extracelulares; neurogénese; neuroprotecção; Doença de Parkinson

Abstract

Parkinson's disease (PD), a progressive and chronic neurological disorder characterized by the selective degeneration of the nigrostriatal dopaminergic pathway, has a huge socioeconomic impact in modern society. Alterations in alpha (α)-synuclein protein expression and aggregation have been regarded as a primary cause of dopaminergic neurons death in the *substantia nigra* (SN) *pars compacta*. So far, there are no treatments that halt or reverse the progression of PD. Recent evidence showed that microRNAs (miRNA), small non-coding RNAs that negatively regulate gene expression, are dysregulated in PD patients. In particular, miR-124 levels were found decreased in plasma and postmortem brain parenchyma of PD patients. Thus, miR-124 has become a relevant molecular therapeutic target for PD. Increasing intracellular levels of miR-124 enhances neurogenesis and neuroprotection in PD models. However, the effect of miR-124 on α-synuclein dynamics has not yet been reported.

One of the main goals of this thesis was to evaluate the role of miR-124-3p in the expression and aggregation of α-synuclein protein using the rat model of PD based on the acute administration of paraquat (PQ). The first research work showed that intranigral administration of miR-124-3p significantly reduces the protein levels of α-synuclein and α-synuclein phosphorylated at serine 129 (present in large amounts in Lewy bodies) in the SN of rats exposed to PQ. Moreover, the protein levels of NADPH oxidase 1 (Nox1), responsible for the oxidative stress production and eventually involved in the development of α-synuclein toxicity, and its activator GTPase Rac1, decreased in SN after miR-124-3p administration in PQ-treated rats. Additionally, the reduced levels of Pitx3 in the SN caused by the administration of PQ were found to increase after the administration of miR-124-3p. This work demonstrates for the first time the role of miR-124-3p in the regulation of α-synuclein toxicity, possibly through the modulation of the Nox1/Rac1 signaling pathway and in the regulation of Pitx3 expression important for the survival and maintenance of dopaminergic neurons.

The efficient delivery of miRNA at the intracellular and intracerebral levels has several limitations since they are highly susceptible to degradation by nucleases and are difficult to take up by cells due to their negative charge. Recently, several approaches capable of guaranteeing an efficient delivery of miRNA have been developed. In particular, small extracellular vesicles (sEV), also referred to as exosomes, have been highlighted as efficient delivery systems for miRNA due to their intrinsic ability to interact with cells

and tissues. The second main goal of this thesis was to use sEV isolated from human umbilical cord blood-derived mononuclear cells as a biological vehicle of miR-124 and to evaluate the efficiency of these sEV transfected with miR-124-3p (miR-124-3p sEV) in inducing neurogenesis and neuroprotection in 6-hydroxydopamine (6-OHDA) PD model. The second research work showed that *in vitro*, sEV efficiently deliver miR-124-3p to subventricular zone (SVZ) neural stem cells (NSC) and to N27 dopaminergic cells. Treatment of NSC with miR-124-3p sEV induced neuronal differentiation of SVZ NSC under physiological conditions and protected N27 dopaminergic cells against 6-OHDA-induced toxicity. *In vivo*, sEV intracerebroventricularly injected in mice were detected in SVZ lining the lateral ventricles and in striatum and midbrain sections, the brain regions most affected by the disease. Although miR-124-3p sEV did not increase the number of new neurons in the 6-OHDA-lesioned striatum, the formulation protected dopaminergic neurons in the SN and striatal fibers, which fully counteracted motor behavior symptoms in mice administered with 6-OHDA.

In conclusion, the results obtained during this thesis provide new evidence on the role of miR-124-3p in α-synuclein protein pathology and evidence supporting the application of sEV as biologic delivery agents for miR-124-3p to promote neuroprotection of dopaminergic neurons. In short, the enrichment of sEV with miR-124-3p may configure a promising therapeutic strategy able to halt or slow-down dopaminergic neuronal death in PD.

Keywords

miR-124; alpha-synuclein; miR-124-enriched small extracellular vesicles; neurogenesis; neuroprotection; Parkinson's disease.

Table of Contents

List of Figures

CHAPTER 1 - Introduction

CHAPTER 3 – MicroRNA-124-3p modulates alpha-synuclein expression levels in a paraquat-induced *in vivo* model for Parkinson's disease

CHAPTER 4 – MicroRNA-124-3p-enriched small extracellular vesicles as a therapeutic approach for Parkinson's disease

List of Abbreviations and Acronyms

6-OHDA	6-Hydroxydopamine
AAV2	Adeno-associated virus-2
AGO	Argonaute
AMPK	5’ Adenosine monophosphate-activated protein kinase
ANXA5	Annexin A5
AP	Anteroposterior
ATP	Adenosine triphosphate
Bax	B-cell lymphoma-2-associated X protein
BBB	Blood-brain barrier
Bcl-2	B-cell lymphoma 2
BDNF	Brain-derived growth factor
Bim	B-cell lymphoma-2-like protein 11
BrdU	5-Bromo-2'-deoxyuridine
CCK-8	Cell Counting Kit-8
Cdk5	Cyclin-dependent kinase 5
cDNA	Complementary deoxyribonucleic acid
CNS	Central nervous system
DAB	3, 3 Diaminobenzidine
DCX	Doublecortin
DG	Dentate gyrus
DGAV	Directorate-General for Food and Veterinary
DGCR8	DiGeorge Syndrome Critical Region 8
DMEM	Dulbecco’s modified Eagle medium
DNA	Deoxyribonucleic acid
DV	Dorsoventral
EDN2	Endothelin 2
EGF	Epidermal growth factor
EGFR	Epidermal growth factor receptor
ERK	Extracellular signal-regulated kinase
ESCRT	Endosomal sorting complex required for transport
EV	Extracellular vesicles
ExoF	Exo-Fect
Ezh2	Enhancer of zeste homolog 2
FBS	Fetal bovine serum
FGF-2	Fibroblast growth factor 2
GAPDH	Glyceraldehyde 3-phosphate dehydrogenase
GCL	Granule cell layer
GDNF	Glial cell line-derived neurotrophic factor
HRP	Horseradish peroxidase
HSC70	Heat shock cognate protein-70
HSP70	Heat shock protein-70
HSP90	Heat shock protein-90
hUCB	Human umbilical cord blood
hUCB-MNC	Human umbilical cord blood-derived mononuclear cells

IP	Intraperitoneal
ICV	Intracerebroventricular
IL-1β	Interleukin 1 beta
IL-2	Interleukin 2
ILV	Intraluminal vesicles
LAMP	Lysosomal-associated membrane protein
LB	Lewy bodies
LRRK2	Leucine-rich repeat kinase 2
LV	Lateral ventricles
MAP-2	Microtubule-associated protein 2
MEKK3	Mitogen-activated protein kinase kinase kinase 3
miR-124-3p sEV	miR-124-3p-loaded small extracellular vesicles
miRISC	MicroRNA-induced silencing complex
miRNA or miR	MicroRNA
ML	Mediolateral
MNC	Mononuclear blood cells
MPP	1-Methyl-4-phenylpyridinium
MPTP	1-Methyl-4-phenyl-1,2,3,6-tetrahydropyridine
mRNA	Messenger ribonucleic acid messenger
mTOR	Mechanistic target of rapamycin
MVB	Multivesicular bodies
NaCl	Sodium chloride
NADPH	Nicotinamide adenine dinucleotide phosphate
NeuN	Neuronal nuclei
NGF	Nerve growth factor
Nox	Nicotinamide adenine dinucleotide phosphate oxidase
Nox1	Nicotinamide adenine dinucleotide phosphate oxidase 1
Nox4	Nicotinamide adenine dinucleotide phosphate oxidase 4
Noxa1	Nicotinamide adenine dinucleotide phosphate oxidase activator 1
Noxo1	Nicotinamide adenine dinucleotide phosphate oxidase organizer 1
NP	Nanoparticles
NPC	Neural progenitor cells
NSC	Neural stem cells
nt	Nucleotides
NTA	Nanoparticle tracking analysis
OB	Olfactory bulb
PACT	Protein kinase R-activating protein
PBS	Phosphate-buffered saline
PBS-T	Phosphate-buffered saline-tween 20
PCNA	Proliferating cell nuclear antigen
PD	Parkinson's disease
PDCD6IP or Alix	Programmed cell death 6 interacting protein
PFA	Paraformaldehyde
PI	Propidium iodide
PINK1	Phosphatase and tensin homolog-induced putative kinase 1
Pitx3	Pituitary homeobox 3
PLGA	Poly (lactic-co-glycolic acid)
PQ	Paraquat

pS129	Phosphorylation of alpha-synuclein at the serine 129
PVDF	Polyvinylidene difluoride
RAN	Ras-related nuclear protein
RhoG	Ras homology growth-related
RMS	Rostral migratory stream
RNA	Ribonucleic acid
ROS	Reactive oxygen species
RPM	Revolutions *per* minute
RT	Room temperature
RVG	Rabies virus glycoprotein
SCR	Scramble
SCR sEV	Scramble-loaded small extracellular vesicles
SDS	Sodium dodecyl sulphate
SEM	Standard error of the mean
sEV	Small extracellular vesicles
SGZ	Subgranular zone
siRNA	Small interfering ribonucleic acid
SN	*Substantia nigra*
SNCA	alpha-synuclein gene
Sox-9	Sex determining region Y-box 9
STAT3	Signal transducer and activator of transcription 3
SVZ	Subventricular zone
TEM	Transmission electron microscopy
TH	Tyrosine hydroxylase
TNF-α	Tumor necrosis factor alpha
TRBP	Transactivation response ribonucleic acid-binding protein
TSG101	Tumor susceptibility gene 101 protein
UCB	Umbilical cord blood
UTR	Untranslated region
VPS4	Vacuolar protein sorting 4
VTA1	Vesicle trafficking 1

Scientific Publications

Publications related to this doctoral thesis

The research work included in this thesis resulted in the publication or preparation for submission of two original research articles in international peer-review journals:

Esteves M, Cristóvão AC, Machado-Pereira M, Ferreira R, Bernardino L, MicroRNA-124-3p modulates alpha-synuclein expression levels in a paraquat-induced in vivo model for Parkinson's disease. (Under revisions) – **Chapter 3**

Esteves M, Abreu R, Fernandes H, Serra-Almeida C, Martins PAT, Barão M, Cristóvão AC, Saraiva C, Ferreira R, Ferreira L, Bernardino L, MicroRNA-124-3p-enriched small extracellular vesicles as a therapeutic approach for Parkinson's disease. Molecular Therapy (2022); 30(10):3176-3192.
DOI: 10.1016/j.ymthe.2022.06.003 – **Chapter 4**

Additionally, two review articles were published:

Esteves M, Serra-Almeida C, Saraiva C, Bernardino L, New insights into the regulatory roles of microRNAs in adult neurogenesis. Current Opinion in Pharmacology (2020); 50:38-45.
DOI: 10.1016/j.coph.2019.11.003 – **Chapter 1**

Saraiva C, Esteves M, Bernardino L, MicroRNA: basic concepts and implications for regeneration and repair of neurodegenerative diseases. Biochemical Pharmacology (2017); 141:118-131.
DOI: 10.1016/j.bcp.2017.07.008 – **Chapter 1**

Publications unrelated to this doctoral thesis

Brito V, Marques M, Esteves M, Serra-Almeida C, Alves G, Almeida P, Bernardino L, Silvestre S, Synthesis, *in vitro* biological evaluation of antiproliferative and neuroprotective effects and in silico studies of novel 16 *E*-Arylidene-5α,6α-epoxyepiandrosterone derivatives. Biomedicines (2023); 11(3):812.
DOI: 10.3390/biomedicines11030812

Saraiva C, Lopes-Nunes J, Esteves M, Santos T, Vale A, Cristóvão AC, Ferreira R, Bernardino L, CtBP neuroprotective role in toxin-based Parkinson's disease models: from expression pattern to dopaminergic survival. Molecular Neurobiology (2023); 60(8):4246-4260.
DOI: 10.1007/s12035-023-03331-w

Serra-Almeida C, Saraiva C, Esteves M, Ferreira R, Santos T, Cristóvão AC, Bernardino L, C-Terminal binding proteins promote neurogenesis and oligodendrogenesis in the subventricular zone. Frontiers in Cell and Development Biology (2021); 8:584220.
DOI: 10.3389/fcell.2020.584220

Cristóvão AC, Campos FL, Je G, Esteves M, Guhathakurta S, Yang L, Beal MF, Fonseca BM, Salgado AJ, Queiroz J, Sousa N, Bernardino L, Alves G, Yoon KS, Kim YS, Characterization of a Parkinson's disease rat model using an upgraded paraquat exposure paradigm. European Journal of Neuroscience (2020), 52(4):3242-3255.
DOI: 10.1111/ejn.14683

Chapter 1

Introduction

Part of this chapter is as in the original publications which I authored:

i) Cláudia Saraiva, Marta Esteves, Liliana Bernardino (2017). MicroRNA: Basic concepts and implications for regeneration and repair of neurodegenerative diseases. Biochemical Pharmacology. 141:118-131.
DOI: https://doi.org/10.1016/j.bcp.2017.07.008

ii) Marta Esteves, Catarina Almeida, Cláudia Saraiva, Liliana Bernardino (2020). New insights into the regulatory roles of microRNAs in adult neurogenesis. Current opinion in Pharmacology. 50:38-45.
DOI: https://doi.org/10.1016/j.coph.2019.11.003

Some alterations to the original publications were introduced to further sustain the aim of the thesis.

1. Parkinson's disease

1.1 Pathology

Parkinson's disease (PD) is the second most common neurodegenerative disorder affecting 1% of the population over 60 years, with significant socioeconomic impact [1]. PD is mainly characterized by the progressive and selective degeneration of the dopaminergic neurons within the substantia nigra (SN) of the midbrain, which results in the depletion of dopamine in the striatum. The deficiency of dopamine signaling contributes to motor and non-motor symptoms [2,3]. So far, there is no effective treatment that can stop or reverse this disease. PD diagnosis typically occurs many years after the disease onset, predominantly based on motor symptoms. Studies revealed that by the time of first motor symptoms, the loss of dopaminergic neurons in the SN is approximately 30%, and around 50-60% of their axon terminals are already perished [4–6]. However, clinical signs of PD are evident when about 80% of striatal dopamine and 50% of SN dopaminergic neurons are lost [7]. Current therapeutic approaches are symptomatic and include pharmacotherapy (mainly levodopa), stereotaxic neurosurgery, deep brain stimulation, and physiotherapy [8]. However, these approaches do not halt neuronal loss as the disease progresses, may lack beneficial long-term effects, and can induce side effects, such as movement complications. Most PD cases are sporadic and likely result from a complex interaction between environmental and genetic risk factors combined with aging, which remains the most significant risk factor [9]. In particular, familial forms of PD include mutations in SNCA (which encodes alpha (α)-synuclein protein), *Parkin*, DJ-1, phosphatase and tensin homolog-induced putative kinase 1 (PINK1), or leucine-rich repeat kinase 2 (LRRK2) genes. The neuropathological hallmark of PD is the presence of intraneural inclusions, the Lewy bodies (LB) and Lewy neurites [10], in surviving SN dopaminergic neurons, which are mainly composed of the protein α-synuclein. However, LB are not confined to the nigrostriatal pathway and can be found in the cortex, amygdala, locus coeruleus, and peripheral autonomic system [11,12]. α-Synuclein is a soluble protein widely expressed in several brain regions and predominantly localized in the presynaptic terminals [13]. Physiologically, α-synuclein protein exists in monomeric and tetrameric forms (Figure 1.1.) [14] and are involved in neurotransmitter release, synaptic function, and synaptic plasticity [15]. However, the misfolding and subsequent aggregation of α-synuclein is a primary cause of dopaminergic degeneration in PD [16,17]. In fact, α-synuclein is abnormally expressed in PD patients' biofluids [18], such as saliva, blood, and cerebrospinal fluid [19], peripheral tissues and organs [20]. Thus, several ongoing studies are aimed at developing α-synuclein-based biomarkers, which are important for

an effective early diagnosis of PD and disease monitoring [18,19]. Besides evidence arguing the role of α-synuclein in PD pathophysiology, other pathogenic mechanisms have been proposed over the years. Postmortem studies strongly implicated oxidative damage and mitochondrial impairment in the pathogenesis of PD [21]. Postmortem analysis of the PD patients' brains and experimental studies also showed that the activation of glial cells and increased pro-inflammatory factor levels lead to the exacerbation of SN dopaminergic neuronal degeneration. Activated microglia were detected in the SN of the postmortem PD brains [22], and proinflammatory cytokines, such as tumor necrosis factor alpha (TNF-α), interleukin 1 beta (IL-1β), and IL-2, were found in the blood [23] and cerebrospinal fluid [24] of PD patients. Despite the diversity of pathogenic mechanisms proposed, the following subsections will emphasize the mechanisms involved in the toxicity of α-synuclein and oxidative stress.

1.1.1 Alpha-synuclein pathogenicity

Evidence of α-synuclein pathogenicity in PD arise from early genetic studies demonstrating that missense mutations or multiplications of the SNCA gene cause autosomal dominant forms of PD. Missense mutations cause α-synuclein misfolding, and multiplications cause α-synuclein overexpression, both promoting α-synuclein aggregation with fibril and oligomer formation [25]. Physiologically, native α-synuclein exists in a dynamic equilibrium between unfolded monomers and α-helically folded tetramers with a low propensity to aggregation [14]. The decline of the tetramer:monomer ratio and the consequent increase in the level of α-synuclein unfolded monomers favors its aggregation [26]. The aggregation process of α-synuclein involves a conformational change whereby it adopts a β-sheet-rich structure which facilitates its aggregation into oligomers, protofibrils, and insoluble fibrils that accumulate in LB (Figure 1.1) [27]. Still on debate, α-synuclein oligomers and fibrils have been considered the pathogenic forms of α-synuclein playing a role in the neurodegenerative process by directly causing dysfunction in neurotransmitter release, cellular oxidative stress, energy depletion, and other pathogenetic pathways, ultimately leading to neuronal death [28–30]. Furthermore, α-synuclein oligomers and fibrils may also spread the neurodegenerative process from neuron-to-neuron causing an immediate dysfunction of the neurons in the vicinity of these species [31]. α-Synuclein fibrils appear to be the most efficient species at propagating in a prion-like manner [32,33]. Interestingly, α-synuclein oligomers (LB) can be secreted via exosomes to the extracellular milieu and taken up by nearby cells, thus spreading disease from cell to cell within the brain [34].

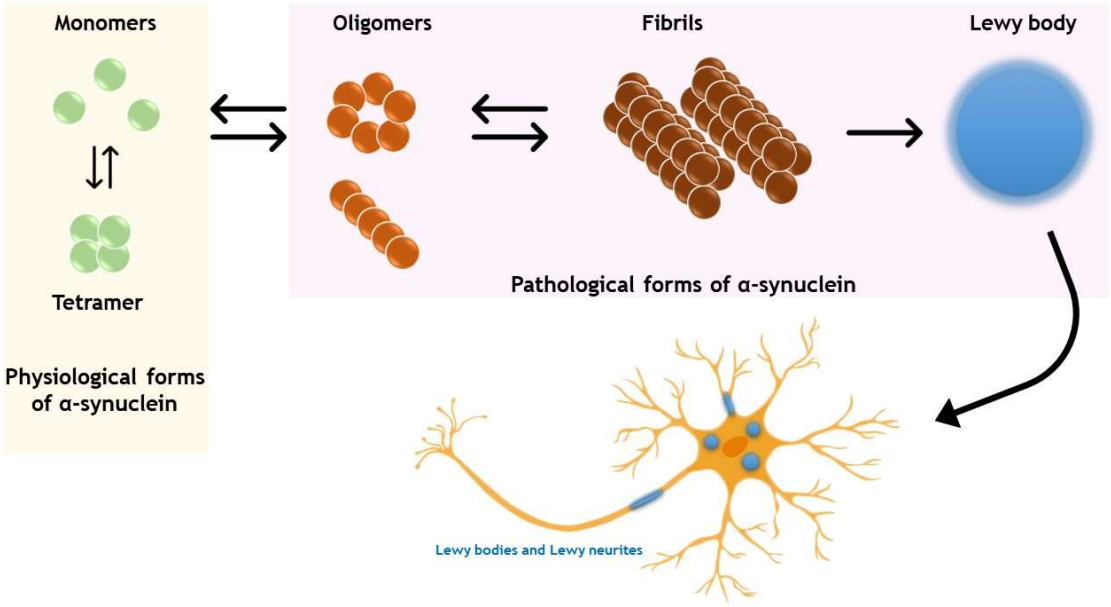

Figure 1.1 Mechanisms of α-synuclein aggregation. Under physiological conditions, α-synuclein exists as unfolded monomers in equilibrium with tetramers that can resist abnormal aggregation. Under pathological conditions, the balance between α-synuclein generation and clearance is disrupted and the monomers aggregate to form oligomers. Cytoplasmic α-synuclein oligomers grow by the addition of soluble monomers, forming fibrils. The accumulation of these fibrils leads to the formation of intracellular inclusions called Lewy bodies. These are localized in the neuronal soma (Lewy bodies) or in the neuronal processes (Lewy neurites). During α-synuclein fibrillogenesis and aggregation, the intermediate species (oligomers and fibrils) are highly toxic, affecting mitochondrial function, endoplasmic reticulum – Golgi trafficking, protein degradation and/or synaptic transmission.

α-Synuclein is also susceptible to specific post-translational modifications, such as nitration, oxidation, truncation, and phosphorylation, among others. Both nitration and oxidation decrease the propensity of α-synuclein to form stable conformations, which might contribute to the progression of PD [35]. Additionally, truncation, typically occurring in the C-terminal domain of the protein, is associated with an increased propensity of α-synuclein to form fibrils and increased toxicity in fly and rat models of PD [36,37]. Truncated α-synuclein species have been found in LB in the SN of postmortem brains of PD patients [38]. Phosphorylation of α-synuclein at the serine 129 residue (pS129-α-synuclein) is one of the major pathological markers of PD. Studies showed that 4% of α-synuclein is phosphorylated in healthy brains, while 90% of phosphorylated α-synuclein is found in the brains of PD patients [39,40]. Experimental studies also revealed that α-synuclein extracted from human LB was phosphorylated at the serine 129 residue [41]. Therefore, this post-translational modification at serine 129 may play an important role in the regulation of α-synuclein aggregation and LB formation, ultimately leading to neuronal degeneration [39]. Dysfunction of autophagy and ubiquitin-proteasome system, the two main pathways to clear toxic α-synuclein [42], lead to the imbalance between formation and clearance of pathological forms of α-

synuclein resulting in α-synuclein accumulation, which is associated with the gradual loss of dopaminergic neurons [43]. In PD patients, lysosomal-associated membrane protein (LAMP) 2A protein levels are decreased in the brain, indicating that chaperone-mediated autophagy activity is attenuated [44,45]. Additionally, aggregated autophagosomes and aberrant lysosomes were detected in SN dopaminergic neurons of the postmortem brain of PD patients [46,47]. Furthermore, colocalization of α-synuclein with the autophagy marker LC3 in LB and elevated LC3-II levels were found in the brains of PD patients [44,48]. p62, another autophagy marker, was also detected in LB from PD patients, further supporting the involvement of macroautophagy in the progression of PD [49]. Therefore, toxicity induced by α-synuclein, that can be triggered by the combination of its overexpression and/or dysregulation of the abovementioned clearance pathways plays a critical role in the PD pathogenesis. Thus, α-synuclein has become the therapeutic target most studied in PD, especially in the pharmaceutical industry, where therapies that modulate the expression or behavior of α-synuclein hold significant promise and investment [50].

1.1.2 Oxidative stress

Reactive oxygen species (ROS), when produced in low concentrations, help regulate cell functions, triggering important signaling events. However, when ROS are produced in excess, it can overwhelm antioxidant defenses and may cause oxidative stress. Thus, oxidative stress defines an imbalance between the generation and accumulation of ROS in the cells and tissues and the ability of the biological system to detoxify them through the production of antioxidants. Excessive ROS, by inducing oxidative stress in lipids, proteins, and nucleic acids, damages the mitochondria and other cellular structures that subsequently leads to the apoptosis of dopaminergic neurons [51]. Thus, oxidative stress plays a crucial role in the progressive neurodegenerative process in PD. Decreased complex I activity in the mitochondrial respiratory chain was observed in the SN of PD patients [52], and it has been shown that SN dopaminergic neurons are sensitive to complex I inhibition [53]. Increased oxidative stress has also been shown to be involved in the aging process, contributing to the increased vulnerability of dopaminergic neurons [54–57]. Oxidative stress can trigger lipid peroxidation, damaging cellular membranes, lipoproteins, and other molecules that contain lipids. The brain is enriched in unsaturated fatty acid levels, being particularly susceptible to lipid peroxidation [21]. Analysis of postmortem brains of PD patients showed increased levels of 4-hydroxyl-2-nonenal, a by-product of lipid peroxidation, carbonyl modifications of soluble proteins, and DNA and RNA oxidation products 8-hydroxy-deoxyguanosine and 8-hydroxy-guanosine [58]. At the cellular level, mitochondria and nicotinamide adenine

dinucleotide phosphate (NADPH) oxidases (Nox) are the main sources of ROS [59]. In PD patients, Nox1 and Nox4 have been detected in dopaminergic neurons [60,61]. Nox1-mediated superoxide generation requires other components, including Rac1, Noxo1 and Noxa1, and homologues $p47^{phox}$ and $p67^{phox}$, respectively [62]. Functional activation of Nox1-derived superoxide generation is dependent on the activation of a Rac1, a small Rho family GTPase. To activate the Nox system, activated Rac1 forms a Nox1 enzyme complex with Noxo1 and Noxa1 (Figure 1.2) [62,63]. It has been suggested that the Nox1 could be a major player in increasing α-synuclein expression and aggregation and consequent dopaminergic degeneration in both rodent PD models and postmortem human PD brain tissue [60,64].

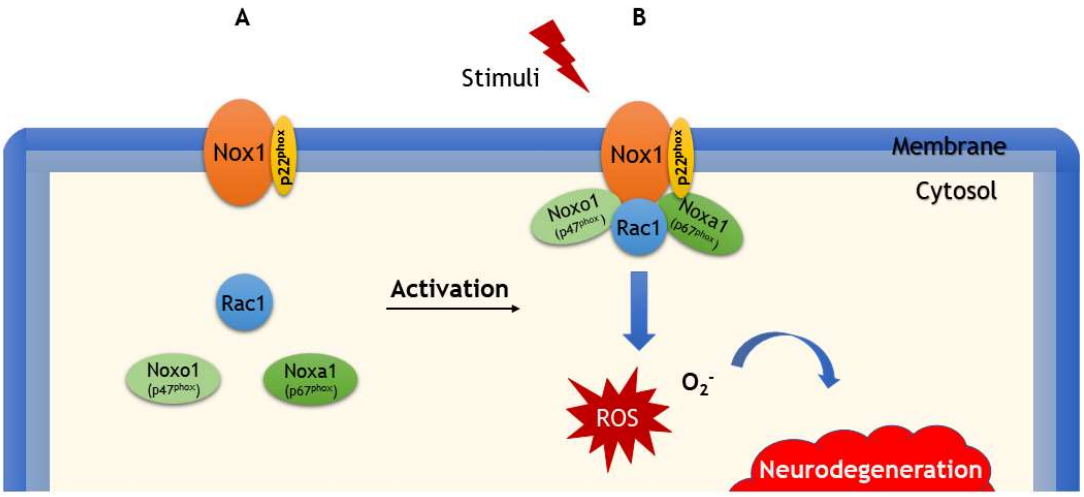

Figure 1.2 Schematic representation of Nox1 activation. Upon a stimulus, the cytosolic regulatory subunits Noxo1 ($p47^{phox}$), Noxa1 ($p67^{phox}$), and Rac1 migrate to the plasma membrane which, together with subunit $p22^{phox}$ in the membrane, activate the Nox1 enzyme system and generate reactive oxygen species (ROS; O_2^-). ROS accumulation results in increased oxidative stress, leading to neuronal degeneration.

1.2 Parkinson's disease models

Animal studies are relevant to better understanding the pathophysiology of diseases and investigating new targets or therapies. PD is a multifactorial disorder, and so far, no animal model fully recapitulates human PD. Therefore, several animal models of PD are used depending on the study purpose. PD animal models induced by neurotoxins or chemical compounds have led to a better understanding of the pathophysiology of PD and to develop new therapies. Genetic models are used to model familial PD, but they have also been helpful in clarifying most common mechanisms of PD. Genetic manipulation of PD-related genes, such as SNCA, LRRK2, *Parkin*, PINK1, and DJ-1, are frequently used in transgenic models [65,66]. 6-Hydroxydopamine (6-OHDA) and 1-

methyl-4-phenyl-1,2,3,6-tetrahydropyridine (MPTP) are the most widely used toxins to mimic PD [67,68]. Agricultural chemicals, such as paraquat (PQ), maneb, and rotenone, when administered systemically, can also induce specific features of PD. In this thesis, the neurotoxin 6-OHDA and the herbicide PQ were used to mimic PD; thus, the next subsections will focus only on these two toxins.

1.2.1 6-Hydroxydopamine model

6-OHDA is a hydroxylated analogue of the natural neurotransmitter dopamine [69]. Being a hydrophilic molecule, it does not penetrate the blood-brain barrier (BBB), thus, the direct stereotaxic administration into the brain parenchyma is required. Although the mechanism is not yet fully understood, studies have shown that 6-OHDA is taken up by dopaminergic neurons via the dopamine transporter, generating a state of oxidative stress [70]. The combination of rapid non-enzymatic auto-oxidation of 6-OHDA which leads to the production of ROS (such as hydrogen peroxide, superoxide radicals, quinones, and hydroxyl radicals) [71] with its interaction with complexes I and IV of the mitochondrial respiratory chain leads to respiratory inhibition and further oxidative stress resulting in dopaminergic neuronal death [72]. 6-OHDA may be injected in the striatum, medial forebrain bundle, or SN to induce parkinsonian features [2,68]. The regimen of the 6-OHDA model with intrastriatal injections may be more useful for neuroprotective studies. 6-OHDA is typically used as a hemiparkinsonian model, in which its unilateral injection in one of the hemispheres causes asymmetric motor behavior (turning, rotation) when apomorphine, a dopaminergic receptor agonist, or amphetamine, a dopamine releasing agent, is administered systemically [67]. In this model, quantifiable motor behavior is a major advantage for screening pharmacological agents based on their effects on the dopaminergic system. 6-OHDA model does not mimic all pathological and clinical features of human parkinsonism. It induces the death of SN dopaminergic neurons and preserves non-dopaminergic neurons, while the formation of cytoplasmatic inclusions (LB) does not occur [73,74].

1.2.2 Paraquat model

PQ, a herbicide used to control the growth of grasses and weeds, is considered a key risk factor for PD in humans and has been used as a preclinical model for PD [3,75,76]. PQ penetrates the BBB possibly through the neutral amino acid transporter system [77], having been detected in the central nervous system (CNS) after its systemic injection into rodents [78]. PQ enters cells in a sodium-dependent manner, acting as an oxidative stressor due to its ability to produce ROS via redox cycling by mitochondrial inhibition [79]. Additionally, PQ exposure increases lipid peroxidation, oxidative stress, impaired mitochondrial function, caspase 3 activation, α-synuclein expression, and aggregation,

deregulates protein degradation, and triggers neuroinflammation [64,77,80–87]. In rodents, PQ exposure induces approximately 36% of dopaminergic neuronal loss [64,88], similar to that observed in the early stages of PD [4–6]. Although the mechanism of toxicity remains unclear, one of the most striking aspects of PQ administration is its ability to induce LB inclusions in SN dopaminergic neurons mimicking PD-like pathology [83,89]. Since oxidative stress is generally considered a factor affecting α-synuclein aggregation [90], PQ-mediated oxidative stress was also shown to increase α-synuclein aggregation and expression levels in the SN of mice [83]. It was also shown that PQ increases the expression of Nox1 and activates its subunit Rac1 in a concentration-dependent manner in dopaminergic cells both *in vitro* and *in vivo* [88].

1.3 Therapeutic approaches to Parkinson's disease

1.3.1 Neuroprotection

Neuroprotection refers to any intervention that delays or prevents neuronal cell death and, therefore, slows or halts the disease progression. In the last few decades, great effort has been made to understand the pathogenic mechanisms involved in PD and to find neuroprotective agents which can protect the dopaminergic neurons from complex damaging cascades, ultimately slowing or halting the neurodegenerative process. The mechanisms that could contribute to the PD pathogenesis include the loss of trophic factors (e.g., glial cell line-derived neurotrophic factor (GDNF), brain-derived growth factor (BDNF), neurturin, *etc.),* ROS production through cellular stress, dysfunction of mitochondria, abnormal protein folding, abnormal cytoplasmic protein inclusions, neuroinflammation and cell death [91]. Currently, there are a plethora of studies focusing on possible therapeutic agents targeting above mechanisms. For example, neurotrophic factors are critical for the differentiation, growth, survival, and function of neuronal cells, so the lack of these factors can trigger cell death pathways in PD. Low levels of these factors, such as BDNF, GDNF, and nerve growth factor (NGF), were found in the SN of PD patients [92,93]. Therefore, increasing its levels could be a promising therapeutic neuroprotective strategy for PD [94,95]. Although some neurotrophic factors have shown promise in conferring neuroprotection in animal models of PD, very few have been translated into the clinic, mainly due to technical limitations. Those that entered human clinical trials, such as GDNF or related factors, resulted in inconclusive data, some of which failed to induce neuroprotection and raised safety concerns [96]. However, the study using the gene transfer-based therapeutic strategy, namely the adeno-associated virus-2 (AAV2)-GDNF administration into the striatum of PD patients is currently in phase 1 of clinical trials (NCT04167540), aiming to investigate the safety

and potential clinical effect. In recent years, non-pharmaceutical treatment approaches, including gene therapy, microRNAs (miRNA or miR), stem cell therapy, and its derived extracellular vesicles (EV) (or exosomes), have been proposed as promising therapies for PD [97,98]. For example, the potential neuroprotective effect of neural stem cells (NSC)-derived EV showed to prevent pathology in PD models. NSC-derived EV reduced ROS production and downregulated the levels of pro-inflammatory cytokines, decreasing dopaminergic neuronal loss both *in vitro* and in *in vivo* models of PD [99]. It was also shown that the administration of human bone marrow mesenchymal stem cells' secretome, enriched in extracellular exosomes, lead to the rescue of dopaminergic neurons and motor function improvement in 6-OHDA-lesioned rats, when compared with transplantation of human bone marrow mesenchymal stem cells [100]. Emerging evidence from postmortem brain analysis and animal model studies has suggested that the dysfunction of miRNA contributes to neurodegenerative diseases. Studies regarding PD also evidenced that miRNA play a role in disease mechanisms and are promising targets for neuroprotection [101]. For instance, a significant decrease in miR-7 was found in the SN of PD patients, and this alteration was proposed to play a role in α-synuclein accumulation [102]. Recently, it was reported that miR-7 attenuates the formation and propagation of hyperphosphorylated α-synuclein, and reduces neuroinflammation, protecting dopaminergic neurons in an *in vivo* model of α-synucleinopathy [103]. Additionally, miR-124, one of the most abundant miRNA expressed in the mammalian brain, was found downregulated in PD patients and experimental models [104–106]. MiR-124 can inhibit neuroinflammation and thus preventing dopaminergic neuronal cell death in PD models [107]. Although many molecules are being extensively tested in preclinical and clinical studies, an effective drug has not yet been found, mainly due to the complexity of this disease, the lack of an animal model that fully recapitulates human PD, and the challenges of designing and performing appropriate clinical trials. Hopefully, despite the several challenges and clinical trial failures, promising novel therapeutic strategies have already emerged [108].

1.3.2 Neurogenesis

Neurogenesis is an active process involving the generation and differentiation/maturation of nerve cells, which comprises several steps, including proliferation, fate specification, neuronal differentiation, and functional integration of newborn neurons into pre-existing neuronal circuits [109]. During embryonic development, neuroepithelial cells and later radial glia cells originate neurons and glia cells based on spatial and temporal cues [110]. These NSC can self-renew, proliferate and possess multipotent features, differentiating into neurons, astrocytes, and

oligodendrocytes [111]. Neurogenesis persists throughout adult life and is restricted to discrete regions of the brain, the neurogenic niches, located in the subventricular zone (SVZ) lining the lateral ventricles and the subgranular zone (SGZ) of the dentate gyrus of the hippocampus [112–114] (Figure 1.3.A). In the adult SVZ, we can find specialized astrocyte-like cells derived from radial glia called adult NSC (Type B cells). These NSC can self-renew, proliferate, and are multipotent (Figure 1.3). The majority of adult NSC are quiescent (slowly dividing cells); nevertheless, a quite fast subtype of NSC (activated NSC) can also be found in these neurogenic niches. Quiescent and activated NSC have different molecular signatures and a fine-tuned control over the amount of each cell type needed to guarantee long-term homeostasis of the neurogenic niches [115,116]. NSC, give rise to neural progenitor cells (NPC), which can differentiate into one of the three major cell lineages of the brain: astrocytes, oligodendrocytes, and neurons. NPC give rise to neuroblasts (Type A cell) which form chains and migrate radially along the rostral migratory stream (RMS) until reaching the olfactory bulb (OB) (Figure 1.3). Once in the OB, neuroblasts differentiate into mature interneurons, which integrate into the existing neuronal circuits. The adult SGZ contains a germinal niche composed of a smaller NSC pool than the SVZ niche [117,118]. In the SGZ, we can find specialized astrocyte-like NSC, derived from radial glia, called adult NSC (Type 1 cells), which can self-renew, proliferate, and are multipotent (Figure 1.3). These NSC proliferate into intermediate progenitors named type II cells and give rise to type III cells (immature neuroblasts), which migrate radially into the granule cell layer to differentiate into dentate granule neurons. These neurons functionally integrate into hippocampal circuitry by extending axons and dendrites, subsequently forming synapses with mature neurons [119,120]. Evidence of adult subventricular and hippocampal neurogenesis were firstly addressed in rodents [121] and subsequently confirmed in human postmortem brains [114]. Nevertheless, contrary to what happens in rodents, the composition and functionality of these germinal zones are still controversial in humans [122,123]. The discussion was recently re-ignited by two prominently published reports with opposite findings [5–7]. Sorrells and collaborators reported that human hippocampal neurogenesis declined sharply during childhood to an almost undetectable level in adults (18-77 years old) [125]. On the other hand, Boldrini *et al* reached the opposite conclusion by showing the existence of newborn neurons in young aged individuals and old patients (14-79 years old) [126]. Interestingly, recent publications reported that new neurons are born throughout adulthood until the late stages of healthy aging [127,128].

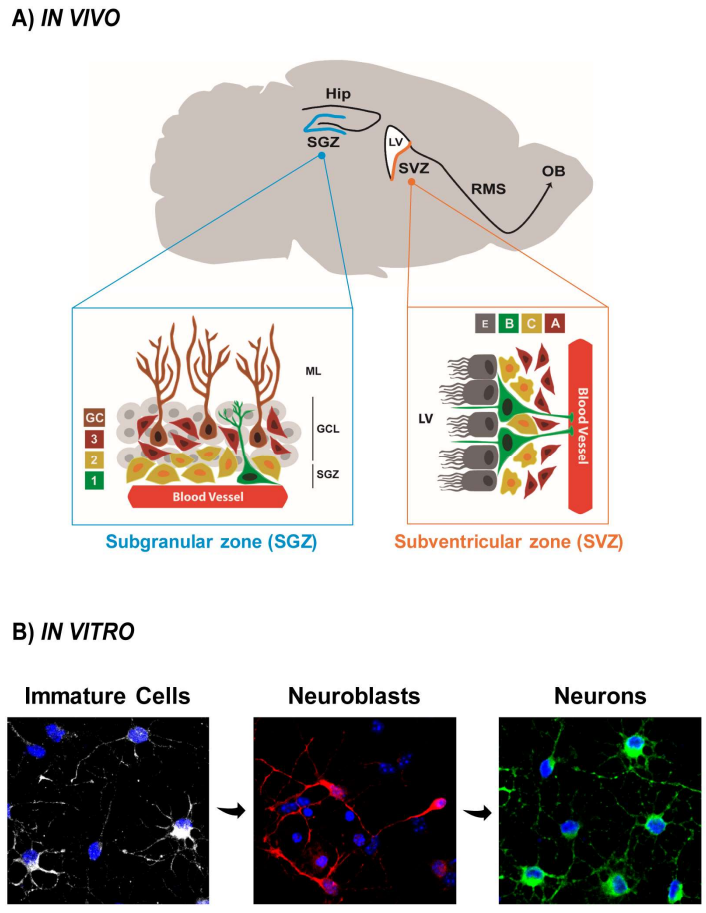

Figure 1.3 Neurogenesis in the adult rodent brain. Adult neurogenesis occurs mainly in the subventricular zone (SVZ) of the lateral ventricles (LV) and the subgranular zone (SGZ) of the hippocampal (Hip) dentate gyrus (DG) of the adult rodent brain. (a) In the SVZ (orange), adult neural stem cells (NSC, type B cells) residing below an ependymal (E) cell layer in the wall of the LV slowly divide, giving rise to transit-amplifying progenitors (type C cells), which in turn develop into neuroblasts or type A cells. Neuroblasts migrate along the rostral migratory stream (RMS) towards the olfactory bulb (OB), where they fully differentiate into mature interneurons. In the SGZ (blue) of the hippocampal DG, NSC which are called type 1 cells, give rise to neural progenitor cells (type 2 cells), which in turn develop into neuroblasts or type 3 cells. Neuroblasts migrate up into the granule cell layer (GCL), where they maturate into granular neurons (GC) and extend their processes out to the molecular layer (ML). (b) Representative images of immunostainings showing immature cells labeled with Nestin (white), neuroblasts with doublecortin (red) and neurons with MAP-2. Hoechst staining (blue) labels cell nuclei. Scale bar: 20 mm. [129]

1.3.2.1 Neurogenesis in Parkinson's disease

The impact of adult neurogenesis in humans is still largely unknown, however, its impairment has been suggested as a possible cause for the onset of neurodegenerative disorders, including PD [130]. Accordingly, studies using brain tissue from patients and animal models have suggested an impairment of adult neurogenesis in PD, although the exact mechanisms are not fully understood [127,131–133]. The limited available data from postmortem brain analysis of PD patients and contradictory experimental findings keep the role of neurogenesis in PD still under debate. The role of dopamine in regulating hippocampal dentate gyrus (DG) and SVZ neurogenesis has been reported. Dopamine

receptors, particularly the D3 type, are widely expressed in the germinative neuroepithelial zones, which are actively involved in neurogenesis in most basal forebrain structures, suggesting a role of dopamine in the modulation of neurogenesis during brain development [134,135]. In the adult brain, high levels of D3 receptor expression have been shown to persist in the germinal SVZ [134]. Studies in mice and humans showed a dense dopaminergic innervation of the SVZ, most likely derived from projections from the midbrain. In turn, evidence have shown that dopamine stimulates SVZ cell proliferation and neurogenesis [131,136,137]. In accordance, a reduction in NSC proliferation at the SVZ and SGZ was found following dopamine denervation in animal models of PD. Interestingly, pharmacologic D2 receptor stimulation significantly recovered NSC proliferation. Moreover, reduced numbers of NPC were found in the OB of postmortem brains of PD patients. PD patients also presented lower levels of cells expressing the proliferation marker proliferating cell nuclear antigen (PCNA) in the SVZ, a decrease of nestin-positive cells (immature neural precursor cells) both in the OB and in the DG of the hippocampus, as well as a reduction in β-III-tubulin-positive cells (neuronal marker) in the SGZ [131]. *In vitro* and *in vivo* studies showed that dopamine stimulates the release of epidermal growth factor (EGF) in the SVZ, which acts on the epidermal growth factor receptor (EGFR) to promote cell proliferation. Thus, reduced numbers of proliferating EGFR-positive cells and a weaker expression of EGFR were observed in the SVZ of human PD patients compared with age-matched controls [138]. Additionally, decreased EGF levels were found in the prefrontal cortex and the striatum of PD patients [139]. However, the specific role of dopamine receptors in SVZ neurogenesis remains controversial [130,133,135,140–142]. Moreover, other studies were not able to show dopaminergic denervation in the SVZ of PD patients [131,133]. By using *in vitro* and *in vivo* approaches, another study proposed that adult neurogenesis is unaffected in PD patients. The treatment of human NSC lines with dopamine and dopamine agonists did not stimulate NSC proliferation, suggesting that dopamine depletion may not affect the neurogenic capacity of the PD brain [143]. α-Synuclein also seems to be involved in neurogenesis impairment in PD. The interplay between accumulated α-synuclein and p53 results in Notch1 signaling dysregulation in adult rat hippocampal NPC, potentially triggering some of the non-motor symptoms associated with the PD pathology [144–147]. Inconsistent data showing a decrease, maintenance, or even an increase of neurogenesis in PD patients and animal models have been reported over the years [148]. The different results obtained can be explained due to the differential activation of dopamine receptors in the NSC [131,149,150] together with a wide diversity of PD models used (transgenic or toxin-based animal models, acute or chronic administrations, different dosages, and different spatial administration of

toxins) [2,133]. For example, in a 6-OHDA rat model of PD, the application of 6-OHDA into the striatum, medial forebrain bundle, or SN caused an increase of SVZ progenitor cell proliferation [151–153]. In contrast, a decrease in SVZ NSC proliferation was observed in rats injected with 6-OHDA in the nigrostriatal pathway or medial forebrain bundle [131,154]. In a 6-OHDA mouse model of PD, the administration of 6-OHDA into both the medial forebrain bundle and SN or only in SN promoted a reduction in SVZ NSC proliferation together with a higher survival rate of newborn neurons in the OB [136,155]. On the other hand, another group reported that the lesion induced by 6-OHDA administrated into the SN does not affect adult SVZ neurogenesis [156]. Besides this contradictory evidence, boosting the generation of new neurons able to replace the dead and degenerating ones may represent a potential therapeutic approach for PD. Restoring the dopamine levels in the striatum of PD patients through stimulation of endogenous SVZ NSC to migrate into the striatum and differentiate into new neurons might thus be an attractive therapeutic approach. Over the years, the pro-neurogenic effect of various molecules in animal models of brain diseases has been studied, namely several growth factors (e.g., fibroblast growth factor 2 (FGF-2) and EGF) [148] and miRNA [101,157]. We were pioneers in showing that the administration of microRNA-124-loaded polymeric nanoparticles (NP) into the lateral ventricles of 6-OHDA-lesioned mice potentiated the migration of SVZ-derived new neurons towards the lesioned striatum and decreased the motor impairments in these mice [158]. This evidence raises the hope for designing novel regenerative medicine applications for PD based on the stimulation of the endogenous repair process mediated by NSC.

2. MicroRNA

In mammals, most of the genome is transcribed into non-coding RNA. Non-coding RNA can be either long non-coding RNA molecules or short non-coding RNA that are subdivided into: “housekeeping RNA” such as ribosomal RNA, transfer RNA; and regulatory RNA, including endogenous small interfering RNA (siRNA), piwi-interacting RNA, and miRNA [159–161]. MiRNA have been the most scrutinized of the regulatory non-coding RNA due to its importance in regulating many biological processes. These molecules have approximately 22 nucleotides (nt) in length and are ubiquitous among plants and animals. Additionally, miRNA are able to regulate post-transcriptionally hundreds of genes by complementary binding to mRNA targets, promoting either mRNA cleavage (mainly in plants), or mRNA translational repression and/or decay (mostly in animals). The tissue and cell-specific expression pattern of miRNA are responsible for their particular biological function within a specific system. Often, this expression signature changes upon a pathological event, suggesting an additional regulatory role of

key signaling pathways in pathology. Moreover, the presence of miRNA in diverse biological fluids such as blood, cerebrospinal fluid, and urine emphasizes their clinical relevance and versatility both as potential modulators of disorders and as possible biomarkers. MiRNA have been highlighted as key modulators of many brain-related functions in both physiological and pathological conditions. While perturbations in their expression pattern have been associated with the etiology and progression of neurological disorders, modulation of their expression levels has been shown to impact neurodegeneration and promote endogenous regenerative programs driven by NSC. A single miRNA can control an entire signaling network associated with neurodegeneration and neuroregeneration/neurogenesis, making these molecules interesting candidates for treating neurodegenerative diseases. Particularly, miRNA-124 (miR-124) was reported to boost neurogenesis leading to motor amelioration of the PD symptoms in a mouse model of PD [158].

2.1 Biogenesis and function

MiRNA were firstly identified in the *Caenorhabditis elegans* but were rapidly found to be ubiquitous among plants and animals, altering the view over the central dogma of molecular biology: DNA is transcribed into RNA, which is then translated into protein. miRNA can be transcribed as independent transcription units or as miRNA genes that lie in introns or exons of other genes [162]. Intronic miRNA originate the majority of the miRNA transcripts in mammals, and it is independently controlled of the host genome by different promotors [163–165]. miRNA genes are generally transcribed by RNA polymerase II, generating an imperfect stem-loop structure with hundreds to thousands of nt, which is flanked by single strand (ss)RNA that is capped on the 5' end and polyadenylated in the 3' end – pri-miRNA (Figure 1.4) [166,167]. The pri-miRNA is further processed by the microprocessor complex and can generate a single or a cluster of mature miRNA [168,169]. The microprocessor complex is composed of two RNA-binding proteins, DiGeorge Syndrome Critical Region 8 (DGCR8), that interacts with pri-miRNA and recruits the RNase III enzyme Drosha responsible for cleaving the pri-miRNA in the stem-loop, forming a precursor-miRNA (pre-miRNA) with a 5' phosphate group, a 2 nt overhang at 3' end and approximately 60 nt long (Figure 1.4) [170,171]. The heterodimer Exportin-5 and its co-factor GTPase Ras-related nuclear protein (RAN) – complex Exportin/RAN – mediates pre-miRNA translocation to the cytoplasm [172,173]. In the cytoplasm, the pre-miRNA is recognized by Dicer that cleaves the pre-miRNA into a 22 nt long miRNA duplex [174]. TRBP (transactivation-response RNA-binding protein) and PACT (protein kinase R-activating protein), although not essential for the process, increase Dicer accuracy resulting in facilitated pre-miRNA processing [175–178]. The

miRNA duplex complex is loaded into the argonaute (AGO) protein in an ATP-dependent manner assisted by the heat shock cognate protein-70 and the heat shock protein-90 (HSC70/HSP90) chaperone machinery [179]. Altogether they form the miRNA-induced silencing complex (miRISC). The N-domain of AGO starts the process of *miRNA duplex unwinding*, which results in: 1) a guide or mature strand, thermodynamically more stable and prevalent, with higher biological activity that is retained in the miRISC complex; and 2) a passenger strand (miR*), which is released to be either degraded or incorporated into another miRISC complex [180–182]. The four AGO proteins expressed in humans (AGO1, 2, 3 and 4) can perform non-cleavage inhibition of mRNA, but only AGO-2, the most abundantly expressed of the four, has nuclease activity (Figure 1.4) [183–185]. The majority of miRNA follow the aforementioned canonical biogenesis pathway. Nevertheless, non-canonical miRNA that bypasses some maturation steps of the canonical pathway have also been described. There are three major alternatives to synthesize these miRNA: i) Drosha/DGCR8-dependent and Dicer-independent pathway; ii) Drosha/DGCR8-independent and Dicer-dependent pathway; iii) Drosha/DGCR8-independent and Dicer-independent pathway [186,187].

MiRNA are able to precisely regulate the expression of hundreds of genes since a single miRNA can bind to numerous different mRNA, and a single mRNA can present multiple miRNA binding sites, either for the same or for different miRNA [188]. The target recognition by the miRNA is mainly based on Watson-Crick pairing of a specific region from nt 2 to 8, seed sequence, and by a match site in the 3'UTR (untranslated region) [189,190]. MiRNA can regulate translation by pairing with the target mRNA in a perfect or near perfect complementary way, followed by the cleavage of the target mRNA by AGO-2 (Figure 1.4) [191–193]. This mechanism occurs mostly in plants. In animals, the miRNA-mRNA interaction is based on incomplete paring with the presence of mismatches and/or bulges. In this case, mRNA translational repression and mRNA destabilization via deadenylation and decapping mechanisms prevail [194,195]. However, there are still some controversies regarding the contribution of each mechanism for miRNA action. Developments in the field indicate that miRNA action is time-dependent, starting with mRNA translational repression followed by a dominant effect of mRNA degradation in the steady-state [194,196–199]. The mRNA destabilization mechanism is the better described miRNA mode of action in humans. The knowledge regarding miRNA mode of action is important to develop and/or enhance the efficacy of therapies based on the use of miRNA. Although miRNA are able to precisely regulate the expression of hundreds of different genes, they may also suffer a tight

regulation. The spatiotemporal expression of miRNA is mainly regulated at transcriptional and post-transcriptional levels.

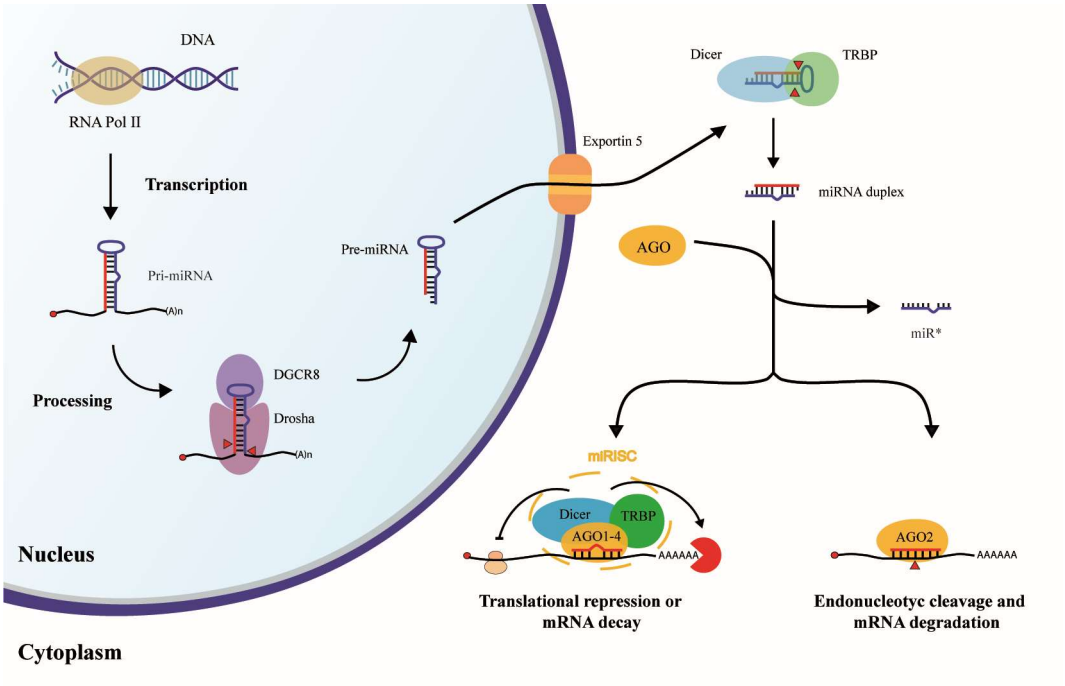

Figure 1.4 Schematic representation of the canonical pathway of microRNA (miRNA) biogenesis. Briefly, miRNA are mostly transcribed by the RNA polymerase II into long transcripts called pri-miRNA that are processed into a miRNA precursor (pre-miRNA) of approximately 60 nucleotides (nt) long, by the microprocessor complex composed of DiGeorge Syndrome Critical Region 8 (DGCR8) and Drosha. The pre-miRNA is exported to the cytoplasm via the Exportin 5 transporter, where it is further processed into a miRNA duplex (~ 22 nt) by Dicer and TRBP (transactivation-response RNA-binding protein) proteins. In the presence of the Argonaut protein family (AGO 1–4), the most thermodynamically stable strand of the miRNA duplex is selected as the guide/mature strand while the other, passenger strand (miR*), is released to be degraded or can be also used as a mature strand. Following processing, miRNA are assembled into miRNA-induced silencing complexes (miRISC complex) composed of miRNA, AGO, Dicer and TBRP proteins. In some cases, mostly seen in plants, miRNA are able to bind mRNA with perfect of near perfect complementarity resulting in endonucleolytic cleavage and mRNA degradation. In other cases, mostly seen in animals, the miRNA bind to the target mRNA with incomplete pairing presenting mismatches and/or bulges which results in mRNA translational repression and/or mRNA decay. [101]

At the transcriptional level, miRNA's expression is regulated similarly to protein-coding genes and represents the major level of control responsible for tissue- or development-specific expression [200,201].Multiple activators and repressors have been described to regulate the miRNA pathway, although transcription factors have been considered the main ones [202–204]. Moreover, several transcription factors cooperate with miRNA within autoregulatory feedback loops to activate or repress their expression [202]. At the post-transcriptional level, the expression of miRNA can be altered due to changes in processing, namely, in the activity of key miRNA biogenesis enzymes, such as Dicer and Drosha [177,205]. Several cofactors and accessory proteins, such as DGCR8, RNA helicases p68 and p72 (cofactors of Drosha microprocessor complex), and AGO-2, assist

Drosha, Dicer, and miRISC in the execution of their functions, which indirectly control miRNA expression [206–210]. In addition, the effects of endogenous (hormones, cytokines) and exogenous (xenobiotics) chemical compounds can also change the expression of miRNA [211]. Due to the profound impact on the regulation of numerous cellular processes, it is clear that any aberration in the regulation of miRNA pathways contributes to several human pathologies, such as neurodegenerative diseases, among others.

2.2 MicroRNA-124

MiR-124 was firstly identified in the mice [212] and is expressed in various tissues, including the brain. It can be transcribed from three different loci, miR-124-1, miR-124-2, and miR-124-3. In the adult brain, miR-124 accounts for 25% to 48% of the total mRNA, being highly expressed among all brain regions except the pituitary gland. In the remaining tissue, miR-124 is 100-times less expressed than in the brain, being also considered a neuronal-specific miRNA since it is mainly expressed in neuronal cells [212–214]. The role of miR-124 in neurogenesis and in the pathological mechanisms of PD will be described in the next subsections.

2.2.1 MicroRNA-124 in neurogenesis

MiRNA play crucial roles in the development and plasticity of the brain [215,216]. The first evidence of the effects of miRNA in brain development has been obtained in zebrafish experiments suppressing miRNA biogenesis. Knockout experiments in the zebrafish Dicer gene were performed resulting in brain morphogenesis defects [217]. In fact, it was reported that an NSC cell line lacking Dicer is unable to differentiate into astrocytes or neurons [218]. Specifically, miR-124, which is highly expressed in the brain, play essential roles in brain development and in adult neurogenesis (Figure 1.5) [219,220]. MiR-124 was reported to regulate the early stages of neurogenesis (neuronal fate commitment), with its activity and expression levels exclusively detected during and after neuronal commitment [221]. The Notch signaling pathway is of utmost importance for maintaining NSC. The interaction between the ligand Jagged1 and the Notch receptor, expressed in NSC, triggers self-renewal and the maintenance of an undifferentiated state. In the rodent SVZ, overexpression of miR-124 represses Jag1 translation leading to NSC differentiation [221,222]. Expression of miR-124 is initiated during the transition of NSC to progenitor cells and is enhanced with neuronal maturation [221,223]. miR-124 promotes not only neuronal commitment but also controls the choice between neuronal and astrocytic differentiation through several reported mechanisms, including the fine-tuning of the expression of a critical epigenetic regulator, Ezh2 (enhancer of zeste homolog 2) [224], inhibition of the signal transducer

and activator of transcription 3 (STAT3) transcription factor signaling [225], and reduction of Sox-9 expression [221].

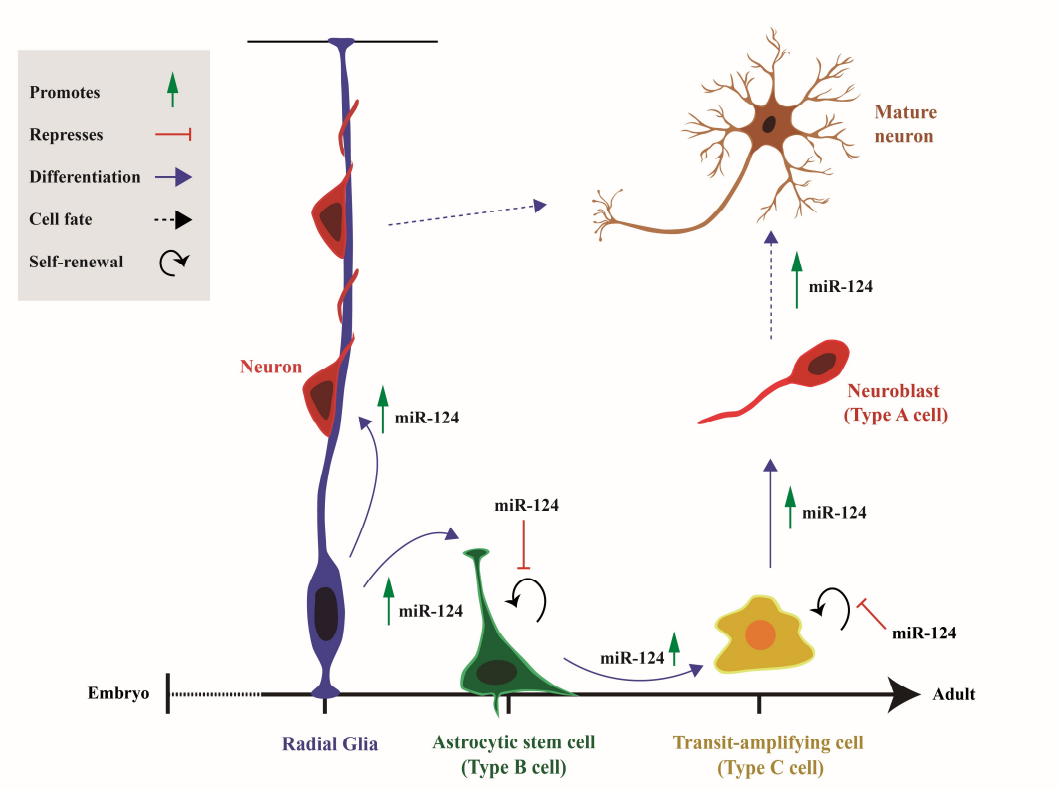

Figure 1.5. Schematic illustration of the miR-124 involvement in the regulation of adult neurogenesis. In the SVZ, the main neurogenic niche in the adult mammalian brain, radial astrocyte-like cells (type B cell) holding stem cell properties generate transient amplifying cells (type C cell) that can finally give rise to immature neuroblasts (type A cell). The newly generated neuronal cells migrate through the rostral migratory stream to the olfactory bulb, where they differentiate into functional interneurons, which are essential for odor discrimination, learning and memory. Adapted from [101].

In vivo, miR-124 overexpression in the mice SVZ niche increased the number of newborn neurons without affecting their migratory capability [221,223], while its downregulation led to a 30% reduction of post-mitotic neurons [221]. Knockdown of miR-124-1 in mice resulted in smaller brain size, neuronal dysfunction, and axonal miss-sprouting in the dentate gyrus [226]. miR-124 expression enhances axonogenesis by regulating cytoskeleton protein levels [227,228] and regulates dendritic differentiation by targeting the ras homology growth-related (RhoG) pathway [229]. Moreover, miR-124 is required for homeostatic plasticity, a compensatory adjustment in neuronal activity [230]. Although many aspects of the miR-124 regulatory network need to be unveiled, these data prove that miR-124 is able to modulate adult neurogenesis, namely in the SVZ. Therefore, an improved understanding of the miRNA-based regulatory mechanisms involved in the multiple steps of adult neurogenesis may lead to the development of novel

approaches to delay or halt neurodegenerative processes or injuries and facilitate regeneration in the adult human brain.

2.2.2 MicroRNA-124 in brain diseases: focus on Parkinson's disease

The unique features of miRNA make them valuable and versatile tools for clinical applications as biomarkers for the diagnosis and prognosis of pathologies and/or therapeutic molecules that can act on diverse key targets or disease-related pathways. Based on the abovementioned, it is clear that miRNA are promising molecules for clinical use, including PD [101]. Interestingly, at the molecular level, 25% of miR-124 validated target genes are deregulated in PD, stressing the relevance of miR-124 in regulating PD [231]. Moreover, levels of miR-124 are decreased in the postmortem brain and the plasma of PD patients [104,106], suggesting it could be a potential biomarker for diagnosing PD. Also, in PD models, miR-124 expression is downregulated in 1-methyl-4-phenylpyridinium (MPP) iodide-treated MN9D dopaminergic neurons [105], MPP^+-treated SH-SY5Y cells [232–234], 6-OHDA-treated PC12 and SH-SY5Y cells [235], as well as in MPTP-treated mice [105,234]. In some of these studies, miR-124 downregulation was observed during the early stages of neurodegeneration, indicating that miR-124 reduction may not reflect dopaminergic neuronal death [105,107] but rather contribute to the initial biological process of neurodegeneration in PD [236].

Thus, increasing intracellular levels of miR-124 levels represent a promising therapeutic strategy. In PD models, miR-124 overexpression counteracted oxidative stress, autophagy dysregulation, apoptosis of dopaminergic neurons, and neuroinflammation [105,107,232–235,237]. Firstly, it was shown that miR-124 overexpression after MPP iodide insult attenuates the expression of the calpain 1/p25/cyclin-dependent kinase 5 (cdk5) proteins while improving cell viability *in vitro* [105]. Then, it was reported that miR-124 overexpression significantly decreased the percentage of apoptotic SH-SY5Y cells and the ratio of LC3 II/LC3 I suggesting that miR-124 functions as a protector of dopaminergic neurons during PD through the involvement of cell apoptosis and autophagy by regulating the 5' adenosine monophosphate-activated protein kinase and mechanistic target of rapamycin (AMPK/mTOR) pathway [233]. The previous research group also showed that the miR-124 agomir administration in MPTP-treated mice inhibited B-cell lymphoma (Bcl)-2-interacting mediator of cell death (Bim) expression, thus suppressing Bax translocation to mitochondria and consequently reducing the number of apoptotic cells in SN. Moreover, the impaired autophagy process, characterized by autophagosomes accumulation and lysosomal depletion, was alleviated by the upregulation of miR-124 in MPTP-treated mice and MPP^+-intoxicated SH-SY5Y cells [234]. Another study showed that miR-124-3p treatment attenuated MPP^+-

induced injury in *in vitro* PD model by suppressing neuronal apoptosis, neuroinflammation, and oxidative stress suggesting the neuroprotective role of miR-124 is triggered by its functional binding to STAT3 [232]. In addition, exogenous delivery of miR-124 suppressed mitogen-activated protein kinase kinase kinase 3 (MEKK3) and p-p65 expression and attenuated the activation of microglia in the SN of MPTP-treated mice, reinforcing the importance of miR-124 in the regulation of inflammatory response in PD [107]. Recently, it was reported that miR-124-3p overexpression significantly increases the survival of 6-OHDA-treated PC12 and SH-SY5Y cells and decreases apoptosis and ROS production via targeting annexin A5 (ANAX5), which was associated with the extracellular signal-regulated kinase (ERK) signaling pathway [235]. In addition, overexpression of miR-124 in a PD mouse model ameliorated motor defects, reduced dopaminergic neuronal loss and oxidative stress by suppressing Axin1 and activating the Wnt/β-catenin pathway [237]. Overall, the ectopic increase of miR-124 has been described to induce neuroprotection in cellular and animal models of PD.

2.2.2.1 MicroRNA-124 delivery into the brain – Therapeutic application for Parkinson's disease

MiRNA are highly susceptible to degradation by nucleases and entrapment in the endosome. Thus, developing safe and efficient methods for miRNA delivery into the cells is challenging due to their short half-life and relatively low stability [238]. For this reason, nucleic acid chemical modifications that improve their stability and effective delivery, including locked nucleic acids, 2′-O-methyl modification and phosphorothioate backbones have been developed [236]. Additionally, in the case of brain diseases, the main obstacle when using miRNA or other molecules/compounds as therapeutic agents is the BBB. Thus, using miRNA transport vehicles capable of crossing the BBB and efficiently delivering miRNA to the brain is necessary. Several drug delivery systems have been developed to carry miRNA into the brain parenchyma. EV, lipid-based carriers, polymeric NP, inorganic NP, viral vectors, micelles, and nanofibers are examples of carriers under intense scrutiny to improve drug delivery into the brain and reduce peripheral accumulation. NP have several advantages, such as: high load and protection of the cargo; high stability and easy storage; easy to modulate in terms of size, shape, surface, and chemistry; which make them the hot spot of the brain-targeted research. Moreover, the use of ligands such as peptides, antibodies, and proteins, to name a few, has been shown to be essential to increase brain uptake of NP and directing them into the lesioned area, thereby decreasing unwanted side effects [239]. In particular, polymeric NP have been successfully used for the delivery of miR-124. Intracerebroventricular administration of miR-124 polymeric NP into the lateral

ventricle of 6-OHDA-based PD mouse model increased the migration of neuroblasts towards the granule cell layer of the OB and the migration of SVZ-derived new neurons into the lesioned striatum. Importantly, these effects were accompanied by amelioration of motor deficits as evaluated by the apomorphine-induced rotation test. Hence, miR-124 polymeric NP represent a promising therapeutic strategy against PD [158]. Moreover, in another study, miR-124 polymeric NP reduced levels of pro-inflammatory cytokines and apoptosis of transfected BV2 microglial cells in an *in vitro* LPS model of PD. Additionally, exogenous delivery of miR-124 polymeric NP significantly downregulated MEKK3 expression, a direct miR-124 target [107], in SN of MPTP-treated mice [240]. To further improve specific brain targeting, Gang and colleagues conjugated rabies virus glycoprotein (RVG) 29 (RVG29) to the NP surface to facilitate its passage through the BBB [240]. RVG29 is a 29-amino acid peptide that binds to nicotinic acetylcholine receptors expressed in capillary endothelial cells, the main components of BBB [241]. This nanoformulation showed great permeability through the *in vitro* BBB model in a time-dependent manner, confirming RVG29 as a promising ligand for BBB crossing.

3. Extracellular vesicles

EV, enclosed by a lipid bilayer, are secreted by many cell types and contain RNA, miRNA, proteins, and lipids, to name a few [242]. These vesicles were initially identified as a cellular mechanism to eliminate unwanted cellular products [243]. Now, EV are also considered an additional mechanism for intercellular communication by transferring functional proteins, metabolites, and genetic material to recipient cells [244–246]. EV influence a broad range of physiological and pathological processes such as immune responses [247], neurogenic processes [248], neuronal communication [246], neurodegeneration [249], cancer [250], among others. In recent years, particular attention has been given to small EV (sEV), vesicles with a small diameter (30–200 nm) capable of permeating biological barriers and delivering their cargo onto target cells. Thus, there has been a growing interest in using these vesicles as diagnostic biomarkers of several diseases, as therapeutic agents, or drug delivery vehicles. As a nano-vesicular system, sEV could be vehicles for several therapeutic agents, including proteins, drugs, and miRNA. Naturally produced sEV overcomes the challenges associated with synthetic drug delivery systems, including polymeric NP and liposomes [251]. Their small size and membrane composition confer reduced immunogenicity and ability to cross biological membranes, including the BBB [252]. Additionally, sEV-based therapy bypasses the disadvantages associated with cell transplantation, such as low cell survival, immune rejection, and risk for blood vessel occlusion [253]. Importantly, sEV can spread and

transport their content into the brain through nasal, intravenous, intraperitoneal (IP), and intracranial administration, highlighting the high flexibility and compatibility of sEV-based therapies in treating CNS diseases [251,254–256]. Brief, in the last years sEV have gained a great clinical research value, emerging as a new method for the diagnosis and treatment of CNS diseases, including PD.

3.1 Biogenesis

Based on intracellular origin and/or biological function, EV are classified into three main classes: sEV (also referred to as exosomes), microvesicles, and apoptotic bodies. Each kind of membranous vesicle has its characteristics, such as differences in size and membrane-associated or matrix-contained marker proteins. Apoptotic bodies (50 to 5000 nm diameter) are released when plasma membrane blebbing occurs during apoptosis. Microvesicles (50 nm–1000 nm) are generated through the outward budding and fission from the plasma membrane, and once formed, they carry specific proteins and lipids and then deliver their cargo to a designated recipient cell. sEV generation differs from microvesicles mainly in terms of their intracellular origin and size [253]. In this section, only the sEV biogenesis will be focused. sEV (30–200 nm) originate from multivesicular bodies (MVB), a specialized endosomal compartment rich in intraluminal vesicles (ILV). First, early endosomes are formed, which are responsible for sorting the cargo for recycling back from the plasma membrane, followed by targeting the endocytic recycling compartment or transferring to late endosomes. Then, ILV are generated by the inward budding of endosomal membranes and accumulate in the lumen of the late endosome forming the MVB. Finally, MVB get transported to the plasma membrane via cytoskeletal and microtubule network and undergo exocytosis post fusion with the cell surface, whereby the ILV are secreted into the extracellular environment as sEV [252,257]. It is noteworthy that not all vesicles within the MVB are sorted for release as sEV; one part of MVB is carried to the lysosomal degradation pathway, where the sEV are removed as debris and recycled for cellular use (Figure 1.6). The underlying mechanisms for certain MVB being fused with the plasma membrane for releasing sEV or sending them to lysosomes for degradation [258] are still unknown [259]. The best-described mechanism for ILV and MVB formation is driven by the endosomal sorting complex required for transport (ESCRT) machinery, a cytoplasmic multi-subunit system essential for membrane remodeling, which enables vesicle budding and cargo sorting in MVB [260]. This process involves the sequential assembly of four ESCRT complexes (ESCRT-0, -I, -II and -III) with associated proteins such as programmed cell death 6 interacting protein (PDCD6IP; also known as ALIX), VPS4, VTA1, and tumor susceptibility gene 101 protein (TSG101) [257]. In addition to ESCRT, other ESCRT-

independent mechanisms have also been proposed [257]. The roles of complex lipids and other proteins in sEV generation have also been reported. For example, in some cells, sEV production requires the lipid ceramide and neutral sphingomyelinase, an enzyme that breaks down sphingolipid to ceramide [261]. sEV are secreted following the fusion of MVB with the cell membrane, a process that is, in some cells, dependent on RAB11, RAB27A, and RAB31, members of the small GTPase family [262,263]. The molecular mechanism of MVB fusion with the plasma membrane remains to be further clarified. Secreted sEV can be taken up by target cells through various proposed mechanisms, including direct interaction with extracellular receptors, direct fusion with the plasma membrane, or endocytosis, and thus deliver their content (specific proteins, lipids, coding, and non-coding RNA, among others) to the recipient cells [252].

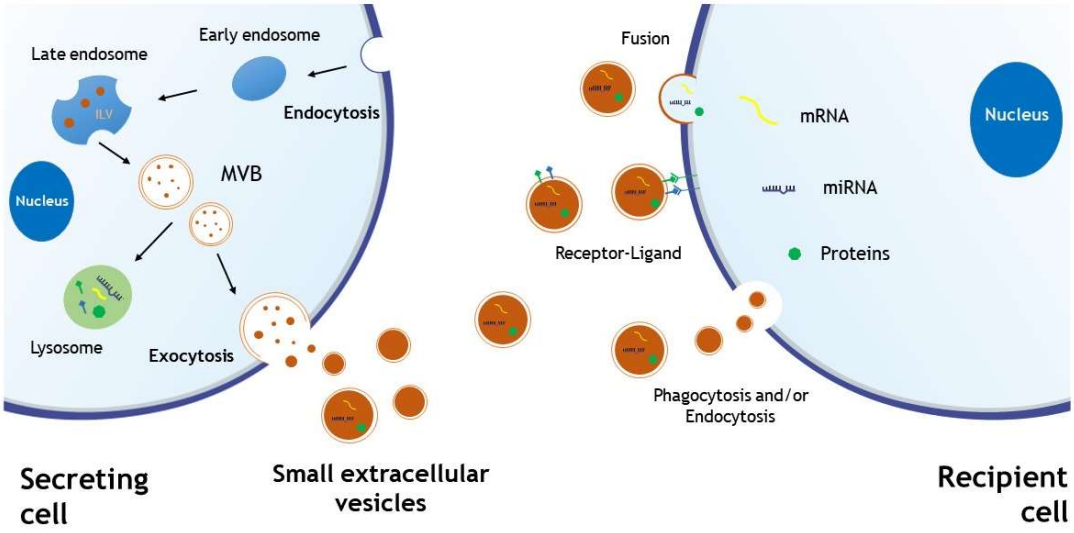

Figure 1.6 Schematic representation of biogenesis, cargo contents, and cellular uptake of small extracellular vesicles (sEV). sEV are derived from the endosome. As early endosomes become late endosomes, inward budding occurs and forms multivesicular bodies (MVB) containing numerous intraluminal vesicles (ILV). MVB can either get degraded by lysosomes or fuse with the membrane to release ILV called sEV. sEV interact with recipient cells by fusion with the plasma membrane, endocytosis, phagocytosis, or receptor-mediated uptake. mRNA, messenger RNA; miRNA, microRNA.

Typically, sEV display a cup-shaped morphology under the transmission electron microscope (TEM). Several defined biomarkers for sEV have been identified, such as tetraspanins CD9, CD63, and CD81, chaperones [heat shock proteins (HSP)] 60, 70, and 90, cytoplasmatic enzymes such as GAPDH, and proteins involved in MVB formation TSG101 and ALIX [264,265]. The biogenesis of sEV is not yet fully understood, and there is still some controversy in the scientific community about sEV research due to all the complexity involved in sEV biogenesis and their signaling pathways. A better

understanding of the intrinsic pathways involved in sEV biology will help ensure the successful development of sEV-based therapies. EV mediate a wide range of effects on recipient cells, indicating that they are either highly multifunctional [253].

Different cell types, including mononuclear blood cells (MNC) and mesenchymal stem cells, release sEV and have demonstrated beneficial paracrine effects in treating neurodegenerative diseases, including PD, therefore representing valuable sources of sEV. The sEV used in this study were obtained from MNC. Thus, this section will focus on these cells as a sEV-secreting cell source. Mononuclear cells from umbilical cord blood (UCB-MNC) are a highly prolific source and relatively easy to obtain from multiple banks [266]. sEV derived from human UCB (hUCB)-MNC are well characterized in composition, show negligent lot-to-lot variability, have low immunogenicity, and are easily accessible in cord blood banks [266–268]. Several clinical trials are using umbilical cord blood cells to treat neurologic diseases, supporting their safety [267]. CD34+ hematopoietic stem/progenitor cells are present in high numbers in UCB and present a less mature and more proliferative phenotype [269,270]. These cells have proven to play a role in neuroprotection in a PD context. Intravenous injection of hUCB-MNC CD34+ improved the motor function, ameliorated striatal dopamine and ATP levels, and restored mitochondrial DNA and nuclear DNA integrity culminating in the protection of dopaminergic neurons in SN of MPTP-parkinsonian mice [271]. Information about the bioactivity of MNC-derived sEV in a PD context is scarce so far. Nevertheless, MNC secretome has been widely used in diseases such as skin tissue regeneration [266], stroke [272], and spinal cord injury [273].

3.2 Small extracellular vesicles in Parkinson's disease

The bioactivity of sEV, due to its membrane composition and bioactive cargo, have highlighted these vesicles as possible therapeutic agents for neurodegenerative diseases, including in PD. SEV isolated from stem cells have shown promising effects in PD. sEV derived from human dental pulp-derived stem cells showed to be protective against 6-OHDA-induced dopaminergic degeneration *in vitro* [274]. Chen and collaborators showed that sEV isolated from human umbilical cord mesenchymal stem cells promoted the proliferation of 6-OHDA-intoxicated SH-SY5Y cells while inhibiting apoptosis by inducing autophagy. *In vivo*, the intravenous administration of these sEV reduced dopaminergic neuronal loss in the SN while increasing dopamine levels in the striatum, alleviating the apomorphine-induced rotational behavior in a 6-OHDA rat model of PD [275]. In another study, exosomes isolated during dopaminergic neurons differentiation from bone marrow mesenchymal stem cells and administrated in the rat striatum of the 6-OHDA induced PD animal model resulted in the downregulation of pro-inflammatory

factors and ROS in the SN [276]. Recently, it was shown that NSC-derived EV reduced the intracellular ROS and associated pro-apoptotic caspase-3/7 in addition to the downregulation of several pro-inflammatory factors leading to significantly decreased 6-OHDA-induced dopaminergic neuronal loss *in vivo* [99]. SEV also play critical roles in inducing pathological processes. Indeed, the cargo transferred by sEV may have detrimental effects, contributing to the spread of the disease [277,278]. SEV released by the different tissues can be collected to evaluate their unique protein or RNA content and be used as disease biomarkers. The potentiality of PD diagnosis using sEV arises from the accumulation of α-synuclein in sEV and transmission among neurons. A potential mechanism for an EV-mediated α-synuclein spreading between neurons in the CNS has been proposed [279,280]. Despite the evidence that sEV are involved in the transmission of α-synuclein between neurons, CD11 positive microglia-derived EV from PD patients also showed higher levels of α-synuclein than healthy individuals. In fact, microglia-derived sEV administered to cortical neurons were able to induce severe α-synuclein aggregation, thus confirming the ability of these sEV to spread α-synuclein protein to neurons [281].

3.3 Small extracellular vesicles as drug delivery vehicles for Parkinson's disease

The exploitation of sEV as drug delivery vehicles offers important advantages compared to other nanoparticulate drug delivery systems such as liposomes and polymeric NP. Due to their biological nature, sEV have the exceptional ability to interact with recipient cells proteins having a specific cell tropism that can target them to disease tissues [282,283]. This contrasts with a relatively lower penetration efficiency of NP because are easily trapped inside the basal lamina, thus limiting their diffusion across the brain parenchyma [284]. The superior uptake of sEV occurs mainly due to their rich composition in adhesion proteins, tetraspanins, and integrins [264,265], which are absent in synthetic NP. Moreover, sEV may comprise additional advantages over synthetic nanocarriers and cell-mediated drug delivery, avoiding the rapid clearance by phagocytosis and engulfment by lysosomes and toxicity [285]. Noteworthy, sEV possess an intrinsic ability to cross biological barriers, such as the BBB, and easily reach their brain targets. Accordingly, sEV loaded with catalase [255], dopamine [286], or *GAPDH* siRNA [256], were detected in the brains of PD mouse models after intravenous administration, indicating their ability to cross the BBB. Therefore, sEV have been considered an attractive platform for drug delivery of nucleic acids or proteins into the brain for the treatment of several neurodegenerative diseases, including PD [255,259,287–289]. As the key pathological feature in PD is the presence of α-synuclein

aggregates, studies using sEV to deliver molecules targeting α-synuclein have increased. Cooper and collaborators used modified exosomes, which specially target the brain by introducing a brain targeting peptide (RVG peptide) in the exterior of the exosomes. RVG peptide specifically binds acetylcholine receptors expressed on neuronal cells [290] and has been employed as a targeting ligand to the brain [291]. The systemic administration of RVG-exosomes loaded with α-synuclein siRNA reduced α-synuclein aggregates in transgenic mice expressing the human S129D α-synuclein [292]. Regarding the limitations of siRNA, such as its short half-life, a new approach was used by Izco and her group. Recently, they used RVG-modified exosomes as delivery vehicles of anti-α-synuclein short hairpin minicircles to induce long-term downregulation of α-synuclein. The administration of these modulated exosomes induced a decrease in the expression and aggregation of α-synuclein, reducing the loss of dopaminergic neurons in the SN and improving clinical symptoms in a mouse model of PD [293]. In addition to delivering small molecules, sEV have also been used to deliver large molecules such as proteins. For example, sEV derived from the bone marrow and loaded with the antioxidant protein catalase was successfully delivered across the BBB and were able to counteract inflammatory reactions and provide potent neuroprotection in 6-OHDA PD mouse model [255]. Furthermore, administration of sEV isolated from mouse blood and loaded with dopamine increased dopamine levels in the brain, culminating in reduced loss of dopaminergic neurons and ameliorated disease phenotype in a PD mouse model [286]. Overall, these studies indicate that sEV are relevant delivery vehicles of several types of molecules, being considered an effective therapeutic platform for PD.

4. References

1. Olesen J, Gustavsson A, Svensson M, Wittchen H-U, Jönsson B, CDBE2010 study group, European Brain Council: The economic cost of brain disorders in Europe. *Eur J Neurol* 2012, 19:155–162.
2. Dauer W, Przedborski S: Parkinson's disease: Mechanisms and models. *Neuron* 2003, 39:889–909.
3. Schapira AHV, Chaudhuri KR, Jenner P: Non-motor features of Parkinson disease. *Nat Rev Neurosci 2017 187* 2017, 18:435–450.
4. Greffard S, Verny M, Bonnet AM, Beinis JY, Gallinari C, Meaume S, Piette F, Hauw JJ, Duyckaerts C: Motor score of the Unified Parkinson Disease Rating Scale as a good predictor of Lewy body-associated neuronal loss in the substantia nigra. *Arch Neurol* 2006, 63:584–588.
5. Ma SY, Röyttä M, Rinne JO, Collan Y, Rinne UK: Correlation between neuromorphometry in the substantia nigra and clinical features in Parkinson's

disease using disector counts. *J Neurol Sci* 1997, 151:83–87.
6. Cheng HC, Ulane CM, Burke RE: Clinical progression in Parkinson disease and the neurobiology of axons. *Ann Neurol* 2010, 67:715–725.
7. Samii A, Nutt JG, Ransom BR: Parkinson's disease. *Lancet* 2004, 363:1783–1793.
8. Gouda NA, Elkamhawy A, Cho J: Emerging Therapeutic Strategies for Parkinson's Disease and Future Prospects: A 2021 Update. *Biomedicines* 2022, 10:371.
9. Cannon JR, Greenamyre JT: Gene-environment interactions in Parkinson's disease: specific evidence in humans and mammalian models. *Neurobiol Dis* 2013, 57:38–46.
10. Xu L, Pu J: Alpha-Synuclein in Parkinson's Disease: From Pathogenetic Dysfunction to Potential Clinical Application. *Parkinsons Dis* 2016, 2016.
11. Braak H, Del Tredici K, Rüb U, De Vos RAI, Jansen Steur ENH, Braak E: Staging of brain pathology related to sporadic Parkinson's disease. *Neurobiol Aging* 2003, 24:197–211.
12. Wakabayashi K, Takahashi H: Neuropathology of autonomic nervous system in Parkinson's disease. *Eur Neurol* 1997, 38 Suppl 2:2–7.
13. Iwai A, Masliah E, Yoshimoto M, Ge N, Flanagan L, Rohan de Silva HA, Kittel A, Saitoh T: The precursor protein of non-A beta component of Alzheimer's disease amyloid is a presynaptic protein of the central nervous system. *Neuron* 1995, 14:467–475.
14. Lashuel HA, Overk CR, Oueslati A, Masliah E: The many faces of α-synuclein: from structure and toxicity to therapeutic target. *Nat Rev Neurosci* 2013, 14:38–48.
15. Tan LY, Tang KH, Lim LYY, Ong JX, Park H, Jung S: α-Synuclein at the Presynaptic Axon Terminal as a Double-Edged Sword. *Biomolecules* 2022, 12:507.
16. Beyer K, Domingo-Sàbat M, Ariza A: Molecular pathology of Lewy body diseases. *Int J Mol Sci* 2009, 10:724–745.
17. Cookson MR: α-Synuclein and neuronal cell death. *Mol Neurodegener 2009 41* 2009, 4:1–14.
18. Chen R, Gu X, Wang X: α-Synuclein in Parkinson's disease and advances in detection. *Clin Chim Acta* 2022, 529:76–86.
19. Kalia L V.: Diagnostic biomarkers for Parkinson's disease: focus on α-synuclein in cerebrospinal fluid. *Parkinsonism Relat Disord* 2019, 59:21–25.
20. Fadda L, Lombardi R, Soliveri P, Lauria G, Giovanni Defazio, Tagliavini F: Skin nerve α-synuclein deposits in a parkinsonian patient with heterozygous parkin mutation. *Parkinsonism Relat Disord* 2019, 60:182–183.
21. Dexter DT, Carter CJ, Wells FR, Javoy-Agid F, Agid Y, Lees A, Jenner P, Marsden

CD: Basal lipid peroxidation in substantia nigra is increased in Parkinson's disease. *J Neurochem* 1989, 52:381–389.

22. McGeer PL, Itagaki S, Boyes BE, McGeer EG: Reactive microglia are positive for HLA-DR in the substantia nigra of Parkinson's and Alzheimer's disease brains. *Neurology* 1988, 38:1285–1291.
23. Williams-Gray CH, Wijeyekoon R, Yarnall AJ, Lawson RA, Breen DP, Evans JR, Cummins GA, Duncan GW, Khoo TK, Burn DJ, et al.: Serum immune markers and disease progression in an incident Parkinson's disease cohort (ICICLE-PD). *Mov Disord* 2016, 31:995–1003.
24. Nagatsu T, Mogi M, Ichinose H, Togari A: Changes in cytokines and neurotrophins in Parkinson's disease. *J Neural Transm Suppl* 2000, doi:10.1007/978-3-7091-6301-6_19.
25. Rosborough K, Patel N, Kalia L V.: α-Synuclein and Parkinsonism: Updates and Future Perspectives. *Curr Neurol Neurosci Rep* 2017, 17:1–11.
26. Nuber S, Rajsombath M, Minakaki G, Winkler J, Müller CP, Ericsson M, Caldarone B, Dettmer U, Selkoe DJ: Abrogating Native α-Synuclein Tetramers in Mice Causes a L-DOPA-Responsive Motor Syndrome Closely Resembling Parkinson's Disease. *Neuron* 2018, 100:75-90.e5.
27. Gómez-Benito M, Granado N, García-Sanz P, Michel A, Dumoulin M, Moratalla R: Modeling Parkinson's Disease With the Alpha-Synuclein Protein. *Front Pharmacol* 2020, 11:1.
28. Cremades N, Cohen SIA, Deas E, Abramov AY, Chen AY, Orte A, Sandal M, Clarke RW, Dunne P, Aprile FA, et al.: Direct observation of the interconversion of normal and toxic forms of α-synuclein. *Cell* 2012, 149:1048–1059.
29. Cascella R, Chen SW, Bigi A, Camino JD, Xu CK, Dobson CM, Chiti F, Cremades N, Cecchi C: The release of toxic oligomers from α-synuclein fibrils induces dysfunction in neuronal cells. *Nat Commun* 2021, 12.
30. Bridi JC, Hirth F: Mechanisms of α-Synuclein Induced Synaptopathy in Parkinson's Disease. *Front Neurosci* 2018, 12.
31. Cascella R, Bigi A, Cremades N, Cecchi C: Effects of oligomer toxicity, fibril toxicity and fibril spreading in synucleinopathies. *Cell Mol Life Sci* 2022, 79:174.
32. Alam P, Bousset L, Melki R, Otzen DE: α-synuclein oligomers and fibrils: a spectrum of species, a spectrum of toxicities. *J Neurochem* 2019, 150:522–534.
33. Mehra S, Sahay S, Maji SK: α-Synuclein misfolding and aggregation: Implications in Parkinson's disease pathogenesis. *Biochim Biophys acta Proteins proteomics* 2019, 1867:890–908.
34. De Toro J, Herschlik L, Waldner C, Mongini C: Emerging roles of exosomes in

normal and pathological conditions: new insights for diagnosis and therapeutic applications. *Front Immunol* 2015, 6.

35. Stefanis L: α-Synuclein in Parkinson's Disease. *Cold Spring Harb Perspect Med* 2012, 2.
36. Periquet M, Fulga T, Myllykangas L, Schlossmacher MG, Feany MB: Aggregated α-Synuclein Mediates Dopaminergic Neurotoxicity In Vivo. *J Neurosci* 2007, 27:3338–3346.
37. Ulusoy A, Febbraro F, Jensen PH, Kirik D, Romero-Ramos M: Co-expression of C-terminal truncated alpha-synuclein enhances full-length alpha-synuclein-induced pathology. *Eur J Neurosci* 2010, 32:409–422.
38. Prasad K, Beach TG, Hedreen J, Richfield EK: Critical Role of Truncated α-Synuclein and Aggregates in Parkinson's Disease and Incidental Lewy Body Disease. *Brain Pathol* 2012, 22:811.
39. Oueslati A: Implication of Alpha-Synuclein Phosphorylation at S129 in Synucleinopathies: What Have We Learned in the Last Decade? *J Parkinsons Dis* 2016, 6:39–51.
40. Ghosh D, Mehra S, Sahay S, Singh PK, Maji SK: α-synuclein aggregation and its modulation. *Int J Biol Macromol* 2017, 100:37–54.
41. Samuel F, Flavin WP, Iqbal S, Pacelli C, Renganathan SDS, Trudeau LE, Campbell EM, Fraser PE, Tandon A: Effects of Serine 129 Phosphorylation on α-Synuclein Aggregation, Membrane Association, and Internalization. *J Biol Chem* 2016, 291:4374–4385.
42. Webb JL, Ravikumar B, Atkins J, Skepper JN, Rubinsztein DC: Alpha-Synuclein is degraded by both autophagy and the proteasome. *J Biol Chem* 2003, 278:25009–25013.
43. Cuervo AM, Wong E: Chaperone-mediated autophagy: roles in disease and aging. *Cell Res* 2014, 24:92.
44. Alvarez-Erviti L, Rodriguez-Oroz MC, Cooper JM, Caballero C, Ferrer I, Obeso JA, Schapira AHV: Chaperone-mediated autophagy markers in Parkinson disease brains. *Arch Neurol* 2010, 67:1464–1472.
45. Murphy KE, Gysbers AM, Abbott SK, Spiro AS, Furuta A, Cooper A, Garner B, Kabuta T, Halliday GM: Lysosomal-associated membrane protein 2 isoforms are differentially affected in early Parkinson's disease. *Mov Disord* 2015, 30:1639–1647.
46. Levine B, Kroemer G: Autophagy in the Pathogenesis of Disease. *Cell* 2008, 132:27.
47. Fellner L, Gabassi E, Haybaeck J, Edenhofer F: Autophagy in α-

Synucleinopathies—An Overstrained System. *Cells* 2021, 10.

48. Dehay B, Bové J, Rodríguez-Muela N, Perier C, Recasens A, Boya P, Vila M: Pathogenic Lysosomal Depletion in Parkinson's Disease. *J Neurosci* 2010, 30:12535.
49. Zatloukal K, Stumptner C, Fuchsbichler A, Heid H, Schnoelzer M, Kenner L, Kleinert R, Prinz M, Aguzzi A, Denk H: p62 Is a common component of cytoplasmic inclusions in protein aggregation diseases. *Am J Pathol* 2002, 160:255–263.
50. Jasutkar HG, Oh SE, Mouradian MM: Therapeutics in the Pipeline Targeting α-Synuclein for Parkinson's Disease. *Pharmacol Rev* 2022, 74:207–237.
51. Guo JD, Zhao X, Li Y, Li GR, Liu XL: Damage to dopaminergic neurons by oxidative stress in Parkinson's disease (Review). *Int J Mol Med* 2018, 41:1817–1825.
52. Schapira AHV, Cooper JM, Dexter D, Clark JB, Jenner P, Marsden CD: Mitochondrial complex I deficiency in Parkinson's disease. *J Neurochem* 1990, 54:823–827.
53. Betarbet R, Sherer TB, MacKenzie G, Garcia-Osuna M, Panov A V., Greenamyre JT: Chronic systemic pesticide exposure reproduces features of Parkinson's disease. *Nat Neurosci 2000 312* 2000, 3:1301–1306.
54. Schapira AH, Jenner P: Etiology and pathogenesis of Parkinson's disease. *Mov Disord* 2011, 26:1049–1055.
55. Zhu J, Chu CT: Mitochondrial dysfunction in Parkinson's disease. *J Alzheimers Dis* 2010, 20 Suppl 2.
56. Beal MF: Mitochondria take center stage in aging and neurodegeneration. *Ann Neurol* 2005, 58:495–505.
57. Rodriguez M, Morales I, Rodriguez-Sabate C, Sanchez A, Castro R, Brito JM, Sabate M: The degeneration and replacement of dopamine cells in Parkinson's disease: The role of aging. *Front Neuroanat* 2014, 8:80.
58. Dias V, Junn E, Mouradian MM: The role of oxidative stress in Parkinson's disease. *J Parkinsons Dis* 2013, 3:461–91.
59. Dan Dunn J, Alvarez LAJ, Zhang X, Soldati T: Reactive oxygen species and mitochondria: A nexus of cellular homeostasis. *Redox Biol* 2015, 6:472–485.
60. Choi DH, Cristóvão AC, Guhathakurta S, Lee J, Joh TH, Beal MF, Kim YS: NADPH oxidase 1-mediated oxidative stress leads to dopamine neuron death in Parkinson's disease. *Antioxidants Redox Signal* 2012, 16:1033–1045.
61. Zawada WM, Mrak RE, Biedermann JA, Palmer QD, Gentleman SM, Aboud O, Griffin WST: Loss of angiotensin II receptor expression in dopamine neurons in

Parkinson's disease correlates with pathological progression and is accompanied by increases in Nox4- and 8-OH guanosine-related nucleic acid oxidation and caspase-3 activation. *Acta Neuropathol Commun* 2015, 3:9.

62. Cheng G, Diebold BA, Hughes Y, Lambeth JD: Nox1-dependent Reactive Oxygen Generation Is Regulated by Rac1 *. *J Biol Chem* 2006, 281:17718–17726.
63. Ueyama T, Geiszt M, Leto TL: Involvement of Rac1 in Activation of Multicomponent Nox1- and Nox3-Based NADPH Oxidases. *Mol Cell Biol* 2006, 26:2160.
64. Cristóvão AC, Guhathakurta S, Bok E, Je G, Yoo SD, Choi DH, Kim YS: Nadph oxidase 1 mediates α-synucleinopathy in Parkinson's disease. *J Neurosci* 2012, 32:14465–14477.
65. Shimohama S, Hisahara S: Toxin-induced and genetic animal models of Parkinson's disease. *Parkinsons Dis* 2010, 2011.
66. Jagmag SA, Tripathi N, Shukla SD, Maiti S, Khurana S: Evaluation of Models of Parkinson's Disease. *Front Neurosci* 2016, 9.
67. Schober A: Classic toxin-induced animal models of Parkinson's disease: 6-OHDA and MPTP. *Cell Tissue Res* 2004, 318:215–224.
68. Kin K, Yasuhara T, Kameda M, Date I: Animal Models for Parkinson's Disease Research: Trends in the 2000s. *Int J Mol Sci* 2019, 20.
69. Blum D, Torch S, Lambeng N, Nissou MF, Benabid AL, Sadoul R, Verna JM: Molecular pathways involved in the neurotoxicity of 6-OHDA, dopamine and MPTP: contribution to the apoptotic theory in Parkinson's disease. *Prog Neurobiol* 2001, 65:135–172.
70. Lehmensiek V, Tan EM, Liebau S, Lenk T, Zettlmeisl H, Schwarz J, Storch A: Dopamine transporter-mediated cytotoxicity of 6-hydroxydopamine in vitro depends on expression of mutant α-synucleins related to Parkinson's disease. *Neurochem Int* 2006, 48:329–340.
71. Dana OF, Gee M: The Generation of Hydrogen Peroxide, Superoxide Radical, and Hydroxyl Radical by 6=Hydroxydopamine, Dialuric Acid, and Related Cytotoxic Agents*. *TEE J OP Biol CHEMIIBTBY* 1974, 249:2447–2452.
72. Glinka Y, Gassen M, Youdim MBH: Mechanism of 6-hydroxydopamine neurotoxicity. *J Neural Transm Suppl* 1997, doi:10.1007/978-3-7091-6842-4_7.
73. Betarbet R, Sherer TB, Timothy Greenamyre J: Animal models of Parkinson's disease. *Bioessays* 2002, 24:308–318.
74. Del Tredici K, Rüb U, De Vos RAI, Bohl JRE, Braak H: Where Does Parkinson Disease Pathology Begin in the Brain? *J Neuropathol Exp Neurol* 2002, 61:413–426.

75. Berry C, La Vecchia C, Nicotera P: Paraquat and Parkinson's disease. *Cell Death Differ 2010 177* 2010, 17:1115–1125.
76. Nandipati S, Litvan I: Environmental Exposures and Parkinson's Disease. *Int J Environ Res Public Heal 2016, Vol 13, Page 881* 2016, 13:881.
77. Shimizu K, Ohtaki K, Matsubara K, Aoyama K, Uezono T, Saito O, Suno M, Ogawa K, Hayase N, Kimura K, et al.: Carrier-mediated processes in blood--brain barrier penetration and neural uptake of paraquat. *Brain Res* 2001, 906:135–142.
78. Corasaniti MT, Strongoli MC, Rotiroti D, Bagetta G, Nisticò G: Paraquat: a useful tool for the in vivo study of mechanisms of neuronal cell death. *Pharmacol Toxicol* 1998, 83:1–7.
79. Drechsel DA, Patel M: Role of Reactive Oxygen Species in the Neurotoxicity of Environmental Agents Implicated in Parkinson's disease. *Free Radic Biol Med* 2008, 44:1873.
80. Castello PR, Drechsel DA, Patel M: Mitochondria are a major source of paraquat-induced reactive oxygen species production in the brain. *J Biol Chem* 2007, 282:14186–14193.
81. Cochemé HM, Murphy MP: Complex I is the major site of mitochondrial superoxide production by paraquat. *J Biol Chem* 2008, 283:1786–1798.
82. Huang CL, Chao CC, Lee YC, Lu MK, Cheng JJ, Yang YC, Wang VC, Chang WC, Huang NK: Paraquat Induces Cell Death Through Impairing Mitochondrial Membrane Permeability. *Mol Neurobiol* 2016, 53:2169–2188.
83. Manning-Bog AB, McCormack AL, Li J, Uversky VN, Fink AL, Di Monte DA: The Herbicide Paraquat Causes Up-regulation and Aggregation of α-Synuclein in Mice: PARAQUAT AND α-SYNUCLEIN. *J Biol Chem* 2002, 277:1641–1644.
84. McCormack AL, Atienza JG, Johnston LC, Andersen JK, Vu S, Di Monte DA: Role of oxidative stress in paraquat-induced dopaminergic cell degeneration. *J Neurochem* 2005, 93:1030–1037.
85. Mitra S, Chakrabarti N, Bhattacharyya A: Differential regional expression patterns of α-synuclein, TNF-α, and IL-1β; and variable status of dopaminergic neurotoxicity in mouse brain after Paraquat treatment. *J Neuroinflammation* 2011, 8.
86. Navarro-Yepes J, Anandhan A, Bradley E, Bohovych I, Yarabe B, de Jong A, Ovaa H, Zhou Y, Khalimonchuk O, Quintanilla-Vega B, et al.: Inhibition of Protein Ubiquitination by Paraquat and 1-Methyl-4-Phenylpyridinium Impairs Ubiquitin-Dependent Protein Degradation Pathways. *Mol Neurobiol 2015 538* 2015, 53:5229–5251.
87. Uversky VN, Li J, Fink AL: Pesticides directly accelerate the rate of α-synuclein

fibril formation: a possible factor in Parkinson's disease. *FEBS Lett* 2001, 500:105–108.

88. Cristóvão AC, Choi D-H, Baltazar G, Beal MF, Kim Y-S: The role of NADPH oxidase 1-derived reactive oxygen species in paraquat-mediated dopaminergic cell death. *Antioxid Redox Signal* 2009, 11:2105–18.
89. Cristóvão AC, Campos FL, Je G, Esteves M, Guhathakurta S, Yang L, Beal MF, Fonseca BM, Salgado AJ, Queiroz J, et al.: Characterization of a Parkinson's disease rat model using an upgraded paraquat exposure paradigm. *Eur J Neurosci* 2020, 52:3242–3255.
90. Krishnan S, Chi EY, Wood SJ, Kendrick BS, Li C, Garzon-Rodriguez W, Wypych J, Randolph TW, Narhi LO, Biere AL, et al.: Oxidative dimer formation is the critical rate-limiting step for Parkinson's disease alpha-synuclein fibrillogenesis. *Biochemistry* 2003, 42:829–837.
91. Sarkar S, Raymick J, Imam S: Neuroprotective and Therapeutic Strategies against Parkinson's Disease: Recent Perspectives. *Int J Mol Sci* 2016, 17.
92. Mogi M, Togari A, Kondo T, Mizuno Y, Komure O, Kuno S, Ichinose H, Nagatsu T: Brain-derived growth factor and nerve growth factor concentrations are decreased in the substantia nigra in Parkinson's disease. *Neurosci Lett* 1999, 270:45–8.
93. Chauhan NB, Siegel GJ, Lee JM: Depletion of glial cell line-derived neurotrophic factor in substantia nigra neurons of Parkinson's disease brain. *J Chem Neuroanat* 2001, 21:277–288.
94. Eslamboli A, Georgievska B, Ridley RM, Baker HF, Muzyczka N, Burger C, Mandel RJ, Annett L, Kirik D: Continuous low-level glial cell line-derived neurotrophic factor delivery using recombinant adeno-associated viral vectors provides neuroprotection and induces behavioral recovery in a primate model of Parkinson's disease. *J Neurosci* 2005, 25:769–777.
95. Gasmi M, Herzog CD, Brandon EP, Cunningham JJ, Ramirez GA, Ketchum ET, Bartus RT: Striatal delivery of neurturin by CERE-120, an AAV2 vector for the treatment of dopaminergic neuron degeneration in Parkinson's disease. *Mol Ther* 2007, 15:62–68.
96. Barker RA, Björklund A, Gash DM, Whone A, Van Laar A, Kordower JH, Bankiewicz K, Kieburtz K, Saarma M, Booms S, et al.: GDNF and Parkinson's Disease: Where Next? A Summary from a Recent Workshop. *J Parkinsons Dis* 2020, 10:875.
97. Yu H, Sun T, An J, Wen L, Liu F, Bu Z, Cui Y, Feng J: Potential Roles of Exosomes in Parkinson's Disease: From Pathogenesis, Diagnosis, and Treatment to

Prognosis. *Front cell Dev Biol* 2020, 8.

98. Chang YH, Wu KC, Harn HJ, Lin SZ, Ding DC: Exosomes and Stem Cells in Degenerative Disease Diagnosis and Therapy. *Cell Transplant* 2018, 27:349–363.
99. Lee EJ, Choi Y, Lee HJ, Hwang DW, Lee DS: Human neural stem cell-derived extracellular vesicles protect against Parkinson's disease pathologies. *J Nanobiotechnology* 2022, 20:198.
100. Mendes-Pinheiro B, Anjo SI, Manadas B, Da Silva JD, Marote A, Behie LA, Teixeira FG, Salgado AJ: Bone Marrow Mesenchymal Stem Cells' Secretome Exerts Neuroprotective Effects in a Parkinson's Disease Rat Model. *Front Bioeng Biotechnol* 2019, 7.
101. Saraiva C, Esteves M, Bernardino L: MicroRNA: Basic concepts and implications for regeneration and repair of neurodegenerative diseases. *Biochem Pharmacol* 2017, 141:118–131.
102. McMillan KJ, Murray TK, Bengoa-Vergniory N, Cordero-Llana O, Cooper J, Buckley A, Wade-Martins R, Uney JB, O'Neill MJ, Wong LF, et al.: Loss of MicroRNA-7 Regulation Leads to α-Synuclein Accumulation and Dopaminergic Neuronal Loss In Vivo. *Mol Ther* 2017, 25:2404–2414.
103. Zhang J, Zhao M, Yan R, Liu J, Maddila S, Junn E, Mouradian MM: MicroRNA-7 Protects Against Neurodegeneration Induced by α-Synuclein Preformed Fibrils in the Mouse Brain. *Neurotherapeutics* 2021, 18:2529–2540.
104. Li N, Pan X, Zhang J, Ma A, Yang S, Ma J, Xie A: Plasma levels of miR-137 and miR-124 are associated with Parkinson's disease but not with Parkinson's disease with depression. *Neurol Sci* 2017, 38:761–767.
105. Kanagaraj N, Beiping H, Dheen ST, Tay SSW: Downregulation of miR-124 in MPTP-treated mouse model of Parkinson's disease and MPP iodide-treated MN9D cells modulates the expression of the calpain/cdk5 pathway proteins. *Neuroscience* 2014, 272:167–79.
106. Xing RX, Li LG, Liu XW, Tian BX, Cheng Y: Down regulation of miR-218, miR-124, and miR-144 relates to Parkinson's disease via activating NF-κB signaling. *Kaohsiung J Med Sci* 2020, 36:786–792.
107. Yao L, Ye Y, Mao H, Lu F, He X, Lu G, Zhang S: MicroRNA-124 regulates the expression of MEKK3 in the inflammatory pathogenesis of Parkinson's disease. *J Neuroinflammation* 2018, 15:13.
108. Charvin D, Medori R, Hauser RA, Rascol O: Therapeutic strategies for Parkinson disease: beyond dopaminergic drugs. *Nat Rev Drug Discov 2018 1711* 2018, 17:804–822.
109. Ming G, Song H: ADULT NEUROGENESIS IN THE MAMMALIAN CENTRAL

NERVOUS SYSTEM. *Annu Rev Neurosci* 2005, 28:223–250.

110. Pearson BJ, Doe CQ: Specification of temporal identity in the developing nervous system. *Annu Rev Cell Dev Biol* 2004, 20:619–647.
111. Reynolds BA, Weiss S: Generation of neurons and astrocytes from isolated cells of the adult mammalian central nervous system. *Science* 1992, 255:1707–10.
112. Keller G: Embryonic stem cell differentiation: emergence of a new era in biology and medicine. *Genes Dev* 2005, 19:1129–1155.
113. Zhao C, Deng W, Gage FH: Mechanisms and functional implications of adult neurogenesis. *Cell* 2008, 132:645–60.
114. Eriksson PS, Perfilieva E, Björk-Eriksson T, Alborn A-M, Nordborg C, Peterson DA, Gage FH: Neurogenesis in the adult human hippocampus. *Nat Med* 1998, 4:1313–1317.
115. Furutachi S, Miya H, Watanabe T, Kawai H, Yamasaki N, Harada Y, Imayoshi I, Nelson M, Nakayama KI, Hirabayashi Y, et al.: Slowly dividing neural progenitors are an embryonic origin of adult neural stem cells. *Nat Neurosci* 2015, 18:657–665.
116. Morizur L, Chicheportiche A, Gauthier LR, Daynac M, Boussin FD, Mouthon M-A: Distinct Molecular Signatures of Quiescent and Activated Adult Neural Stem Cells Reveal Specific Interactions with Their Microenvironment. *Stem Cell Reports* 2018, 11:565–577.
117. Lois C, Alvarez-Buylla A: Proliferating subventricular zone cells in the adult mammalian forebrain can differentiate into neurons and glia (neurogenesis/subependymal zone/brain repair/stem cells). *Proc Natl Acad Sci USA* 1993, 90:2074–2077.
118. Morshead CM, Reynolds BA, Craig CG, McBurney MW, Staines WA, Morassutti D, Weiss S, van der Kooy D: Neural stem cells in the adult mammalian forebrain: A relatively quiescent subpopulation of subependymal cells. *Neuron* 1994, 13:1071–1082.
119. Liu Y, Zhang J, Han R, Liu H, Sun D, Liu X: Downregulation of serum brain specific microRNA is associated with inflammation and infarct volume in acute ischemic stroke. *J Clin Neurosci* 2015, 22:291–5.
120. Kempermann G, Jessberger S, Steiner B, Kronenberg G: Milestones of neuronal development in the adult hippocampus. *Trends Neurosci* 2004, 27:447–452.
121. Altman J, Das GD: Autoradiographic and histological evidence of postnatal hippocampal neurogenesis in rats. *J Comp Neurol* 1965, 124:319–35.
122. Kempermann G, Song H, Gage FH: Neurogenesis in the Adult Hippocampus. *Cold Spring Harb Perspect Biol* 2015, 7:a018812.

123. Pino A, Fumagalli G, Bifari F, Decimo I: New neurons in adult brain: distribution, molecular mechanisms and therapies. *Biochem Pharmacol* 2017, 141:4–22.
124. Kempermann G, Gage FH, Aigner L, Song H, Curtis MA, Thuret S, Kuhn HG, Jessberger S, Frankland PW, Cameron HA, et al.: Human Adult Neurogenesis: Evidence and Remaining Questions. *Cell Stem Cell* 2018, 23:25–30.
125. Sorrells SF, Paredes MF, Cebrian-Silla A, Sandoval K, Qi D, Kelley KW, James D, Mayer S, Chang J, Auguste KI, et al.: Human hippocampal neurogenesis drops sharply in children to undetectable levels in adults. *Nature* 2018, 555:377–381.
126. Boldrini M, Fulmore CA, Tartt AN, Simeon LR, Pavlova I, Poposka V, Rosoklija GB, Stankov A, Arango V, Dwork AJ, et al.: Human Hippocampal Neurogenesis Persists throughout Aging. *Cell Stem Cell* 2018, 22:589-599.e5.
127. Tobin MK, Musaraca K, Disouky A, Shetti A, Bheri A, Honer WG, Kim N, Dawe RJ, Bennett DA, Arfanakis K, et al.: Human Hippocampal Neurogenesis Persists in Aged Adults and Alzheimer's Disease Patients. *Cell Stem Cell* 2019, 24:974-982.e3.
128. Moreno-Jiménez EP, Flor-García M, Terreros-Roncal J, Rábano A, Cafini F, Pallas-Bazarra N, Ávila J, Llorens-Martín M: Adult hippocampal neurogenesis is abundant in neurologically healthy subjects and drops sharply in patients with Alzheimer's disease. *Nat Med* 2019, 25:554–560.
129. Esteves M, Serra-Almeida C, Saraiva C, Bernardino L: New insights into the regulatory roles of microRNAs in adult neurogenesis. *Curr Opin Pharmacol* 2020, 50:38–45.
130. Winner B, Winkler J: Adult Neurogenesis in Neurodegenerative Diseases. *Cold Spring Harb Perspect Biol* 2015, 7:a021287.
131. Höglinger GU, Rizk P, Muriel MP, Duyckaerts C, Oertel WH, Caille I, Hirsch EC: Dopamine depletion impairs precursor cell proliferation in Parkinson disease. *Nat Neurosci 2004 77* 2004, 7:726–735.
132. Nuber S, Petrasch-Parwez E, Winner B, Winkler J, Von Hörsten S, Schmidt T, Boy J, Kuhn M, Nguyen HP, Teismann P, et al.: Neurobiology of Disease Neurodegeneration and Motor Dysfunction in a Conditional Model of Parkinson's Disease. 2008, doi:10.1523/JNEUROSCI.3040-07.2008.
133. Marxreiter F, Regensburger M, Winkler J: Adult neurogenesis in Parkinson's disease. *Cell Mol Life Sci* 2013, 70:459–473.
134. Diaz J, Ridray S, Mignon V, Griffon N, Schwartz JC, Sokoloff P: Selective Expression of Dopamine D3 Receptor mRNA in Proliferative Zones during Embryonic Development of the Rat Brain. *J Neurosci* 1997, 17:4282.
135. Borta A, Höglinger GU: Dopamine and adult neurogenesis. *J Neurochem* 2007,

100:587–595.

136. Baker SA, Baker KA, Hagg T: Dopaminergic nigrostriatal projections regulate neural precursor proliferation in the adult mouse subventricular zone. *Eur J Neurosci* 2004, 20:575–579.

137. Freundlieb N, François C, Tandé D, Oertel WH, Hirsch EC, Höglinger GU: Dopaminergic Substantia Nigra Neurons Project Topographically Organized to the Subventricular Zone and Stimulate Precursor Cell Proliferation in Aged Primates. *J Neurosci* 2006, 26:2321.

138. O'Keeffe GC, Tyers P, Aarsland D, Dalley JW, Barker RA, Caldwellf MA: Dopamine-induced proliferation of adult neural precursor cells in the mammalian subventricular zone is mediated through EGF. *Proc Natl Acad Sci U S A* 2009, 106:8754–8759.

139. Iwakura Y, Piao YS, Mizuno M, Takei N, Kakita A, Takahashi H, Nawa H: Influences of dopaminergic lesion on epidermal growth factor-ErbB signals in Parkinson's disease and its model: neurotrophic implication in nigrostriatal neurons. *J Neurochem* 2005, 93:974–983.

140. Baker SA, Baker KA, Hagg T: D3 dopamine receptors do not regulate neurogenesis in the subventricular zone of adult mice. *Neurobiol Dis* 2005, 18:523–527.

141. Kim Y, Wang WZ, Comte I, Pastrana E, Tran PB, Brown J, Miller RJ, Doetsch F, Molnár Z, Szele FG: Dopamine stimulation of postnatal murine subventricular zone neurogenesis via the D3 receptor. *J Neurochem* 2010, 114:750–760.

142. Garcia-Garrote M, Parga JA, Labandeira PJ, Labandeira-Garcia JL, Rodriguez-Pallares J: Dopamine Regulates Adult Neurogenesis in the Ventricular-Subventricular Zone via Dopamine D3 Angiotensin Type 2 Receptor Interactions. *Stem Cells* 2021, 39:1778–1794.

143. Van Den Berge SA, Van Strien ME, Korecka JA, Dijkstra AA, Sluijs JA, Kooijman L, Eggers R, De Filippis L, Vescovi AL, Verhaagen J, et al.: The proliferative capacity of the subventricular zone is maintained in the parkinsonian brain. *Brain* 2011, 134:3249–3263.

144. Winner B, Lie DC, Rockenstein E, Aigner R, Aigner L, Masliah E, Kuhn HG, Winkler J: Human wild-type alpha-synuclein impairs neurogenesis. *J Neuropathol Exp Neurol* 2004, 63:1155–1166.

145. Winner B, Rockenstein E, Lie DC, Aigner R, Mante M, Bogdahn U, Couillard-Despres S, Masliah E, Winkler J: Mutant alpha-synuclein exacerbates age-related decrease of neurogenesis. *Neurobiol Aging* 2008, 29:913–925.

146. Crews L, Mizuno H, Desplats P, Rockenstein E, Adame A, Patrick C, Winner B, Winkler J, Masliah E: α-Synuclein Alters Notch-1 Expression and Neurogenesis

in Mouse Embryonic Stem Cells and in the Hippocampus of Transgenic Mice. *J Neurosci* 2008, 28:4250.

147. Desplats P, Spencer B, Crews L, Pathel P, Morvinski-Friedmann D, Kosberg K, Roberts S, Patrick C, Winner B, Winkler J, et al.: α-Synuclein Induces Alterations in Adult Neurogenesis in Parkinson Disease Models via p53-mediated Repression of Notch1. *J Biol Chem* 2012, 287:31691.
148. Van Den Berge SA, Van Strien ME, Hol EM: Resident adult neural stem cells in Parkinson's disease - The brain's own repair system? *Eur J Pharmacol* 2013, 719:117–127.
149. Coronas V, Bantubungi K, Fombonne J, Krantic S, Schiffmann SN, Roger M: Dopamine D3 receptor stimulation promotes the proliferation of cells derived from the post-natal subventricular zone. *J Neurochem* 2004, 91:1292–1301.
150. Kippin TE, Kapur S, Van Der Kooy D: Dopamine Specifically Inhibits Forebrain Neural Stem Cell Proliferation, Suggesting a Novel Effect of Antipsychotic Drugs. *J Neurosci* 2005, 25:5815–5823.
151. Aponso PM, Faull RLM, Connor B: Increased progenitor cell proliferation and astrogenesis in the partial progressive 6-hydroxydopamine model of Parkinson's disease. *Neuroscience* 2008, 151:1142–1153.
152. Liu B fang, Gao E jing, Zeng X zhi, Ji M, Cai Q, Lu Q, Yang H, Xu Q yuan: Proliferation of neural precursors in the subventricular zone after chemical lesions of the nigrostriatal pathway in rat brain. *Brain Res* 2006, 1106:30–39.
153. Arias-Carrión O, Hernández-López S, Ibañez-Sandoval O, Bargas J, Hernández-Cruz A, Drucker-Colín R: Neuronal precursors within the adult rat subventricular zone differentiate into dopaminergic neurons after substantia nigra lesion and chromaffin cell transplant. *J Neurosci Res* 2006, 84:1425–1437.
154. Winner B, Geyer M, Couillard-Despres S, Aigner R, Bogdahn U, Aigner L, Kuhn G, Winkler J: Striatal deafferentation increases dopaminergic neurogenesis in the adult olfactory bulb. *Exp Neurol* 2006, 197:113–121.
155. Sui Y, Horne MK, Stanić D: Reduced Proliferation in the Adult Mouse Subventricular Zone Increases Survival of Olfactory Bulb Interneurons. *PLoS One* 2012, 7:e31549.
156. Fricke IB, Viel T, Worlitzer MM, Collmann FM, Vrachimis A, Faust A, Wachsmuth L, Faber C, Dollé F, Kuhlmann MT, et al.: 6-hydroxydopamine-induced Parkinson's disease-like degeneration generates acute microgliosis and astrogliosis in the nigrostriatal system but no bioluminescence imaging-detectable alteration in adult neurogenesis. *Eur J Neurosci* 2016, 43:1352–1365.
157. Sun P, Liu DZ, Jickling GC, Sharp FR, Yin KJ: MicroRNA-based therapeutics in

central nervous system injuries. *J Cereb Blood Flow Metab* 2018, 38:1125.

158. Saraiva C, Paiva J, Santos T, Ferreira L, Bernardino L: MicroRNA-124 loaded nanoparticles enhance brain repair in Parkinson's disease. *J Control Release* 2016, 235:291–305.
159. Carninci P: Molecular biology: The long and short of RNAs. *Nature* 2009, 457:974–975.
160. Carninci P, Kasukawa T, Katayama S, Gough J, Frith MC, Maeda N, Oyama R, Ravasi T, Lenhard B, Wells C, et al.: The Transcriptional Landscape of the Mammalian Genome. *Science (80-)* 2005, 309:1559–1563.
161. Okazaki Y, Furuno M, Kasukawa T, Adachi J, Bono H, Kondo S, Nikaido I, Osato N, Saito R, Suzuki H, et al.: Analysis of the mouse transcriptome based on functional annotation of 60,770 full-length cDNAs. *Nature* 2002, 420:563–573.
162. Rodriguez A, Griffiths-Jones S, Ashurst JL, Bradley A: Identification of mammalian microRNA host genes and transcription units. *Genome Res* 2004, 14:1902–10.
163. Godnic I, Zorc M, Jevsinek Skok D, Calin GA, Horvat S, Dovc P, Kovac M, Kunej T: Genome-wide and species-wide in silico screening for intragenic MicroRNAs in human, mouse and chicken. *PLoS One* 2013, 8:e65165.
164. Monteys AM, Spengler RM, Wan J, Tecedor L, Lennox KA, Xing Y, Davidson BL: Structure and activity of putative intronic miRNA promoters. *RNA* 2010, 16:495–505.
165. Ramalingam P, Palanichamy JK, Singh A, Das P, Bhagat M, Kassab MA, Sinha S, Chattopadhyay P: Biogenesis of intronic miRNAs located in clusters by independent transcription and alternative splicing. *RNA* 2014, 20:76–87.
166. Lee Y, Kim M, Han J, Yeom K-H, Lee S, Baek SH, Kim VN: MicroRNA genes are transcribed by RNA polymerase II. *EMBO J* 2004, 23:4051–60.
167. Cai X, Hagedorn CH, Cullen BR: Human microRNAs are processed from capped, polyadenylated transcripts that can also function as mRNAs. *RNA* 2004, 10:1957–66.
168. Hertel J, Lindemeyer M, Missal K, Fried C, Tanzer A, Flamm C, Hofacker IL, Stadler PF, Students of Bioinformatics Computer Labs 2004 and 2005 TS of BCL 2004 and: The expansion of the metazoan microRNA repertoire. *BMC Genomics* 2006, 7:25.
169. Altuvia Y, Landgraf P, Lithwick G, Elefant N, Pfeffer S, Aravin A, Brownstein MJ, Tuschl T, Margalit H: Clustering and conservation patterns of human microRNAs. *Nucleic Acids Res* 2005, 33:2697–706.
170. Zeng Y, Cullen BR: Efficient Processing of Primary microRNA Hairpins by Drosha

Requires Flanking Nonstructured RNA Sequences. *J Biol Chem* 2005, 280:27595–27603.

171. Lee Y, Ahn C, Han J, Choi H, Kim J, Yim J, Lee J, Provost P, Rådmark O, Kim S, et al.: The nuclear RNase III Drosha initiates microRNA processing. *Nature* 2003, 425:415–419.
172. Lund E: Nuclear Export of MicroRNA Precursors. *Science (80-)* 2004, 303:95–98.
173. Yi R, Qin Y, Macara IG, Cullen BR: Exportin-5 mediates the nuclear export of pre-microRNAs and short hairpin RNAs. *Genes Dev* 2003, 17:3011–6.
174. MacRae IJ, Zhou K, Doudna JA: Structural determinants of RNA recognition and cleavage by Dicer. *Nat Struct Mol Biol* 2007, 14:934–940.
175. Lee Y, Hur I, Park S-Y, Kim Y-K, Suh MR, Kim VN: The role of PACT in the RNA silencing pathway. *EMBO J* 2006, 25:522–32.
176. Wilson RC, Tambe A, Kidwell MA, Noland CL, Schneider CP, Doudna JA: Dicer-TRBP Complex Formation Ensures Accurate Mammalian MicroRNA Biogenesis. *Mol Cell* 2015, 57:397–407.
177. Chendrimada TP, Gregory RI, Kumaraswamy E, Norman J, Cooch N, Nishikura K, Shiekhattar R: TRBP recruits the Dicer complex to Ago2 for microRNA processing and gene silencing. *Nature* 2005, 436:740–744.
178. Kim Y, Yeo J, Lee JH, Cho J, Seo D, Kim J-S, Kim VN: Deletion of Human tarbp2 Reveals Cellular MicroRNA Targets and Cell-Cycle Function of TRBP. *Cell Rep* 2014, 9:1061–1074.
179. Iwasaki S, Kobayashi M, Yoda M, Sakaguchi Y, Katsuma S, Suzuki T, Tomari Y: *Hsc70/Hsp90 Chaperone Machinery Mediates ATP-Dependent RISC Loading of Small RNA Duplexes*. 2010.
180. Meijer HA, Smith EM, Bushell M: Regulation of miRNA strand selection: follow the leader? *Biochem Soc Trans* 2014, 42:1135–1140.
181. Kwak PB, Tomari Y: The N domain of Argonaute drives duplex unwinding during RISC assembly. *Nat Struct Mol Biol* 2012, 19:145–151.
182. Noland CL, Doudna JA: Multiple sensors ensure guide strand selection in human RNAi pathways. *RNA* 2013, 19:639–48.
183. Valdmanis PN, Gu S, Schuermann N, Sethupathy P, Grimm D, Kay MA: Expression determinants of mammalian argonaute proteins in mediating gene silencing. *Nucleic Acids Res* 2012, 40:3704–3713.
184. González-González E, López-Casas PP, del Mazo J: The expression patterns of genes involved in the RNAi pathways are tissue-dependent and differ in the germ and somatic cells of mouse testis. *Biochim Biophys Acta - Gene Regul Mech* 2008,

1779:306–311.
185. Wang D, Zhang Z, O'Loughlin E, Lee T, Houel S, O'Carroll D, Tarakhovsky A, Ahn NG, Yi R: Quantitative functions of Argonaute proteins in mammalian development. *Genes Dev* 2012, 26:693–704.
186. Abdelfattah AM, Park C, Choi MY: Update on non-canonical microRNAs. *Biomol Concepts* 2014, 5:275–87.
187. Daugaard I, Hansen TB: Biogenesis and Function of Ago-Associated RNAs. *Trends Genet* 2017, doi:10.1016/j.tig.2017.01.003.
188. Friedman RC, Farh KK-H, Burge CB, Bartel DP: Most mammalian mRNAs are conserved targets of microRNAs. *Genome Res* 2009, 19:92–105.
189. Bartel DP: MicroRNAs: Target Recognition and Regulatory Functions. *Cell* 2009, 136:215–233.
190. Wang X: Composition of seed sequence is a major determinant of microRNA targeting patterns. *Bioinformatics* 2014, 30:1377–1383.
191. Karginov F V, Cheloufi S, Chong MMW, Stark A, Smith AD, Hannon GJ: Diverse endonucleolytic cleavage sites in the mammalian transcriptome depend upon microRNAs, Drosha, and additional nucleases. *Mol Cell* 2010, 38:781–8.
192. Yekta S, Shih I-H, Bartel DP: MicroRNA-directed cleavage of HOXB8 mRNA. *Science* 2004, 304:594–6.
193. Bartel DP: MicroRNAs: genomics, biogenesis, mechanism, and function. *Cell* 2004, 116:281–297.
194. Eichhorn SW, Guo H, McGeary SE, Rodriguez-Mias RA, Shin C, Baek D, Hsu S, Ghoshal K, Villén J, Bartel DP: mRNA Destabilization Is the Dominant Effect of Mammalian MicroRNAs by the Time Substantial Repression Ensues. *Mol Cell* 2014, 56:104–115.
195. Huntzinger E, Izaurralde E: Gene silencing by microRNAs: contributions of translational repression and mRNA decay. *Nat Rev Genet* 2011, 12:99–110.
196. Béthune J, Artus-Revel CG, Filipowicz W: Kinetic analysis reveals successive steps leading to miRNA-mediated silencing in mammalian cells. *EMBO Rep* 2012, 13:716–23.
197. Djuranovic S, Nahvi A, Green R: miRNA-Mediated Gene Silencing by Translational Repression Followed by mRNA Deadenylation and Decay. *Science (80-)* 2012, 336:237–240.
198. Larsson O, Nadon R: Re-analysis of genome wide data on mammalian microRNA-mediated suppression of gene expression. *Transl (Austin, Tex)* 2013, 1:e24557.
199. Meijer HA, Kong YW, Lu WT, Wilczynska A, Spriggs R V, Robinson SW, Godfrey JD, Willis AE, Bushell M: Translational repression and eIF4A2 activity are critical

for microRNA-mediated gene regulation. *Science* 2013, 340:82–5.

200. Corcoran DL, Pandit K V., Gordon B, Bhattacharjee A, Kaminski N, Benos P V.: Features of Mammalian microRNA Promoters Emerge from Polymerase II Chromatin Immunoprecipitation Data. *PLoS One* 2009, 4:e5279.
201. Ozsolak F, Poling LL, Wang Z, Liu H, Liu XS, Roeder RG, Zhang X, Song JS, Fisher DE: Chromatin structure analyses identify miRNA promoters. *Genes Dev* 2008, 22:3172–3183.
202. Krol J, Loedige I, Filipowicz W: The widespread regulation of microRNA biogenesis, function and decay. *Nat Rev Genet* 2010, 11:597–610.
203. Martinez NJ, Ow MC, Reece-Hoyes JS, Barrasa MI, Ambros VR, Walhout AJM: Genome-scale spatiotemporal analysis of Caenorhabditis elegans microRNA promoter activity. *Genome Res* 2008, 18:2005–15.
204. Johnson SM, Lin SY, Slack FJ: The time of appearance of the C. elegans let-7 microRNA is transcriptionally controlled utilizing a temporal regulatory element in its promoter. *Dev Biol* 2003, 259:364–79.
205. Rupaimoole R, Wu SY, Pradeep S, Ivan C, Pecot C V., Gharpure KM, Nagaraja AS, Armaiz-Pena GN, McGuire M, Zand B, et al.: Hypoxia-mediated downregulation of miRNA biogenesis promotes tumour progression. *Nat Commun* 2014, 5:5202.
206. Gregory RI, Yan K, Amuthan G, Chendrimada T, Doratotaj B, Cooch N, Shiekhattar R: The Microprocessor complex mediates the genesis of microRNAs. *Nature* 2004, 432:235–240.
207. Han J, Pedersen JS, Kwon SC, Belair CD, Kim Y-K, Yeom K-H, Yang W-Y, Haussler D, Blelloch R, Kim VN: Posttranscriptional Crossregulation between Drosha and DGCR8. *Cell* 2009, 136:75–84.
208. Triboulet R, Chang H-M, LaPierre RJ, Gregory RI: Post-transcriptional control of DGCR8 expression by the Microprocessor. *RNA* 2009, 15:1005–1011.
209. Newman MA, Hammond SM: Emerging paradigms of regulated microRNA processing. *Genes Dev* 2010, 24:1086–1092.
210. Hammond SM, Boettcher S, Caudy AA, Kobayashi R, Hannon GJ: Argonaute2, a Link Between Genetic and Biochemical Analyses of RNAi. *Science (80-)* 2001, 293:1146–1150.
211. Gulyaeva LF, Kushlinskiy NE: Regulatory mechanisms of microRNA expression. *J Transl Med* 2016, 14:143.
212. Lagos-Quintana M, Rauhut R, Yalcin A, Meyer J, Lendeckel W, Tuschl T: Identification of Tissue-Specific MicroRNAs from Mouse. *Curr Biol* 2002, 12:735–739.
213. Baroukh NN, Van Obberghen E: Function of microRNA-375 and microRNA-124a

in pancreas and brain. *FEBS J* 2009, 276:6509–21.

214. Mishima T, Mizuguchi Y, Kawahigashi Y, Takizawa T, Takizawa T: RT-PCR-based analysis of microRNA (miR-1 and -124) expression in mouse CNS. *Brain Res* 2007, 1131:37–43.
215. Ziats MN, Rennert OM: Identification of differentially expressed microRNAs across the developing human brain. *Mol Psychiatry* 2014, 19:848–52.
216. Chen W, Qin C: General hallmarks of microRNAs in brain evolution and development. *RNA Biol* 2015, 12:701–8.
217. Giraldez AJ, Cinalli RM, Glasner ME, Enright AJ, Thomson JM, Baskerville S, Hammond SM, Bartel DP, Schier AF: MicroRNAs Regulate Brain Morphogenesis in Zebrafish. *Science (80-)* 2005, 308:833–838.
218. Andersson T, Rahman S, Sansom SN, Alsiö JM, Kaneda M, Smith J, O'Carroll D, Tarakhovsky A, Livesey FJ: Reversible block of mouse neural stem cell differentiation in the absence of dicer and microRNAs. *PLoS One* 2010, 5:e13453.
219. Coolen M, Katz S, Bally-Cuif L: miR-9: a versatile regulator of neurogenesis. *Front Cell Neurosci* 2013, 7:220.
220. Åkerblom M, Jakobsson J: MicroRNAs as Neuronal Fate Determinants. *Neurosci* 2014, 20:235–242.
221. Cheng L-C, Pastrana E, Tavazoie M, Doetsch F: miR-124 regulates adult neurogenesis in the subventricular zone stem cell niche. *Nat Neurosci* 2009, 12:399–408.
222. Liu XS, Chopp M, Zhang RL, Tao T, Wang XL, Kassis H, Hozeska-Solgot A, Zhang L, Chen C, Zhang ZG: MicroRNA profiling in subventricular zone after stroke: MiR-124a regulates proliferation of neural progenitor cells through notch signaling pathway. *PLoS One* 2011, 6:1–11.
223. Akerblom M, Sachdeva R, Barde I, Verp S, Gentner B, Trono D, Jakobsson J: MicroRNA-124 Is a Subventricular Zone Neuronal Fate Determinant. *J Neurosci* 2012, 32:8879–8889.
224. Neo WH, Yap K, Lee SH, Looi LS, Khandelia P, Neo SX, Makeyev E V., Su IH: MicroRNA miR-124 controls the choice between neuronal and astrocyte differentiation by fine-tuning Ezh2 expression. *J Biol Chem* 2014, 289:20788–20801.
225. Krichevsky AM, Sonntag K-C, Isacson O, Kosik KS: Specific microRNAs modulate embryonic stem cell-derived neurogenesis. *Stem Cells* 2006, 24:857–64.
226. Sanuki R, Onishi A, Koike C, Muramatsu R, Watanabe S, Muranishi Y, Irie S, Uneo S, Koyasu T, Matsui R, et al.: miR-124a is required for hippocampal axogenesis and retinal cone survival through Lhx2 suppression. *Nat Neurosci* 2011, 14:1125–

34.
227. Gu X, Meng S, Liu S, Jia C, Fang Y, Li S, Fu C, Song Q, Lin L, Wang X: MiR-124 Represses ROCK1 Expression to Promote Neurite Elongation Through Activation of the PI3K/Akt Signal Pathway. *J Mol Neurosci* 2014, 52:156–165.
228. Yu J-Y, Chung K-H, Deo M, Thompson RC, Turner DL: MicroRNA miR-124 regulates neurite outgrowth during neuronal differentiation. *Exp Cell Res* 2008, 314:2618–2633.
229. Franke K, Otto W, Johannes S, Baumgart J, Nitsch R, Schumacher S: miR-124-regulated RhoG reduces neuronal process complexity via ELMO/Dock180/Rac1 and Cdc42 signalling. *EMBO J* 2012, 31:2908–2921.
230. Hou Q, Ruan H, Gilbert J, Wang G, Ma Q, Yao W-D, Man H-Y: MicroRNA miR124 is required for the expression of homeostatic synaptic plasticity. *Nat Commun* 2015, 6:10045.
231. Sonntag K-C: MicroRNAs and deregulated gene expression networks in neurodegeneration. *Brain Res* 2010, 1338:48–57.
232. Geng L, Liu W, Chen Y: miR-124-3p attenuates MPP+-induced neuronal injury by targeting STAT3 in SH-SY5Y cells. *Exp Biol Med* 2017, 242:1757–1764.
233. Gong X, Wang H, Ye Y, Shu Y, Deng Y, He X, Lu G, Zhang S: miR-124 regulates cell apoptosis and autophagy in dopaminergic neurons and protects them by regulating AMPK/mTOR pathway in Parkinson's disease. *Am J Transl Res* 2016, 8:2127–37.
234. Wang H, Ye Y, Zhu Z, Mo L, Lin C, Wang Q, Wang H, Gong X, He X, Lu G, et al.: MiR-124 Regulates Apoptosis and Autophagy Process in MPTP Model of Parkinson's Disease by Targeting to Bim. *Brain Pathol* 2015, doi:10.1111/bpa.12267.
235. Dong RF, Zhang B, Tai LW, Liu HM, Shi FK, Liu NN: The Neuroprotective Role of MiR-124-3p in a 6-Hydroxydopamine-Induced Cell Model of Parkinson's Disease via the Regulation of ANAX5. *J Cell Biochem* 2018, 119:269–277.
236. Angelopoulou E, Paudel YN, Piperi C: miR-124 and Parkinson's disease: A biomarker with therapeutic potential. *Pharmacol Res* 2019, 150.
237. Zhang F, Yao Y, Miao N, Wang N, Xu X, Yang C: Neuroprotective effects of microRNA 124 in Parkinson's disease mice. *Arch Gerontol Geriatr* 2022, 99:104588.
238. Pereira P, Queiroz JA, Figueiras A, Sousa F: Current progress on microRNAs-based therapeutics in neurodegenerative diseases. *Wiley Interdiscip Rev RNA* 2017, 8:e1409.
239. Kreuter J: Influence of the Surface Properties on Nanoparticle-Mediated

Transport of Drugs to the Brain. *J Nanosci Nanotechnol* 2004, 4:484–488.

240. Gan L, Li Z, Lv Q, Huang W: Rabies virus glycoprotein (RVG29)-linked microRNA-124-loaded polymeric nanoparticles inhibit neuroinflammation in a Parkinson's disease model. *Int J Pharm* 2019, 567:118449.
241. Kumar P, Wu H, McBride JL, Jung KE, Hee Kim M, Davidson BL, Kyung Lee S, Shankar P, Manjunath N: Transvascular delivery of small interfering RNA to the central nervous system. *Nature* 2007, 448:39–43.
242. Raposo G, Stoorvogel W: Extracellular vesicles: Exosomes, microvesicles, and friends. *J Cell Biol* 2013, 200:373–383.
243. Johnstone RM, Adam M, Hammond JR, Orr L, Turbide C: Vesicle formation during reticulocyte maturation. Association of plasma membrane activities with released vesicles (exosomes). *J Biol Chem* 1987, 262:9412–9420.
244. Valadi H, Ekström K, Bossios A, Sjöstrand M, Lee JJ, Lötvall JO: Exosome-mediated transfer of mRNAs and microRNAs is a novel mechanism of genetic exchange between cells. *Nat Cell Biol* 2007, 9:654–659.
245. Van Niel G, D'Angelo G, Raposo G: Shedding light on the cell biology of extracellular vesicles. *Nat Rev Mol Cell Biol 2018 194* 2018, 19:213–228.
246. Men Y, Yelick J, Jin S, Tian Y, Chiang MSR, Higashimori H, Brown E, Jarvis R, Yang Y: Exosome reporter mice reveal the involvement of exosomes in mediating neuron to astroglia communication in the CNS. *Nat Commun* 2019, 10.
247. Nolte-'t Hoen ENM, Buschow SI, Anderton SM, Stoorvogel W, Wauben MHM: Activated T cells recruit exosomes secreted by dendritic cells via LFA-1. *Blood* 2009, 113:1977–1981.
248. Losurdo M, Grilli M: Extracellular Vesicles, Influential Players of Intercellular Communication within Adult Neurogenic Niches. *Int J Mol Sci* 2020, 21:1–28.
249. Howitt J, Hill AF: Exosomes in the Pathology of Neurodegenerative Diseases. *J Biol Chem* 2016, 291:26589–26597.
250. Osaki M, Okada F: Exosomes and Their Role in Cancer Progression. *Yonago Acta Med* 2019, 62:182–190.
251. Ouerdane Y, Hassaballah MY, Nagah A, Ibrahim TM, Mohamed HAH, El-Baz A, Attia MS: Exosomes in Parkinson: Revisiting Their Pathologic Role and Potential Applications. *Pharmaceuticals* 2022, 15.
252. Gurung S, Perocheau D, Touramanidou L, Baruteau J: The exosome journey: from biogenesis to uptake and intracellular signalling. *Cell Commun Signal 2021 191* 2021, 19:1–19.
253. EL Andaloussi S, Mäger I, Breakefield XO, Wood MJA: Extracellular vesicles: biology and emerging therapeutic opportunities. *Nat Rev Drug Discov* 2013,

12:347–57.

254. Xia X, Wang Y, Huang Y, Zhang H, Lu H, Zheng JC: Exosomal miRNAs in central nervous system diseases: biomarkers, pathological mediators, protective factors and therapeutic agents. *Prog Neurobiol* 2019, 183.
255. Haney MJ, Klyachko NL, Zhao Y, Gupta R, Plotnikova EG, He Z, Patel T, Piroyan A, Sokolsky M, Kabanov A V., et al.: Exosomes as drug delivery vehicles for Parkinson's disease therapy. *J Control Release* 2015, 207:18–30.
256. Alvarez-Erviti L, Seow Y, Yin H, Betts C, Lakhal S, Wood MJA: Delivery of siRNA to the mouse brain by systemic injection of targeted exosomes. *Nat Biotechnol 2011 294* 2011, 29:341–345.
257. Colombo M, Raposo G, Théry C: Biogenesis, secretion, and intercellular interactions of exosomes and other extracellular vesicles. *Annu Rev Cell Dev Biol* 2014, 30:255–289.
258. Pant S, Hilton H, Burczynski ME: The multifaceted exosome: biogenesis, role in normal and aberrant cellular function, and frontiers for pharmacological and biomarker opportunities. *Biochem Pharmacol* 2012, 83:1484–1494.
259. Yuan L, Li JY: Exosomes in parkinson's disease: Current perspectives and future challenges. *ACS Chem Neurosci* 2019, 10:964–972.
260. Schmidt O, Teis D: The ESCRT machinery. *Curr Biol* 2012, 22.
261. Trajkovic K, Hsu C, Chiantia S, Rajendran L, Wenzel D, Wieland F, Schwille P, Brügger B, Simons M: Ceramide triggers budding of exosome vesicles into multivesicular endosomes. *Science (80-)* 2008, 319:1244–1247.
262. Bobrie A, Colombo M, Raposo G, Théry C: Exosome Secretion: Molecular Mechanisms and Roles in Immune Responses. *Traffic* 2011, 12:1659–1668.
263. Ostrowski M, Carmo NB, Krumeich S, Fanget I, Raposo G, Savina A, Moita CF, Schauer K, Hume AN, Freitas RP, et al.: Rab27a and Rab27b control different steps of the exosome secretion pathway. *Nat Cell Biol* 2010, 12:19–30.
264. Théry C, Zitvogel L, Amigorena S: Exosomes: composition, biogenesis and function. *Nat Rev Immunol 2002 28* 2002, 2:569–579.
265. Zhang Y, Liu Y, Liu H, Tang WH: Exosomes: biogenesis, biologic function and clinical potential. *Cell Biosci* 2019, 9.
266. Henriques-Antunes H, Cardoso RMS, Zonari A, Correia J, Leal EC, Jiménez-Balsa A, Lino MM, Barradas A, Kostic I, Gomes C, et al.: The Kinetics of Small Extracellular Vesicle Delivery Impacts Skin Tissue Regeneration. *ACS Nano* 2019, 13:8694–8707.
267. Steel HC, Alessandrini M, Mellet J, Dessels C, Oloyo AK, Pepper MS: Cord Blood Stem Cell Banking. In *Stem Cell Processing. Stem Cells in Clinical Applications*.

Edited by Van Pham P. Springer; 2016:163–180.

268. de Abreu RC, Ramos C V., Becher C, Lino M, Jesus C, da Costa Martins PA, Martins PAT, Moreno MJ, Fernandes H, Ferreira L: Exogenous loading of miRNAs into small extracellular vesicles. *J Extracell Vesicles* 2021, 10:e12111.
269. Brown JA, Boussiotis VA: Umbilical cord blood transplantation: basic biology and clinical challenges to immune reconstitution. *Clin Immunol* 2008, 127:286–297.
270. Verneris MR, Miller JS: The Phenotypic and Functional Characteristics of Umbilical Cord Blood and Peripheral Blood Natural Killer Cells. *Br J Haematol* 2009, 147:185.
271. Abo-Grisha N, Essawy S, Abo-Elmatty DM, Abdel-Hady Z: Effects of intravenous human umbilical cord blood CD34+ stem cell therapy versus levodopa in experimentally induced Parkinsonism in mice. *Arch Med Sci* 2013, 9:1138.
272. Ankersmit HJ, Altmann P, Mildner M, Haider T, Traxler D, Beer L, Ristl R, Golabi B, Gabriel C, Leutmezer F: Secretomes of apoptotic mononuclear cells ameliorate neurological damage in rats with focal ischemia. *F1000Research* 2014, 3.
273. Yoo J, Kim HS, Seo JJ, Eom JH, Choi SM, Park S, Kim DW, Hwang DY: Therapeutic effects of umbilical cord blood plasma in a rat model of acute ischemic stroke. *Oncotarget* 2016, 7:79131–79140.
274. Jarmalavičiūtė A, Tunaitis V, Pivoraitė U, Venalis A, Pivoriūnas A: Exosomes from dental pulp stem cells rescue human dopaminergic neurons from 6-hydroxy-dopamine–induced apoptosis. *Cytotherapy* 2015, 17:932–939.
275. Chen H, Liang F, Gu P, Xu B, Xu H, Wang W, Hou J: Exosomes derived from mesenchymal stem cells repair a Parkinson ' s disease model by inducing autophagy. *Cell Death Dis* 2020, 11.
276. Li Y, Li Z, Gu J, Xu X, Chen H, Gui Y: Exosomes isolated during dopaminergic neuron differentiation suppressed neuronal inflammation in a rodent model of Parkinson's disease. *Neurosci Lett* 2022, 771:136414.
277. Isola A, Chen S: Exosomes: The Messengers of Health and Disease. *Curr Neuropharmacol* 2017, 15:157–165.
278. Ciregia F, Urbani A, Palmisano G: Extracellular Vesicles in Brain Tumors and Neurodegenerative Diseases. *Front Mol Neurosci* 2017, 10.
279. Desplats P, Lee HJ, Bae EJ, Patrick C, Rockenstein E, Crews L, Spencer B, Masliah E, Lee SJ: Inclusion formation and neuronal cell death through neuron-to-neuron transmission of alpha-synuclein. *Proc Natl Acad Sci U S A* 2009, 106:13010–13015.
280. Hansen C, Angot E, Bergström AL, Steiner JA, Pieri L, Paul G, Outeiro TF, Melki R, Kallunki P, Fog K, et al.: α-Synuclein propagates from mouse brain to grafted

dopaminergic neurons and seeds aggregation in cultured human cells. *J Clin Invest* 2011, 121:715–725.

281. Guo M, Wang J, Zhao Y, Feng Y, Han S, Dong Q, Cui M, Tieu K: Microglial exosomes facilitate α-synuclein transmission in Parkinson's disease. *Brain* 2020, 143:1476–1497.
282. Perets N, Betzer O, Shapira R, Brenstein S, Angel A, Sadan T, Ashery U, Popovtzer R, Offen D: Golden Exosomes Selectively Target Brain Pathologies in Neurodegenerative and Neurodevelopmental Disorders. *Nano Lett* 2019, 19:3422–3431.
283. Betzer O, Perets N, Angel A, Motiei M, Sadan T, Yadid G, Offen D, Popovtzer R: In Vivo Neuroimaging of Exosomes Using Gold Nanoparticles. *ACS Nano* 2017, 11:10883–10893.
284. Arends F, Lieleg O: Biophysical Properties of the Basal Lamina: A Highly Selective Extracellular Matrix. In *Composition and Function of the Extracellular Matrix in the Human Body*. Edited by Francesco Travascio. InTechOpen; 2016.
285. Conlan RS, Pisano S, Oliveira MI, Ferrari M, Mendes Pinto I: Exosomes as Reconfigurable Therapeutic Systems. *Trends Mol Med* 2017, 23:636–650.
286. Qu M, Lin Q, Huang L, Fu Y, Wang L, He S, Fu Y, Yang S, Zhang Z, Zhang L, et al.: Dopamine-loaded blood exosomes targeted to brain for better treatment of Parkinson's disease. *J Control Release* 2018, 287:156–166.
287. Xin H, Li Y, Cui Y, Yang JJ, Zhang ZG, Chopp M: Systemic administration of exosomes released from mesenchymal stromal cells promote functional recovery and neurovascular plasticity after stroke in rats. *J Cereb Blood Flow Metab* 2013, 33:1711–5.
288. Luarte A, Bátiz LF, Wyneken U, Lafourcade C: Potential Therapies by Stem Cell-Derived Exosomes in CNS Diseases: Focusing on the Neurogenic Niche. *Stem Cells Int* 2016, 2016:1–16.
289. Ha D, Yang N, Nadithe V: Exosomes as therapeutic drug carriers and delivery vehicles across biological membranes: current perspectives and future challenges. *Acta Pharm Sin B* 2016, 6:287–296.
290. Lentz TL, Burrage TG, Smith AL, Crick J, Tignor GH: Is the Acetylcholine Receptor a Rabies Virus Receptor? *Science (80-)* 1982, 215:182–184.
291. Son S, Hwang DW, Singha K, Jeong JH, Park TG, Lee DS, Kim WJ: RVG peptide tethered bioreducible polyethylenimine for gene delivery to brain. *J Control Release* 2011, 155:18–25.
292. Cooper JM, Wiklander PBO, Nordin JZ, Al-Shawi R, Wood MJ, Vithlani M, Schapira AH V., Simons JP, El-Andaloussi S, Alvarez-Erviti L: Systemic exosomal

siRNA delivery reduced alpha-synuclein aggregates in brains of transgenic mice. *Mov Disord* 2014, 29:1476–1485.

293. Izco M, Blesa J, Schleef M, Schmeer M, Porcari R, Al-Shawi R, Ellmerich S, De Toro M, Gardiner C, Seow Y, et al.: Systemic Exosomal Delivery of shRNA Minicircles Prevents Parkinsonian Pathology. *Mol Ther* 2019, 27:2111–2122.

Chapter 2

Global Aims

2.1 Global aims

PD is the second most prevalent neurodegenerative disorder worldwide and the most common movement disorder with substantial health and socioeconomic impact on modern society. Due to the current lack of effective PD treatments, the development of novel therapies is timely. MiRNA, small non-coding RNAs that post-transcriptionally regulate gene expression, are promising candidates for PD therapy. miR-124 is particularly promising, as it is downregulated in the SN of PD models and in plasma of PD patients, and conversely, enhancing its expression boosts neuroprotection and neurogenesis. However, the effect of miR-124 in the modulation of α-synuclein accumulation and aggregation, the pathological hallmarks of the disease, has not yet been reported.

Thus, one of the main objectives of this thesis was:

1) Evaluate the effects of miR-124-3p on α-synuclein accumulation and aggregation, and dopaminergic neuroprotection in a rat model of PD.

The development of efficient miRNA-based therapies faces several challenges such as the hydrophilicity and negative charge of miRNA, which limit its delivery into tissues, particularly to the brain. Intracellular delivery of miRNA can be improved by chemical modification, liposomes or nanoparticles encapsulation, and viral infection, to name a few. However, these strategies raise safety issues, limitations in stability and versatility, and do not allow an accurate delivery within the cells. Alternatively, sEV are a promising delivery system for miR-124, due to their intrinsic ability to target tissues, biocompatibility, and safety. In this thesis we used sEV isolated from hUCB-MNC and loaded with miR-124-3p as a new therapeutic approach for PD.

The other main goals of this thesis were:

2) Evaluate the effects of miR-124-3p delivered by sEV (miR-124-3p sEV) on dopaminergic neuroprotection and SVZ neurogenesis, *in vitro*.
3) Assess the therapeutic potential of miR-124-3p sEV in a pre-clinical mouse model of PD, *in vivo*.

Chapter 3

MicroRNA-124-3p modulates alpha-synuclein expression levels in a paraquat-induced *in vivo* model for Parkinson's disease

This chapter is under revisions in an international peer-review journal:

Marta Esteves, Ana Clara Cristóvão, Ana Vale, Marta Machado-Pereira, Raquel Ferreira, Liliana Bernardino. MicroRNA-124-3p modulates alpha-synuclein expression levels in a paraquat-induced *in vivo* model for Parkinson's disease.

3.1 Abstract

PD is the second most prevalent neurodegenerative disease and the most common movement disorder. Although PD etiology is not fully understood, α-synuclein is a key protein involved in PD pathology. MiRNA, small gene regulatory RNAs that control gene expression, have been identified as biomarkers and potential therapeutic targets for brain diseases, including PD. In particular, miR-124 is downregulated in the plasma and brain samples of PD patients. Recently we showed that the brain delivery of miR-124 counteracts 6-OHDA-induced motor deficits. However, its role in α-synuclein pathology has never been addressed. Here we used a PQ-induced rat PD model to evaluate the role of miR-124-3p in modulating monomeric and phosphorylated forms of α-synuclein levels and dopaminergic neuroprotection. Our results showed that an intranigral administration of miR-124-3p reduced the expression levels of both monomeric and phosphorylated (pS129) α-synuclein in the SN of rats exposed to PQ. Nox, responsible for ROS generation, have been considered major players in the development of α-synuclein pathology. Accordingly, miR-124-3p decreased protein expression levels of Nox1 and its activator, small GTPase Rac1, in the SN of PQ-lesioned rats. Moreover, miR-124-3p was able to counteract the reduced levels of pituitary homeobox 3 (Pitx3) induced by PQ in the SN, suggesting an impact on dopaminergic maintenance and survival. This is the first study showing that miR-124-3p decreases PQ-induced α-synuclein levels and the associated Nox1/Rac1 signaling pathway, and impacts Pitx3 protein levels, supporting the potential of using miR-124-3p as a disease-modifying agent for PD and related α-synucleinopathies.

Keywords

miR-124; alpha-synuclein; paraquat; Parkinson’s disease; Nox1; Rac1; Pitx3

3.2 Introduction

PD, the most common movement disorder, is characterized by the progressive degeneration of dopaminergic neurons in the SN of the midbrain, resulting in striatal dopamine depletion. The deficiency of dopamine signaling contributes to both motor and non-motor symptoms [1]. While the etiology of PD is likely multifactorial, the accumulation of cytoplasmic protein inclusions including insoluble α-synuclein (LB) within dopaminergic neurons has been largely recognized as a key pathologic component of the disease. Evidence suggests that misfolded α-synuclein seeds recruit monomeric α-synuclein to form aggregates, which can propagate across brain regions, a phenomenon that correlates with clinical disease progression [2,3]. These pathologic α-synuclein aggregates are typically hyperphosphorylated at serine 129 (pS129) [4]. Several factors have been identified to potentiate the formation and propagation of α-synuclein aggregates, including increased expression of α-synuclein, impaired dephosphorylation, decreased clearance, and oxidative stress [5]. However, the precise mechanisms responsible for α-synuclein-induced toxicity and dopaminergic neuronal death are unclear. Evidence suggest that the dysregulation of α-synuclein may increase neuroinflammation, oxidative stress, and mitochondrial dysfunction, leading to dopaminergic degeneration [6]. It is therefore imperative to identify factors that can counteract α-synuclein toxicity and subsequent dopaminergic degeneration. A growing body of evidence has suggested that the dysfunction of miRNA, small non-coding RNA that regulate gene expression at the post-transcriptional level, are promising therapeutic targets for PD [7]. In particular, the levels of brain-enriched miR-124 are decreased in lesioned human brain samples and plasma and in PD models [8,9], suggesting it could be a potential biomarker for the diagnosis of PD. At the molecular level, 24% of miR-124 validated target genes are deregulated in PD [10]. In in vivo PD models, miR-124 overexpression counteracted neurotoxin-induced dopaminergic neuronal injury, oxidative stress, and dysregulated autophagy, while its knockdown had the opposite effect. These effects were associated with the modulation of AMPK/mTOR, p62/p38, annexinA5 (ANXA5), and Bim signaling pathways [11–14]. However, so far, the molecular effects induced by miR-124 are unknown, particularly regarding α-synuclein accumulation and aggregation in an in vivo model of PD.

Herein, we evaluated the role of miR-124-3p as modulator of monomeric and phosphorylated forms of α-synuclein in the PQ rat model of PD. The PQ, a commonly used herbicide, increases α-synuclein levels and aggregation in dopaminergic neurons in the SN, induces degeneration of nigrostriatal dopaminergic neurons, and consequent dopamine depletion in the nigrostriatal pathway, and lipid peroxidation [15,16]. Our

results showed that the intranigral administration of miR-124-3p decreased α-synuclein and phosphorylated α-synuclein at serine 129 (pS129-α-synuclein) protein levels in the SN of PQ-intoxicated rats. Moreover, miR-124-3p counteracted the increased protein levels of Nox1 and its activator Rac1 in the SN triggered by PQ administration. We also showed that PQ reduced protein levels of tyrosine hydroxylase (TH) in the SN and striatum and of Pitx3 in the SN. Pitx3 is responsible for regulating TH expression and maintaining the dopaminergic phenotype. Our data showed that miR-124-3p counteracted PQ-induced decrease of Pitx3 protein levels in the SN. Overall, these results suggest a role for miR-124-3p in regulating α-synuclein levels, likely through modulation of the Nox1/Rac1 signaling pathway and regulating the expression of Pitx3 which is important for the survival and maintenance of midbrain dopaminergic neurons.

3.3 Materials and Methods

3.3.1 Animals

Male Wistar rats (3- to 8-month-old) were used for this study. The experimental procedures were performed following protocols approved by the Directorate-General for Food and Veterinary (DGAV), the Portuguese National Authority for Animal Health (21/01/2019; reference number 0421/000/000/2019), and by the Directive 2010/63/EU of the European Parliament and the Council on the protection of animals used for scientific purposes. All animals were maintained in temperature/humidity-controlled conditions under a 12 h light/dark cycle with free access to food and water. All efforts were made to reduce the number of animals used and minimize their suffering.

3.3.2 Treatment paradigm

As depicted in Figure 3.1.A, each animal received four IP injections, separated by one day, of either PQ (10 mg/Kg of body weight) or sterile saline (0.1 M phosphate-buffered saline (PBS)), according to a previously published dose [21]. Three days before starting PQ IP injections, rats were anesthetized with IP injection of ketamine (100 mg/kg of rat weight) and xylazine (10 mg/kg of rat weight) and then stereotaxically injected with 250 nM miR-124-3p at the right SN using the following coordinates: mediolateral (ML), - 2.1; anteroposterior (AP), – 5.0; dorsoventral (DV), – 7.7. Three experimental groups were designed: Saline: stereotaxic injection in the SN and IP injection with saline solution (0.1 M PBS) (n = 4); PQ: stereotaxic injection with saline solution and IP injection with PQ (n = 5); miR-124-3p + PQ: stereotaxic injection with miR-124-3p and then IP injection with PQ (n = 4). Five days after the last PQ IP injection, animals were sacrificed. For Western-blot analysis, rats were anesthetized with isoflurane and then sacrificed by

decapitation. Brains were collected, and total protein lysates from striatum and the SN were prepared.

3.3.3 Western blot

Striatum and substantia nigra tissues were lysed on ice in RIPA lysis buffer (50 mM Tris/HCl, pH 8.0, 150 mM NaCl, 5 mM ethylene glycol tetraacetic acid, 1% Triton X-100, 0.5% sodium deoxycholate, 0.1% sodium dodecyl sulphate (SDS) and 10 mM DDT) with a cocktail of protease and phosphatase inhibitors (Roche Diagnostics Ltd., Mannheim, Germany) by mechanical dissociation. Lysates were then centrifuged, the supernatant collected, and the total protein concentration was quantified using the BCA assay kit (Thermo Scientific) according to the manufacturer's instructions. Then, 30 μg of total protein was loaded in a 12.5% or 15% polyacrylamide gel, followed by electrophoresis and transfer onto a PVDF membrane (GE Healthcare, Little Chalfont, UK) for 90 min. Membranes were blocked using 5% milk or 5% bovine serum albumin (BSA) and then incubated with the primary antibodies (mouse anti-TH (1:5000; BD Biosciences), rabbit anti-Pitx3 (1:1000; Invitrogen), mouse anti-α-synuclein (1:500; BD Biosciences); rabbit anti-pS129-α-synuclein (1:200; Santa Cruz Biotechnology), goat anti-Nox1 (1:200; Santa Cruz Biotechnology), mouse anti-rac1 (1:750; Millipore), rabbit anti-$p47^{phox}$ (1:1000; Santa Cruz Biotechnology), mouse anti-actin (1:5000; BD Biosciences) and mouse anti-beta-tubulin (1:5000; BD Biosciences) and secondary antibodies conjugated to horseradish peroxidase—HRP (chicken anti-goat, goat anti-rabbit or goat anti-mouse; 1:5000; all from Santa Cruz Biotechnology). Protein bands were detected by enhanced chemiluminescence (ECL) detection using the ChemiDoc™ MP Imaging System (BioRad Laboratories, CA, USA) and quantified by densitometry analyses using the Image Lab 5.1 software (Bio-Rad Laboratories).

3.3.4 Statistical analysis

All data are expressed as mean ± standard error of the mean (SEM) of at least three different animals. Statistical analysis was performed using the GraphPad Prism 7.0 Software (GraphPad Software Inc.), using one-way ANOVA followed by the Sidak's or Tukey's multiple comparison tests. Values of $p < 0.05$ were considered significant.

3.4 Results

3.4.1 miR-124-3p impacts dopaminergic neurons in the PQ-induced model of PD

Recent evidence has shown the neuroprotective role of miR-124 in PD models. In this work, we evaluated the putative neuroprotective effects of miR-124-3p in a PQ-induced

PD model. Wistar rats were stereotaxically injected with 250 nM miR-124-3p in the right SN and then exposed to PQ (Figure 3.1.A). First, dopaminergic neuronal toxicity induced by PQ was investigated evaluating TH protein levels in the striatum and SN by western blot. We found that PQ exposure reduced TH protein levels in the SN (Figure 3.1.B) and striatum (Figure 3.1.C) compared to the saline group. The administration of 250 nM of miR-124-3p was not able to counteract the reduction of TH levels induced by PQ exposure (Figure 3.1.B and C, respectively). Next, the protein levels of Pitx3, an important transcription factor involved in the survival and maintenance of midbrain dopaminergic neurons, were also evaluated. PQ exposure significantly reduced Pitx3 protein levels in SN (Figure 3.1.D and E; $p < 0.05$) compared to the saline group. The miR-124-3p administration significantly increased Pitx3 protein levels compared to the PQ-intoxicated group reaching levels similar to saline-treated animals (Figure 3.1.D and E; $p < 0.01$). Altogether, these results showed that 250 nM miR-124-3p is not able to counteract PQ-induced decrease of TH protein levels but is able to increase Pitx3 protein levels similar to saline animals, suggesting a putative neuroprotective effect.

3.4.2 miR-124-3p modulates PQ-induced alpha-synuclein expression levels

To disclose if miR-124-3p affects α-synuclein accumulation, we evaluated the expression of monomeric α-synuclein in the SN and striatum of rats exposed to PQ, by western blot. As shown in Figure 3.2, PQ exposure significantly increased α-synuclein levels in the SN (Figure 3.2.A and D; $p < 0.001$) and in the striatum (Figure 3.2.B and D; $p < 0.05$), when compared with the saline group. The administration of miR-124-3p significantly prevented the increase of α-synuclein levels induced by PQ administration in the SN (Figure 3.2.A and D; $p < 0.0001$) and striatum (Figure 3.2.B and D; $p < 0.01$). As a proof-of-concept of the role of miR-124-3p in preventing α-synucleinopathy, we then investigated the expression of pS129-α-syn in the SN of rats exposed to PQ. As shown in Figure 3.2.C, PQ exposure significantly increased the levels of pS129-α-syn in the SN (Figure 3.2.C and D; $p < 0.05$), when compared with the saline group, and the administration of miR-124-3p prevented this increase to levels similar to saline animals (Figure 3.2.C and D; $p < 0.01$). Therefore, miR-124-3p reduced monomeric α-synuclein expression, including the phosphorylated S129-α-syn form, induced by PQ *in vivo*.

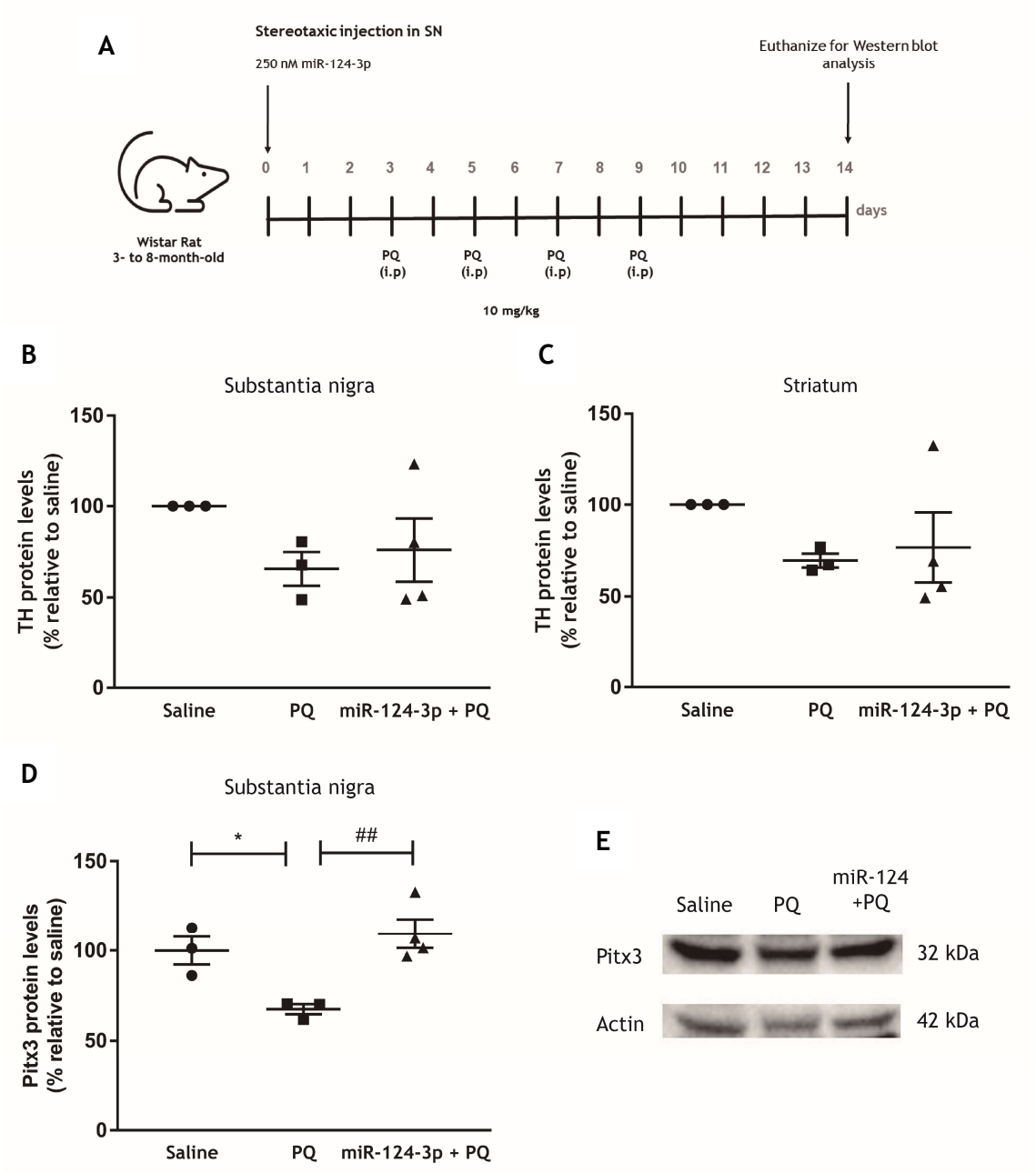

Figure 3.1. Effects of miR-124-3p in the expression of dopaminergic neuronal markers in a rat PQ model *in vivo*. (A) Design and timeline of the experimental animal procedure. Male Wistar rats were subjected to intranigral injection with 250 nM miR-124-3p, or saline, followed by four IP injections of saline or PQ (10 mg/kg), separated by one day. Five days after the last PQ injection, rats' brains were collected for western blot analysis. Expression levels of TH in the **(B)** SN and **(C)** striatum, and **(D)** Pitx3 in the SN, of adult Wistar rats treated with saline, PQ or 250 nM miR-124-3p + PQ. **(E)** Representative western blot protein bands of Pitx3 (32 kDa), and actin (42 kDa). TH and Pitx3 protein levels were normalized against actin. Data are expressed as a percentage of the controls (saline) ± SEM. Protein expression in control condition (saline) was set to 100%. N = 3 or 4 rats. $^{*}p < 0.05$ compared to the saline group and $^{\#\#}p < 0.01$ compared to the PQ-treated rat group using the one-way ANOVA followed by Sidak's multiple comparison test. Abbreviations: IP, intraperitoneal; TH, tyrosine hydroxylase; Pitx3, pituitary homeobox 3; PQ, paraquat; SN, substantia nigra.

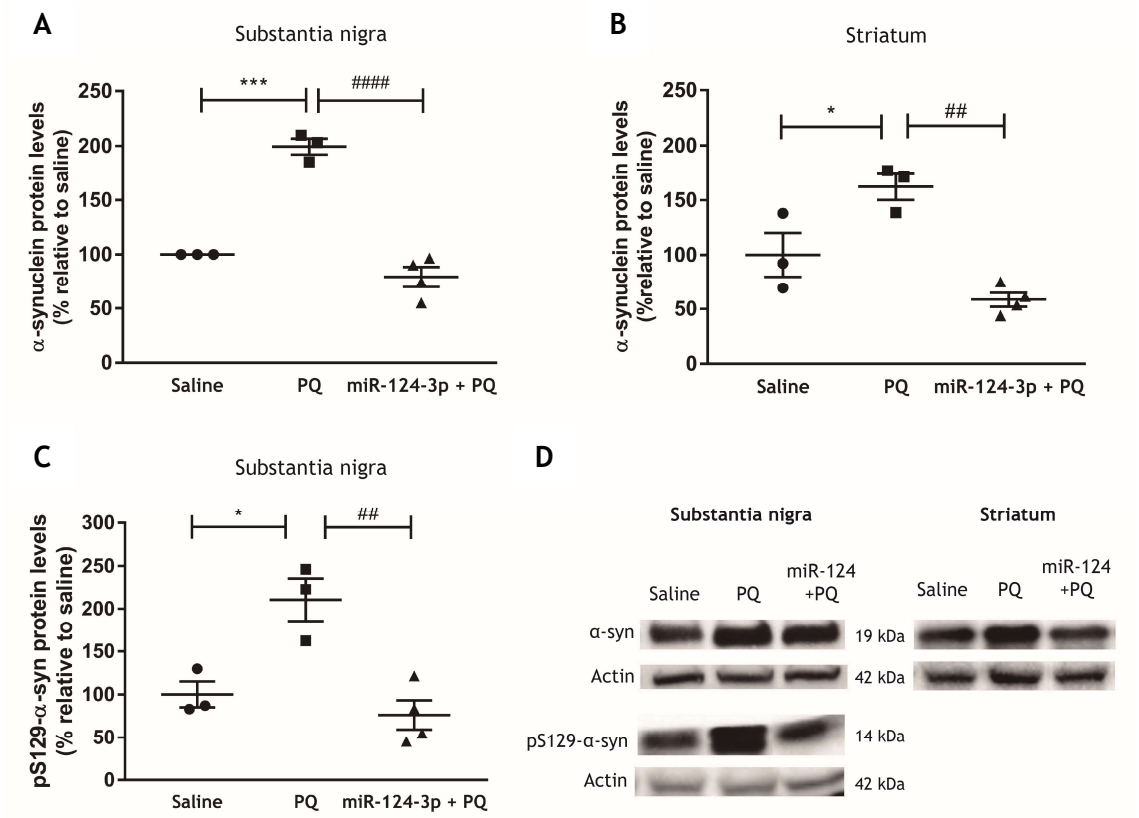

Figure 3.2. miR-124-3p counteracts the increased levels of total monomeric and phosphorylated α-synuclein at serine 129 (pS129-α-syn) induced by PQ in vivo. Expression levels of α-synuclein in the **(A)** SN and **(B)** striatum, and **(C)** pS129-α-syn in the SN of adult Wistar rats treated with saline, PQ or 250 nM miR-124-3p + PQ. **(D)** Representative western blot protein bands of α-syn (19 kDa), pS129-α-syn (14 kDa), and actin (42 kDa). α-Syn and pS129-α-syn protein levels were normalized against actin. Data are expressed as a percentage of control (saline) ± SEM. Protein expression in the control condition (saline) was set to 100%. N = 3 or 4 rats. *p < 0.05 or ***p < 0.001 compared to saline-treated animals and ##p < 0.01 or ####p < 0.0001 compared to the PQ-treated group using the one-way ANOVA followed by Sidak's **(a)** or Tukey's **(b** and **c)** multiple comparison tests. Abbreviations: α-syn, α-synuclein; pS129-α-syn, α-synuclein phosphorylated at serine 129; PQ, paraquat; SN, substantia nigra

3.4.3 miR-124-3p counteracts the increased levels of Nox1 and Rac1 induced by PQ

Nox1-derived oxidative stress has a role in α-synuclein pathology development [15]. Thus, we then disclosed the effect of miR-124-3p in the expression of Nox1, of its organizer Noxo1 homologue, p47^{phox}, and of Rac1, in the SN of PQ-exposed rats. As expected, administration of PQ induced a significant increase in protein levels of Nox1 (Figure 3.3.A and D, $p < 0.01$) and Rac1 (Figure 3.3.B and D, $p < 0.05$) in the SN, compared with the saline-treated group. Contrarily, the intranigral injection of miR-124-3p counteracted the increased protein levels of Nox1 (Figure 3.3.A and D; $p < 0.01$) and Rac1 (Figure 3.3.B and D; $p < 0.01$) induced by PQ administration to levels similar to saline-treated rats. Regarding its subunits Noxo1 homologue, p47^{phox}, neither PQ nor

miR-124-3p induced significant alterations in their protein levels compared with the saline-treated group (3.3.C). These results suggest that miR-124-3p modulates Nox1/Rac1 signaling pathway in the PQ-induced PD *in vivo* model.

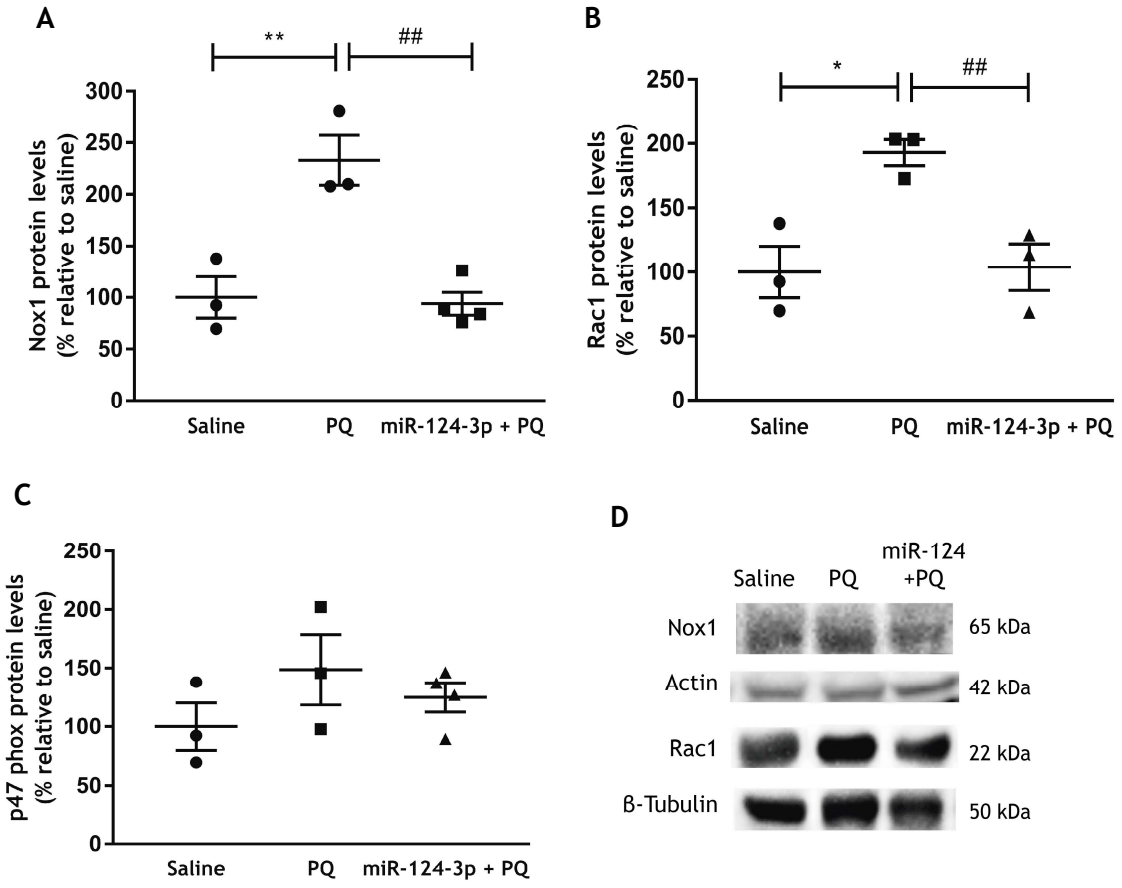

Figure 3.3 miR-124-3p counteracts the Nox1 signaling pathway induced by PQ in the SN *in vivo*. Expression levels of **(A)** Nox1, **(B)** Rac1, and **(C)** $p47^{phox}$ in the SN of adult Wistar rats treated with saline, PQ or 250 nM miR-124-3p + PQ. **(D)** Representative western blot protein bands of Nox1 (65 kDa), Rac1 (22 kDa), actin (42 kDa) and β-tubulin (50 kDa). Nox1 and Rac1 were normalized against actin and β-tubulin, respectively. Data are expressed as a percentage of control (saline) ± SEM. N = 3 or 4 rats. $^{*}p < 0.05$ and $^{**}p < 0.01$ compared to the saline-treated group and $^{\#\#}p < 0.01$ compared to the PQ-treated group using the one-way ANOVA followed by Sidak's multiple comparison test. Abbreviations: PQ, paraquat; SN, substantia nigra.

3.5 Discussion

At the present, there are no effective treatments for the neurodegenerative process in PD. Efforts have been made to establish experimental animal models that recapitulate key pathologic hallmarks to obtain greater insight into the PD pathophysiologic mechanisms and test new therapeutic targets/strategies. The administration of neurotoxins like MPTP, 6-OHDA, rotenone, or PQ or the overexpression of genetically modified genes related to PD, such as SNCA, are the most commonly used models of PD [18]. PQ exposure is considered a key risk factor for sporadic PD in humans and has been widely

used to induce *in vivo* models of PD [17,19–22]. In this study, we used PQ as a PD model due to its ability to increase α-synuclein levels in the SN [16,17]. The systemic exposure to PQ in rodents induces oxidative stress, loss of dopaminergic striatal fibers, and loss of about 36% of dopaminergic neurons in the SN [16,17,20]. A large body of evidence highlights α-synuclein dysregulation as the primary cause of various cellular dysfunctions that lead to the degeneration of dopaminergic neurons [2]. In addition, α-synuclein extracted from human LB revealed to be phosphorylated at serine 129 residue. In fact, phosphorylation of α-synuclein at serine 129 was reported to be implicated in the aggregation, LB formation, and consequent dopaminergic neurotoxicity [23]. For this reason, several studies have been trying to identify targets able to counteract α-synuclein pathology and dopaminergic neurodegeneration. So far, no study has analyzed the role of miR-124 in the modulation of α-synuclein in a PD context.

This study showed for the first time that miR-124-3p is able to down-regulate PQ-induced α-synuclein expression in the striatum and SN. Recent studies have already reported the regulation of α-synuclein levels by other miRNAs. For example, miR-7, which is found decreased in the SN of PD patients, downregulates α-synuclein expression by binding to the *SNCA* mRNA 3'-UTR, thus protecting against neurodegeneration [24]. Therefore, strategies that reduce α-synuclein protein levels might modulate the equilibrium between soluble and misfolded forms leading to gradual clearance of existing pathology. α-Synuclein may contribute to PD pathogenesis in a number of ways, but it is generally thought its oligomeric and fibrillary conformations, the toxic species that mediate disruption of cellular homeostasis, protein clearance pathology and neuronal death [25–28]. Further studies are needed to understand through which mechanisms miR-124-3p affects oligomeric forms of α-synuclein and the downstream pathological aggregation mechanisms responsible for PD pathology. Understanding these molecular mechanisms is warranted to further develop novel disease-modifying therapeutic approaches. Nox, considered one of the main sources of ROS in dopaminergic neurons, has been implicated in the pathology of PD. Specifically, the isoform Nox1, which is upregulated in dopaminergic neurons under oxidative stress has been regarded as a relevant player in dopaminergic neuronal degeneration in PD rodent models [15,29]. Moreover, Nox1 can be a major player in increasing α-synuclein expression and aggregation and consequent dopaminergic degeneration in both rodent PD models and postmortem human PD brains [15,17]. The full activation of Nox1 requires the membrane-bound component $p22^{phox}$ and the cytosolic partners Rac1, and Noxo1 and Noxa1 or homologous regulators $p47^{phox}$ and $p67^{phox}$, respectively [30]. Here we showed that the administration of miR-124-3p reduced protein levels of Nox1 and

Rac1, a GTPase involved in its activation, in the SN of rats exposed to PQ. The modulation of the Nox1/Rac1 signaling pathway by miR-124-3p may be responsible for the decreased accumulation of α-synuclein in the SN of PQ-exposed rats. In accordance with previous studies [29,31], we showed that PQ increases the protein levels of Nox1 and Rac1. Although no significant increase in $p47^{phox}$ protein levels was observed, there is an increased tendency in its levels, which is in accordance with the animal model exposed to PQ plus maneb (dithiocarbamate fungicide), which shows an increase in $p47^{phox}$ protein levels [32–34]. Future studies to analyze in depth the effect of miR-124-3p in $p47^{phox}$, $p67^{phox}$ and Rac1 activation will allow to discriminate the modulatory effect on the Nox1 signaling pathway and indirectly in alpha-synucleinopathy. Additional functional validation studies, such as luciferase reporter and qPCR are needed to disclose if α-synuclein, Nox1 or Rac1 are miR-124 targets. Moreover, while western-blot analysis provides total protein expression levels, previously we showed that PQ induced toxicity and oxidative stress in dopaminergic neurons *in vitro* and *in vivo* [17,20]. This acute model induces high systemic toxicity [19,20]. Therefore, future studies aiming to evaluate in depth the molecular mechanisms induced by miR-124-3p in dopaminergic neurons should be done in an upgraded PQ exposure paradigm inducing progressive dopaminergic degeneration and consequent motor dysfunction with low systemic toxicity [20]. Additionally, the effects of miR-124 should be also tested in other relevant PD models to investigate misfolding, aggregation and spreading of α-synuclein-related pathology, including transgenic rodent models overexpressing α-synuclein (wild-type or mutated), the injection of AAV systems to overexpress wild-type or mutated forms of α-synuclein, or the injection of preformed fibrils of recombinant α-synuclein (PFFs).

Previous studies have shown that miR-124 has neuroprotective effects in rodent PD models. miR-124 attenuates dopaminergic degeneration by targeting several signaling pathways, including the ANXA5/ERK pathway [14], STAT3 [35], AMPK/mTOR pathway [12], the calpain 1/p25/cdk5 signaling [8], EDN2 [36], and Bim [13], in *in vitro* and *in vivo* PD models. Recently, others showed that the overexpression of miR-124 in the 6-OHDA-induced PD mouse model ameliorated dopaminergic neuronal loss and improved motor deficits by targeting Axin1 and activating the Wnt/β-catenin pathways [37]. Previously, we also showed that polymeric nanoparticles and small extracellular vesicles loaded with miR-124 were able to trigger neurogenesis and protect dopaminergic neurons, respectively, culminating in the amelioration of motor deficits in the 6-OHDA mouse model of PD [38,39]. So far, no study has explored the effect of miR-124 in neuronal dopaminergic survival using the PQ-induced model. In our study, we found that miR-124-3p was able to counteract the reduced protein levels of Pitx3 triggered by

PQ in the SN. Pitx3 is an important transcription factor for dopaminergic neurons specification during neuronal development, being also involved in the maintenance of TH expression and in the survival of dopaminergic neurons throughout adulthood [40]. In addition, it protects dopaminergic neurons against insults by regulating GDNF and BDNF [40,41]. In PD patients, the number of Pitx3-positive neurons is reduced which correlates with dopaminergic neuron loss and accumulation and potential aggregation of α-synuclein. Recently, Wang and colleagues observed an increased accumulation of α-synuclein in the Pitx3-deficient dopaminergic neurons of 15-month-old mice, suggesting that the deficiency of Pitx3 leads to α-synuclein accumulation which may trigger the pathogenic cascades leading to neurodegeneration [40]. However, our results showed that miR-124-3p is not able to counteract the decrease of TH protein levels in the striatum and in the SN induced by PQ. Considering the neuroprotective effects of miR-124 reported in other PD models, we may hypothesize that the miRNA concentration and/or the exposure paradigm used in this study are not appropriate to induce an increase of TH expression while is able to increase Pitx3 levels similar to controls. Moreover, the direct delivery of naked miRNA into the brain parenchyma is a limitation for miRNA-based therapies. Due to high susceptibility to degradation by nucleases, and entrapment in the endosome [42], the amount of miRNA reaching targeted regions may not be sufficient to counteract TH reduced levels induced by PQ. In addition, a single administration of miR-124-3p three days before the administration of PQ may also diminish the miRNA effect. However, the mortality rate observed and previously reported by others [20,43,44], due to the exacerbated inflammatory response and the systemic toxicity provoked by acute administration of PQ impeded the stereotaxic injection of miR-124-3p during the PQ exposure. Additionally, the systemic toxicity induced by the acute exposure to the high dose of PQ, lead to non-brain related motor dysfunction, which limits further evaluations of dopamine-dependent motor behaviors. Thus, future experiments using alternative chronic PQ models, depicting no systemic toxicity or with additional miRNA doses and delivery strategies are needed. An interesting approach would be to use delivery vehicles, for example, the small extracellular vesicles or exosomes, to protect, transport, and deliver the miRNA into target cells. Moreover, choosing non-invasive administration routes, such as the intranasal route, may be suitable approach to overcome the limitations above. Despite the need for further studies, here we report for the first time the effect of miR-124-3p on the modulation of α-synuclein expression, the Nox1/Rac1 signaling pathway and Pitx3 protein levels in the PQ-induced model of PD.

3.6 Conclusions

In conclusion, the present work demonstrates for the first time that miR-124-3p reduces the expression of monomeric and phosphorylated forms of α-synuclein and downregulates the Nox1/Rac1 signaling pathway in the SN of rats exposed to PQ. These findings suggest that the miR-124-3p is able to counteract α-synuclein-induced pathology, likely through this signaling pathway. Moreover, miR-124-3p was able to counteract Pitx3 levels which were decreased in PQ-lesioned rats. Altogether these findings open a new avenue about the role of miR-124-3p as a disease-modifying therapeutic agent for PD and related synucleinopathies.

3.7 References

1. Jankovic J: Parkinson's disease: Clinical features and diagnosis. *J Neurol Neurosurg Psychiatry* 2008, 79:368–376.
2. Luk KC, Kehm V, Carroll J, Zhang B, O'Brien P, Trojanowski JQ, Lee VMY: Pathological α-synuclein transmission initiates Parkinson-like neurodegeneration in nontransgenic mice. *Science* 2012, 338:949–953.
3. Volpicelli-Daley LA, Luk KC, Patel TP, Tanik SA, Riddle DM, Stieber A, Meaney DF, Trojanowski JQ, Lee VMY: Exogenous α-synuclein fibrils induce Lewy body pathology leading to synaptic dysfunction and neuron death. *Neuron* 2011, 72:57–71.
4. Anderson JP, Walker DE, Goldstein JM, De Laat R, Banducci K, Caccavello RJ, Barbour R, Huang J, Kling K, Lee M, et al.: Phosphorylation of Ser-129 is the dominant pathological modification of alpha-synuclein in familial and sporadic Lewy body disease. *J Biol Chem* 2006, 281:29739–29752.
5. Bingol B: Autophagy and lysosomal pathways in nervous system disorders. *Mol Cell Neurosci* 2018, 91:167–208.
6. Rocha EM, De Miranda B, Sanders LH: Alpha-synuclein: Pathology, mitochondrial dysfunction and neuroinflammation in Parkinson's disease. *Neurobiol Dis* 2018, 109:249–257.
7. Saraiva C, Esteves M, Bernardino L: MicroRNA: Basic concepts and implications for regeneration and repair of neurodegenerative diseases. *Biochem Pharmacol* 2017, 141:118–131.
8. Kanagaraj N, Beiping H, Dheen ST, Tay SSW: Downregulation of miR-124 in MPTP-treated mouse model of Parkinson's disease and MPP iodide-treated MN9D cells modulates the expression of the calpain/cdk5 pathway proteins. *Neuroscience* 2014, 272:167–79.
9. Li N, Pan X, Zhang J, Ma A, Yang S, Ma J, Xie A: Plasma levels of miR-137 and

miR-124 are associated with Parkinson's disease but not with Parkinson's disease with depression. *Neurol Sci* 2017, 38:761–767.

10. Sonntag K-C: MicroRNAs and deregulated gene expression networks in neurodegeneration. *Brain Res* 2010, 1338:48–57.
11. Yao L, Zhu Z, Wu J, Zhang Y, Zhang H, Sun X, Qian C, Wang B, Xie L, Zhang S, et al.: MicroRNA-124 regulates the expression of p62/p38 and promotes autophagy in the inflammatory pathogenesis of Parkinson's disease. *FASEB J* 2019, 33:8648–8665.
12. Gong X, Wang H, Ye Y, Shu Y, Deng Y, He X, Lu G, Zhang S: miR-124 regulates cell apoptosis and autophagy in dopaminergic neurons and protects them by regulating AMPK/mTOR pathway in Parkinson's disease. *Am J Transl Res* 2016, 8:2127–37.
13. Wang H, Ye Y, Zhu Z, Mo L, Lin C, Wang Q, Wang H, Gong X, He X, Lu G, et al.: MiR-124 Regulates Apoptosis and Autophagy Process in MPTP Model of Parkinson's Disease by Targeting to Bim. *Brain Pathol* 2016, 26:167–176.
14. Dong RF, Zhang B, Tai LW, Liu HM, Shi FK, Liu NN: The Neuroprotective Role of MiR-124-3p in a 6-Hydroxydopamine-Induced Cell Model of Parkinson's Disease via the Regulation of ANAX5. *J Cell Biochem* 2018, 119:269–277.
15. Choi DH, Cristóvão AC, Guhathakurta S, Lee J, Joh TH, Beal MF, Kim YS: NADPH oxidase 1-mediated oxidative stress leads to dopamine neuron death in Parkinson's disease. *Antioxidants Redox Signal* 2012, 16:1033–1045.
16. Manning-Bog AB, McCormack AL, Li J, Uversky VN, Fink AL, Di Monte DA: The Herbicide Paraquat Causes Up-regulation and Aggregation of α-Synuclein in Mice: PARAQUAT AND α-SYNUCLEIN. *J Biol Chem* 2002, 277:1641–1644.
17. Cristóvão AC, Guhathakurta S, Bok E, Je G, Yoo SD, Choi DH, Kim YS: Nadph oxidase 1 mediates α-synucleinopathy in Parkinson's disease. *J Neurosci* 2012, 32:14465–14477.
18. Cenci MA, Björklund A: Animal models for preclinical Parkinson's research: An update and critical appraisal. *Prog Brain Res* 2020, 252:27–59.
19. Berry C, La Vecchia C, Nicotera P: Paraquat and Parkinson's disease. *Cell Death Differ 2010 177* 2010, 17:1115–1125.
20. Cristóvão AC, Campos FL, Je G, Esteves M, Guhathakurta S, Yang L, Beal MF, Fonseca BM, Salgado AJ, Queiroz J, et al.: Characterization of a Parkinson's disease rat model using an upgraded paraquat exposure paradigm. *Eur J Neurosci* 2020, 52:3242–3255.
21. Ahmad MH, Fatima M, Ali M, Rizvi MA, Mondal AC: Naringenin alleviates paraquat-induced dopaminergic neuronal loss in SH-SY5Y cells and a rat model

of Parkinson's disease. *Neuropharmacology* 2021, 201.

22. Wang K, Zhang B, Tian T, Zhang B, Shi G, Zhang C, Li G, Huang M: Taurine protects dopaminergic neurons in paraquat-induced Parkinson's disease mouse model through PI3K/Akt signaling pathways. *Amino Acids* 2022, 54:1–11.
23. Oueslati A: Implication of Alpha-Synuclein Phosphorylation at S129 in Synucleinopathies: What Have We Learned in the Last Decade? *J Parkinsons Dis* 2016, 6:39–51.
24. Zhang J, Zhao M, Yan R, Liu J, Maddila S, Junn E, Mouradian MM: MicroRNA-7 Protects Against Neurodegeneration Induced by α-Synuclein Preformed Fibrils in the Mouse Brain. *Neurotherapeutics* 2021, 18:2529–2540.
25. Cremades N, Cohen SIA, Deas E, Abramov AY, Chen AY, Orte A, Sandal M, Clarke RW, Dunne P, Aprile FA, et al.: Direct observation of the interconversion of normal and toxic forms of α-synuclein. *Cell* 2012, 149:1048–1059.
26. Bridi JC, Hirth F: Mechanisms of α-Synuclein Induced Synaptopathy in Parkinson's Disease. *Front Neurosci* 2018, 12.
27. Cascella R, Chen SW, Bigi A, Camino JD, Xu CK, Dobson CM, Chiti F, Cremades N, Cecchi C: The release of toxic oligomers from α-synuclein fibrils induces dysfunction in neuronal cells. *Nat Commun* 2021, 12.
28. Koziorowski D, Figura M, Milanowski ŁM, Szlufik S, Alster P, Madetko N, Friedman A: Mechanisms of Neurodegeneration in Various Forms of Parkinsonism—Similarities and Differences. *Cells* 2021, 10:1–29.
29. Cristóvão AC, Choi D-H, Baltazar G, Beal MF, Kim Y-S: The role of NADPH oxidase 1-derived reactive oxygen species in paraquat-mediated dopaminergic cell death. *Antioxid Redox Signal* 2009, 11:2105–18.
30. Ueyama T, Geiszt M, Leto TL: Involvement of Rac1 in Activation of Multicomponent Nox1- and Nox3-Based NADPH Oxidases. *Mol Cell Biol* 2006, 26:2160.
31. Cristóvão AC, Barata J, Je G, Kim YS: PKCδ mediates paraquat-induced Nox1 expression in dopaminergic neurons. *Biochem Biophys Res Commun* 2013, 437:380.
32. Hou L, Zhang C, Wang K, Liu X, Wang H, Che Y, Sun F, Zhou X, Zhao X, Wang Q: Paraquat and maneb co-exposure induces noradrenergic locus coeruleus neurodegeneration through NADPH oxidase-mediated microglial activation. *Toxicology* 2017, 380:1–10.
33. Hou L, Sun F, Sun W, Zhang L, Wang Q: Lesion of the Locus Coeruleus Damages Learning and Memory Performance in Paraquat and Maneb-induced Mouse Parkinson's Disease Model. *Neuroscience* 2019, 419:129–140.

34. Wang K, Shi Y, Liu W, Liu S, Sun MZ: Taurine improves neuron injuries and cognitive impairment in a mouse Parkinson's disease model through inhibition of microglial activation. *Neurotoxicology* 2021, 83:129–136.
35. Geng L, Liu W, Chen Y: miR-124-3p attenuates MPP+-induced neuronal injury by targeting STAT3 in SH-SY5Y cells. *Exp Biol Med* 2017, 242:1757–1764.
36. Wang J, Wang W, Zhai H: MicroRNA-124 Enhances Dopamine Receptor Expression and Neuronal Proliferation in Mouse Models of Parkinson's Disease via the Hedgehog Signaling Pathway by Targeting EDN2. *Neuroimmunomodulation* 2019, 26:174–187.
37. Zhang F, Yao Y, Miao N, Wang N, Xu X, Yang C: Neuroprotective effects of microRNA 124 in Parkinson's disease mice. *Arch Gerontol Geriatr* 2022, 99:104588.
38. Saraiva C, Paiva J, Santos T, Ferreira L, Bernardino L: MicroRNA-124 loaded nanoparticles enhance brain repair in Parkinson's disease. *J Control Release* 2016, 235:291–305.
39. Esteves M, Abreu R, Fernandes H, Serra-Almeida C, Martins PAT, Barão M, Cristóvão AC, Saraiva C, Ferreira R, Ferreira L, et al.: MicroRNA-124-3p-enriched small extracellular vesicles as a therapeutic approach for Parkinson's disease. *Mol Ther* 2022, doi:10.1016/J.YMTHE.2022.06.003.
40. Wang Y, Chen X, Wang Y, Li S, Cai H, Le W: The essential role of transcription factor Pitx3 in preventing mesodiencephalic dopaminergic neurodegeneration and maintaining neuronal subtype identities during aging. *Cell Death Dis 2021 1211* 2021, 12:1–11.
41. Gao D-S, Chen J, Kang X-Y, Tang C-X: Impact of Pitx3 gene knockdown on glial cell line-derived neurotrophic factor transcriptional activity in dopaminergic neurons. 2017, 12.
42. Pereira P, Queiroz JA, Figueiras A, Sousa F: Current progress on microRNAs-based therapeutics in neurodegenerative diseases. *Wiley Interdiscip Rev RNA* 2017, 8:e1409.
43. Prasad K, Tarasewicz E, Mathew J, Strickland PAO, Buckley B, Richardson JR, Richfield EK: Toxicokinetics and toxicodynamics of paraquat accumulation in mouse brain. *Exp Neurol* 2009, 215:358.
44. Gao L, Yuan H, Xu E, Liu J: Toxicology of paraquat and pharmacology of the protective effect of 5-hydroxy-1-methylhydantoin on lung injury caused by paraquat based on metabolomics. *Sci Reports 2020 101* 2020, 10:1–16.

Chapter 4

MicroRNA-124-3p-enriched small extracellular vesicles as a therapeutic approach for Parkinson's disease

This chapter corresponds to the original research article:

Marta Esteves, Ricardo Abreu, Hugo Fernandes, Catarina Serra-Almeida, Patrícia A. T. Martins, Marta Barão, Ana Clara Cristóvão, Cláudia Saraiva, Raquel Ferreira, Lino Ferreira, Liliana Bernardino (2022). MicroRNA-124-3p-enriched small extracellular vesicles as a therapeutic approach for Parkinson's disease. Molecular Therapy, S1525-0016(22)00363-X. DOI: https://doi.org/10.1016/j.ymthe.2022.06.003

Some alterations to the original publication and additional information were included to further sustain the aim of the thesis.

4.1 Abstract

PD is a neurodegenerative disease characterized by the loss of dopaminergic neurons in the SN with no effective cure available. MicroRNA-124 (miR-124) has been regarded as a promising therapeutic entity for PD due to its pro-neurogenic and neuroprotective roles. However, its efficient delivery to the brain remains challenging. Here, we used UCB-MNC-derived EV as a biological vehicle to deliver miR-124-3p and evaluate its therapeutic effects in a mouse model of Parkinson's disease. *In vitro*, miR-124-3p-loaded small extracellular vesicles (miR-124 sEV) induced neuronal differentiation in SVZ NSC and protected N27 dopaminergic cells against 6-OHDA-induced toxicity. *In vivo*, intracerebroventricularly administered sEV were detected in the SVZ lining the lateral ventricles, and in the striatum and SN, the brain regions most affected by the disease. Most importantly, although miR-124 sEV did not increase the number of new neurons in the 6-OHDA-lesioned striatum, the formulation protected dopaminergic neurons in the SN and striatal fibers, which fully counteracted motor behavior symptoms in 6-OHDA-treated mice. Our findings reveal a novel promising therapeutic application of sEV as delivery agents for miR-124-3p in the context of Parkinson's disease.

Keywords

miR-124; microRNA; small extracellular vesicles; 6-OHDA; dopaminergic degeneration; neurogenesis; neuroprotection; motor behavior; Parkinson's disease

4.2 Introduction

PD is the second most common neurodegenerative disease and currently has no effective treatment available. PD is mainly characterized by the progressive degeneration of dopaminergic neurons in the SN of the midbrain, which results in the depletion of dopamine in the striatum. The deficiency of dopamine signaling contributes to motor deficits such as resting tremor, muscle rigidity, and bradykinesia [1]. Recent evidence highlight miRNA, small non-coding RNAs that regulate gene expression at the post-transcriptional level, as promising therapeutic targets for neurodegenerative diseases, including PD [2]. In particular, the levels of miR-124 are decreased in the lesioned brain regions (SN) of PD models and the plasma of PD patients [3,4], suggesting it could be a potential biomarker for the diagnosis of PD. At the molecular level, 24% of miR-124 validated target genes are deregulated in PD, stressing the relevance of miR-124 in the regulation of PD [5]. In *in vivo* PD models, miR-124 overexpression counteracted oxidative stress, autophagy, and apoptosis of DA, while its knockdown had the opposite effect. These effects were associated with the modulation of AMPK/mTOR, p62/p38, ANXA5 and Bim signaling pathways [6–8]. Despite this characterization of the cellular and molecular mechanisms that potentially delay/halt disease progression, its therapeutic use is hampered due to its limited and inefficient ability to reach lesioned brain regions. Previously, we have shown that the intracerebroventricular (ICV) delivery of miR-124-loaded polymeric nanoparticles (miR-124 NP) boosts endogenous neurogenesis in the SVZ, and increases the number of new neurons in the lesioned striatum, which were associated with the amelioration of PD-related motor deficits [9]. However, polymeric delivery systems still have limitations for the delivery of miRNA to dopaminergic neurons. In fact, ICV injected polymeric NP remain in the SVZ, lining the lateral ventricles, and were not able to migrate to the SN [9]. Due to their biocompatibility, safety, and intrinsic ability to target lesioned tissues/cells, sEV, also commonly referred to as exosomes, are likely a superior choice, overcoming the limitations observed with viral, liposomal or polymeric drug delivery systems (e.g. bioaccumulation and toxicity) [10–13]. Accordingly, recent strategies based on native or modulated sEV have been proposed for treating PD [11,14,15]. Nevertheless, the therapeutic use of sEV enriched with miR-124 in PD has not been addressed yet. Herein, we used sEV as a biological carrier of the therapeutic entity, miR-124, to boost neuroprotection, neurogenesis, and functional motor recovery in PD preclinical models.

In this work, sEV were isolated from hUCB-MNC and enriched with miR-124-3p (miR-124-3p sEV) as a strategy to deliver miR-124-3p to the brain and induce therapeutic effects in PD. sEV derived from hUCB-MNC are well characterized in composition, have

low immunogenicity, and are easily accessible in cord blood banks [10,16]. Several clinical trials are using umbilical cord blood cells to treat neurologic diseases, supporting their safety [16]. We found that miR-124-3p sEV protect dopaminergic neurons from 6-OHDA-induced toxicity both *in vitro* and *in vivo*, culminating in a full motor function recovery *in vivo*. This study provides a new and efficient biological sEV-based delivery system for miR-124-3p capable of halting the progression of PD neurodegeneration.

4.3 Materials and Methods

4.3.1 sEV isolation

sEV were isolated from conditioned medium of hUCB-derived MNC culture. All hUCB samples were obtained upon signed informed consent, in compliance with Portuguese legislation. The collection was approved by the ethics committee of Centro Hospitalar e Universitário de Coimbra, Portugal (HUC-01-11, approved on March 3rd, 2011). The samples were stored and transported to the laboratory in sterile bags with anticoagulant solution (citrate-phosphate-dextrose) and processed within 48 h after collection. Briefly, MNC were isolated by density gradient separation (Lymphoprep™ - StemCell Technologies SARL, Grenoble, France). To obtain MNC-derived sEV, hUCB-MNC were cultured in X-VIVO 15 serum-free cell culture medium (Lonza Group, Basel, Switzerland) supplemented with Flt-3 (100 ng/mL, PeproTech) and stem-cell factor (100 ng/mL, PeproTech) under hypoxia (0.5% O_2) conditions for 18 h. Conditioned medium was collected and centrifuged at 300 g, for 10 min, at 4°C to remove cells (pellet). Supernatant was collected for a new tube and centrifuged at 2,000 g, for 20 min, at 4°C to deplete cellular debris. Then, sEV were purified by differential centrifugation as described previously [17]. Briefly, samples were ultracentrifuged twice at 10 000 g, for 30 min, at 4°C, and the pellet was discarded. The supernatant was ultracentrifuged at 100 000 g, for 2 h, at 4°C, to pellet sEV. Finally, the pellet obtained was washed with cold PBS, ultracentrifuged again at 100 000 g, for 2 h, at 4°C, resuspended in 150 µL of cold PBS and stored at -80°C. Ultracentrifugation steps were performed using Optima™ XPN 100K ultracentrifuge (Beckman Coulter, California, USA) with a swinging bucket rotor SW 32 Ti and 28.7 mL polyallomer conical tubes (Beckman Coulter). We have submitted all relevant data of our experiments to the EV-TRACK knowledgebase (EV-TRACK ID: EV210107) (Van Deun J, et al. EV-TRACK: transparent reporting and centralizing knowledge in extracellular vesicle research. Nature methods. 2017;14(3):228-32).

4.3.2 sEV characterization by Nanoparticle tracking analysis

Analysis of sEV size distribution and concentration was performed through Nanoparticle tracking analysis (NTA) by NanoSight NS300 (Malvern Instruments, Malvern, U.K.).

The system used an O-Ring Top Plate and the sample was injected manually at an approximate flow of 1 mL every 20 s. sEV were diluted in PBS until it reached a concentration between 15 and 45 particles/frame. Five 30 s measurements were done for each sample with the camera level set at 16. All the videos were processed with NTA 3.2 analytical software, using the software threshold between 2 and 4 depending on the quality of the videos.

4.3.3 sEV characterization by protein quantification

The total protein content of sEV was measured by Micro BCA™ protein assay kit (Thermo Fisher Scientific, Massachusetts, USA), according to the manufacturer's instructions. Briefly, sEV samples were diluted 22 times in 2% (v/v) SDS to disrupt the sEV membrane and subsequently, 50 µL of the previous mix was pipetted, in duplicate, into a 96-well cell culture plates. Reaction solution provided in the kit was added and incubated for 2 h at 37°C. Next, the plates were equilibrated at room temperature (RT) for 15 min, and the absorbance was read at 562 nm in the microplate reader Synergy™ H1 (Biotek, Vermont, USA). Total protein concentration was determined using a linear standard curve established with BSA.

4.3.4 sEV characterization by Zeta potential

NanoBrook ZetaPALS Potential Analyzer (Brookhaven Instruments Corporation, Long Island, USA) was used for sEV surface charge measurement. Briefly, 5 µL of purified sEV were diluted in 1500 µL of biological grade ultrapure water (Fisher Scientific, New Hampshire, USA), filtered twice through a 0.2 µM filter. sEV were then placed in a disposable polystyrene cuvette and the electrode was immersed within the cuvette. Each sample was measured five times (using Smoluchowski module) at RT.

4.3.5 Western blot analysis

Western blot analysis was performed to detect EV markers and contaminants in EV samples, as previously described [17]. Briefly, up to 15 µL of concentrated EV preparations in PBS (0.5 to 4 µg) were mixed with 5 µL 4x Laemmli buffer (0.25 M Tris base, 8% SDS, 40% glycerol, 200 mg bromophenol blue, 10% 2-mercaptoethanol) and boiled at 96°C for 10 min. For the analysis of tetraspanins, Laemmli buffer was prepared without reducing agents. Samples were loaded in 30 µL wells of Any kD™ Mini-PROTEAN® TGX Stain-Free™ Protein Gel (Bio-Rad) and electrophoresis was performed in 1x Tris/Glycine/SDS buffer prepared from a commercial 10x concentrated stock (10x Tris/Glycine/SDS Electrophoresis Buffer; Bio-Rad), at the constant voltage of 120V, for 75 min. Afterwards, gels were placed in blotting buffer (25 mM Tris, 192 mM glycine, 20% methanol in water) for 10 min to equilibrate. Then the gel was stacked on

top of a nitrocellulose membrane (GE Healthcare), and both were assembled within a transfer system. The transfer was performed in wet conditions at 200 mA for 90 min. Then, the membrane was blocked in a 1:1 PBS-Tween 20 (0.2% (v/v)) with Intercept Blocking Buffer (Li-cor) solution for 1 h at RT. Afterwards, membranes were incubated overnight at 4°C with the appropriate primary antibodies and according to the manufacturer recommendation (antibody details below). Then, membranes were incubated for 1 h at RT with secondary antibodies. Membranes were viewed in the Odyssey CLx system (Li-cor) at the 700 nm and 800 nm wavelengths. Antibodies used in this study were: CD63 (BD Pharmingen, Franklin Lakes, USA), ApoA-1 (Santa Cruz Biotechnology), Calnexin (Santa Cruz Biotechnology), HSP70 (Enzo Life Sciences), CD9 (BD Pharmingen) and IRDye® 800CW Goat anti-Mouse IgG Secondary Antibody (Li-cor). To detect non-EV markers in hUCB-MNC samples, MNC were lysed in 2x RIPA buffer for 30 min, in ice. The cellular extracts were centrifuge at 16 000 rpm for 10 min at 4°C and the supernatant containing the proteins was stored at -80°C. The protein (4 µg) was boiled in 1x Laemmli buffer for 5 min and then loaded in a 12% SDS-polyacrylamide gel electrophoresis and transferred to PVDF membranes (Amersham™ Hybond™ 0.45 PVDF). The membranes were blocked with 5% BSA in TBS-T for 1 h. Then, the membrane was incubated with the monoclonal antibodies against calnexin (Abcam) or apoA-1 (Affinity Biosciences) overnight at 4°C. In the next day, the membranes were washed (3x for 5 min in TBS-T) and then incubated with polyclonal goat anti-mouse immunoglobulins/HRP (Cell Signaling) for 1 h at RT. Proteins were visualized using the enhanced chemiluminescence detection system (ECL®, Advansta).

4.3.6 sEV characterization by TEM

TEM analysis of sEV were performed as previously described.[17] Briefly, samples were diluted 1:1 in 4% (v/v) paraformaldehyde (PFA) and placed on Formvar-carbon coated grids (TAAB Technologies) for 20 min at RT. After washing 4 times with PBS, grids were placed on a drop of 1% (v/v) glutaraldehyde for 5 min, followed by 5 washes with distilled water, one minute each. The grids were incubated in the dark with uranyl-oxalate solution with pH=7 for 5 min, and then placed on ice in contact with a solution of methyl cellulose (9:1) for 10 min. sEV imaging was obtained using a Tecnai G2 Spirit BioTWIN electron microscope (FEI) at 80 kV.

4.3.7 Exo-Fect™ loading of sEV

sEV were loaded with miR-124-3p or scramble (SCR) (GE Healthcare Dharmacon, Inc., Lafayette, CO, USA) by Exo-Fect™ Exosome Transfection Reagent (10 µL; System Biosciences, USA) for 10 min at 37°C. Samples were purified using ExoQuick, according to the manufacturer's instructions. Briefly, samples were incubated with ExoQuick

reagent in 1:5 (v/v) for 30 min on ice, centrifuged at 13,000 g for 3 min, the supernatant was discarded, and the pellet were resuspended in PBS. For *in vitro* studies, final samples contained 20 pmol (0.27 μg) of miR-124-3p or SCR *per* 3.5x1010 – 7.5x1010 particles (80-90 μg sEV) whereas *for in vivo* studies the final samples contained 20 pmol (0.27 μg) of miR-124-3p or SCR *per* 2.3x1010 part (10 μg of sEV) in a total volume of 5 μL. 20 pmol miR-124 was incubated with Exo-Fect™ in the absence of sEV and was used as control. SEV, SCR sEV and miR-124-3p sEV formulations were eventually stored at -80°C for the next experiments. The emission spectra of all samples, excited at λex=5 nm, was measured from λem=5 nm until λem=700 nm in a microplate reader SynergyTM H1 (Biotek) and the highest point for each sample was considered to calculate the loading efficiency of each method. The loading efficiency on each condition, including the control without sEV, was calculated using the formula: fluorescence intensity of the pellet / (fluorescence intensity of the pellet + fluorescence intensity of the supernatant). For each condition and each type of sEV, the fluorescence value of the respective control was subtracted to the measured value and this number was expressed, in percentage, as the loading efficiency.

4.3.8 qPCR analysis

To evaluate miR-124-3p expression in sEV, total RNA was extracted using the RNeasy Micro Kit (Qiagen) as *per* the manufacturer´s instructions and quantified using the Qubit 2.0 system (Thermo Fisher Scientific). cDNA was synthesized for each sample from the amount of RNA extracted from 40 μg ($9.2x10^{10}$ particles) of sEV using the Mir-X™ miRNA First-Strand Synthesis Kit (Takara), from which the amount corresponding to roughly 3 μg (6.9×10^9 particles) of Evs was used *per* qPCR reaction. Finally, qPCR was performed on the CFX Connect Real-Time System (Bio-Rad) using the NZYSpeedy qPCR Green Master Mix (2x) (Nzytech). Reverse primer was the universal 3' mRQ primer (Takara). The forward primer sequence for miR-124-3p was 5'-TAAGGCACGCGGTGAATGCC-3' and for RNU6 (RNA, U6 small nuclear) amplification, the forward primer 5'- TCGGCAGCACATATACTAA-3' and the reverse primer 5'-GAATTTGCGTGTCATCCT- 3' were used. U6 RNA served as housekeeping control, and the native EV samples (non-transfected) as a sample control. To estimate the number of copies of miR-124-3p in sEV, serial dilutions were prepared from miR-124-3p standards ranging from $2x10^{-6}$ to 20 pmol, being then correlated with respective Cq values. The resultant value, obtained in pmol, was converted to copy number by multiplication through Avogadro's constant (6.022×10^{23} mol^{-1}).

4.3.9 Treatment of sEV with RNase

SEV ($2x10^{10}$ total particles) were loaded with miR-124-Cy5 (10 pmol) through Exo-Fect™. Samples where then purified via ExoQuick as described above. Subsequently, purified sEV pellets were exposed to 2 μg/mL RNase (Sigma- Aldrich), in a final volume of 150 μL, for 30 min at RT and re-purified via ExoQuick. Finally, qPCR was performed on the RNase treated and non-treated samples.

4.3.10 sEV labelling with PKH67

sEV were labelled with PKH67 (Sigma-Aldrich, St. Louis, MO, USA) according to the manufacturer´s instructions. Briefly, 20 μg of sEV were diluted in the kit buffer (diluent C) 1:1 and then PKH67 in diluent C (1:75) was mixed with the diluted sample. Subsequently, samples were incubated at RT for 3 min, following purification by ultracentrifugation.

4.3.11 Primary SVZ cell cultures and experimental treatments

1-3 days old C57BL/6J mice were used to obtain SVZ cell cultures as previously described by us.[9] Briefly, SVZ fragments were dissected from 450 μm-thick coronal brain sections and digested in 0.025% trypsin, 0.265 mM EDTA (all from Life Technologies), followed by mechanical dissociation. The cell suspension was diluted in serum-free medium composed of Dulbecco's modified Eagle medium [(DMEM)/F12 + GlutaMAX™-l)] supplemented with 100 U/mL penicillin, 100 μg/mL streptomycin, 1% B27 supplement, 10 ng/mL EGF, and 5 ng/mL FGF-2 (all from Life Technologies) and plated onto uncoated petri dishes (Corning Life Science, NY, USA). Five to six-day-old neurospheres were then seeded onto 0.1 mg/mL poly-D-lysine- (Sigma-Aldrich) coated glass coverslips in 24-well plates in serum-free medium devoid of growth factors. SVZ cells were allowed to form a cell monolayer for two days, and then were treated with 1.5 (3 μg/mL sEV) or $3x10^9$ part/mL (6 μg/mL sEV) of sEV loaded or not with miR-124-3p or SCR or Exo-Fect™ plus miR-124-3p (the same volume as the miR-124-3p sEV condition was added). Two or seven days after the treatments, cell death and commitment or neuronal differentiation were evaluated by immunocytochemistry, respectively.

4.3.12 Propidium iodide incorporation

Propidium iodide (PI; 5 μg/mL; Sigma-Aldrich) was used to quantify the number of necrotic and late apoptotic cells. PI was added to SVZ cells 10 min before the end of the 48 h treatments, at 37°C. Thereafter, cells were fixed using 10% formalin solution, for 15 min, at RT, and then rinsed with PBS. Cell nuclei were stained with Hoechst-33342 (1:500; Life Technologies) for 5 min and then mounted in Fluoroshield Mounting

Medium (Abcam Plc.). Five random microscopic fields were acquired *per* replicate using an Axio Imager microscope (from Carl Zeiss) under a magnification of 40x.

4.3.13 Immunocytochemistry

SVZ cells were fixed with 10% formalin, washed with PBS, and then incubated in PBS containing 0.3% Triton X-100 and 3% BSA (cytoplasmatic staining) or 6% BSA (nuclear staining) for 30 min or 1 h at RT, respectively. Cells were subsequently incubated overnight at 4°C with the following primary antibodies: rabbit polyclonal anti-Ki-67 (1:50; Abcam Plc.); goat polyclonal anti-doublecortin (DCX) (1:200; Santa Cruz Biotechnology, Inc.); mouse monoclonal anti-Nestin (1:100; Abcam Plc.); mouse monoclonal anti-NeuN (1:100; Merck Millipore, Darmstadt, Germany), all prepared in 0.3% BSA and 0.1% Triton X-100. On the next day, after washing with PBS, cells were incubated for 1 h with the corresponding secondary antibody followed by Hoechst-33342 nuclear staining and then mounted in Fluoroshield mounting medium (Abcam Plc.). Secondary antibodies used were Alexa Fluor 488 donkey anti-rabbit, Alexa Fluor 546 donkey anti-goat, Alexa Fluor 594 or 647 donkey anti-mouse (all 1:200; Life Technologies), all prepared in PBS. Photomicrographs were taken using LSM 710 confocal microscope (Carl Zeiss). Analysis of immunocytochemistry experiments was performed at the border of seeded neurospheres, where cells formed a pseudo-monolayer. The experiments were performed in three independent SVZ cultures from C57BL/6 pups, and for each experimental condition at least 2 coverslips were analyzed *per* culture. Percentage of PI-positive, Ki-67$^+$/Nestin$^+$, Ki-67$^+$/DCX$^+$, and NeuN-positive cells were calculated from cell counts in five independent microscopic fields (an average of 150 cells *per* field) from each coverslip with a 40x magnification.

4.3.14 N27 cell line and experimental treatments

Immortalized N27 cell line, derived from rat mesencephalon, were grown in RPMI 1640 medium containing 2 g/L sodium bicarbonate and supplemented with 10% fetal bovine serum (FBS; Millipore), 100 IU/L penicillin, and 10 g/mL streptomycin in humidified 95% air and 5% CO_2, at 37°C. For experiments, the cells were seeded at a density of $1x10^4$ cells/well in 96-well culture plates. After 24 h cells were fed with fresh medium and treated with 50 μM 6-OHDA (Sigma-Aldrich Inc.) and/or 1.5 (3 μg/mL) or $3x10^9$ part/mL (6 μg/mL) of miR-124-3p sEV or sEV, for 24 h.

4.3.15 Cell viability assay in N27 cells

Viability of N27 cells was evaluated by using Cell Counting Kit-8 (CCK-8; Dojindo Laboratories, Kumamoto, Japan) following the manufacturer's instructions with modifications. Briefly, 24 h after the treatments, 5 μL CCK-8 solution were added to each

well. Cells were incubated in humidified 95% air and 5% CO_2, for 3 h at 37°C. The absorbance was measured at 450 nm using a microplate reader XMark™ Microplate Spectrophotometer (Bio-Rad).

4.3.16 Animals

Young adult (2- to 3-month-old) male C57BL/6 were used for this study. The experimental procedures were performed following protocols approved by the DGAV, the Portuguese National Authority for Animal Health (21/01/2019; reference number 0421/000/000/2019) and by the Directive 2010/63/EU of the European Parliament and the Council on the protection of animals used for scientific purposes. All animals were kept in appropriate cages in the same room under temperature-controlled conditions with a fixed 12 h light/dark cycle, with free access to food and water. All efforts were made to reduce the number of animals used and to minimize their suffering.

4.3.16.1 Stereotaxic injections and BrdU administration

Mice were anesthetized with an IP injection of ketamine (90 mg/kg of mouse weight) and xylazine (10 mg/kg of mouse weight) and placed in a stereotaxic apparatus (51900 Stoelting, Dublin, Ireland). The skull was exposed, and the scales were defined after setting the zero at the bregma point. Mice were then injected in the right lateral ventricle with 10 μg of miR-124-3p sEV ($2.3x10^{10}$ particles loaded with 20 pmol of miR-124-3p/mouse), SCR sEV ($2.3x10^{10}$ particles loaded with 20 pmol of SCR /mouse) non-loaded sEV (sEV; $2.3x10^{10}$ particles /mouse) or sterile 0.1 M PBS (saline) (AP: -0.5 mm; ML: -0.7 mm, DV: -2.9 mm from bregma) through a 10 μL Hamilton syringe at a speed of 0.5 μL/min in a total volume of 5 μL.[9] To find out the effect of the miR sEV formulation in a mouse model of PD, mice were subjected to another stereotaxic injection to deliver 10 μg 6-OHDA (dissolved in 0.02% of ascorbic acid) into the right striatum (AP: -0.6 mm; ML: -2.0 mm, DV: -3.0 mm from bregma) using a 10 μL Hamilton syringe at a speed of 0.2 μL/min, in a total volume of 2 μL. [9] The needle was left in place for an additional 5 min before being slowly withdrawn. After the injections, mice were kept warm (37°C) until they fully recovered from the surgery. Four experimental groups were tested: 1) “Saline mice” injected with saline both in the right striatum and in the lateral ventricle; 2) “6-OHDA” mice injected with 6-OHDA in the right striatum and saline in the lateral ventricle; 3) “sEV + 6-OHDA” mice injected with 6-OHDA in the right striatum and sEV in the lateral ventricle; 4) “miR-124-3p sEV + 6-OHDA” mice injected with 6-OHDA in the right striatum and miR-124-3p sEV in the lateral ventricle; and 4) “SCR sEV + 6-OHDA” mice injected with 6-OHDA in the right striatum and SCR sEV in the lateral ventricle. To label dividing cells, BrdU dissolved in a sterile solution of 0.9%

NaCl was administered IP (50 mg/kg of animal weight) for 3 days (every 12 h) after the stereotaxic procedure. Then, animals were maintained in appropriate cages for 4 weeks until they were euthanized. To evaluate the distribution of the sEV in the brain, mice were injected ICV with PKH67-labeled sEV ($2.3x10^{10}$ particles), as described above, and 24 h after stereotaxic injections mice were euthanized, and the brain removed for posterior analysis.

4.3.17 Behavioral studies

All behavioral tests were performed during the light cycle. Mice were transferred to the experimental room at least 20 min before the test to let them acclimatize to the environment.

4.3.17.1 Rotarod

Motor coordination, balance and grip strength function was analyzed using a mice rotarod apparatus (Ugo Basile, Italy). Rotarod test was performed at week 1 and 2 after stereotaxic injections under an accelerating protocol, starting at 4 revolutions *per* min (rpm) and reaching 40 rpm over 5 min, and the latency to fall was recorded. The trial stopped when the mouse fell (activating a switch that automatically stopped the timer) or when 5 min had been completed. Each animal was given four independent trials with a 30 min inter-trial period to reduce stress and fatigue. All mice were pre-trained on the rotarod to reach a stable performance. The training consisted of one session *per* day during 2 consecutive days under a fixed accelerating protocol. Each session included 4 separate test trials, each lasting 5 min. Mice were trained at 12 rpm on day 1 and 22 rpm on day 2. The animals were allowed to rest 30 min between each trial. Each full passive rotation performed by mice onto the rod was considered as a fall.

4.3.17.2 Apomorphine-induced rotation test

Apomorphine-induced rotation was measured at week 2 and 4 after stereotaxic injections. Mice received a subcutaneous injection of freshly prepared apomorphine hydrochloride (Sigma-Aldrich) (0.5 mg/kg), a dopamine D1/D2 receptor agonist, dissolved in 1% ascorbic acid and 0.9% NaCl. They were placed in individual round glass bowls and were allowed to adapt to their environment for 5 min before the test. After apomorphine administration, full body ipsilateral and contralateral turns were recorded using a digital camera for 45 min. Subsequently, each 360° rotation of the body axes was manually counted as a rotation. Values were expressed as a mean of net contralateral turns (equal to the number of contralateral turns minus ipsilateral turns).

4.3.18 Tissue preparation

Four weeks post-injections, mice were deeply anesthetized through ip injection of ketamine (90 mg/kg of mouse weight) and xylazine (10 mg/kg of mouse weight) and euthanized by transcardial perfusion with saline followed by 4% PFA. Following perfusion, brains were removed, post-fixed overnight with 4% PFA and cryoprotected in 30% sucrose solution. Thereafter, brains were snap-frozen in liquid nitrogen and stored at -80°C until further use. Brains were cut into 40 µm-thick coronal sections on a cryostat (Leica CM 3050S, Leica Microsystems, Germany). The sections corresponding to the striatum and SN of each animal were collected sequentially in 6 compartments of 24-well plate containing cryopreservation solution and stored at -20°C until processing for immunohistostaining.

4.3.19 Immunohistochemistry

Free-floating coronal brain sections were rinsed in PBS-Tween 20 (PBS-T) and then incubated with 10% FBS and 0.1% Triton X-100 in PBS for at least 1 h at RT. Endogenous peroxidase activity was inhibited by incubation with 3% hydrogen peroxide in water for 10 min at RT and the sections were then washed with PBS-T. Sections were incubated with primary antibody mouse anti-TH (1:2500; BD Biosciences) diluted in PBS containing 5% FBS, overnight at 4°C. After several rinses with PBS-T, sections were incubated with a biotinylated goat anti-mouse secondary antibody (dilution 1:200; Vector Laboratories, Burlingame, CA, USA) diluted in PBS containing 1% FBS for 1 h at RT. The avidin-biotin peroxidase complex reagent (Vectastain ABC KIT, Vector Laboratories Inc., Burlingame, CA, USA) was then added for at least 30 min at RT. The reaction product was visualized using DAB chromogen/HRP substrate-buffer (Dako) until color develops (5-10 min). The reaction was stopped by adding TBS. Sections were mounted on slides, dried, and dehydrated in graded ethanol dilutions, cleared in xylene and cover slipped using a permanent mounting medium (Entellan, Merck, NJ, USA). Quantitative analysis of dopaminergic neurons in SN was carried out by serial section analysis of the total number of TH-positive neurons throughout the rostro-caudal axis. The region corresponding to the ipsilateral SN *pars compacta* was carefully delineated and the total number of TH-positive neurons in the full extent of this structure was counted *per* section. The total number of TH-positive neurons for each representative mesencephalic section was quantified in four coronal sections *per* mouse from -2.80 to -3.88 mm relative to bregma, under the magnification of 10x at the Axio Imager A1 microscope (Carl Zeiss, Germany). Quantitative analysis of the intensity and area occupied by TH-positive fibers staining in striatum was carried out in 4 coronal sections of ipsilateral striatum, from 1.34 to 0.38 mm relative to bregma of each mouse, selected

throughout the rostro-caudal axis, under the magnification of 5x at the Axio Imager A1 microscope.

For BrdU staining, tissue sections were rinsed in PBS and incubated with 2 M HCl for 25 min at 37°C to induce DNA denaturation and exposure of BrdU. Tissue sections were then incubated in blocking solution 2% of horse serum (Life Technologies) and 0.3% Triton X-100 in PBS, for 2 h at RT, followed by a 48 h incubation at 4°C with the following primary antibodies: rat monoclonal anti-BrdU (1:500, AbD Serotec, Raleigh, NC, USA) and mouse monoclonal anti-NeuN (1:1000, Merck Millipore). Thereafter, sections were incubated for 2 h at RT with Hoechst-33342 (1:10,000) and the respective secondary antibodies: Alexa Fluor 488 donkey anti-rat and Alexa Fluor 594 donkey anti-mouse (all 1:1000; from Life Technologies). Then, a simplified version of this protocol was used for sEV distribution/location studies. Briefly, 40 μm-thick coronal sections were incubated in a blocking solution for 2 h at RT and then incubated for 48 h at 4°C with the mouse anti-TH (1:1000, BD Biosciences). Thereafter, sections were incubated for 2 h at RT with Hoechst (1:10,000) and the secondary antibody, Alexa Fluor 594 donkey anti-mouse (1:1000, Abcam Plc.). Finally, sections were mounted in Fluoroshield mounting medium (Abcam Plc.). Photomicrographs were obtained using LSM 710 confocal microscope. Quantification of NeuN/BrdU-double positive cell number was performed in the striatum of 3 animals, as described previously by us [9]. Two different Z axis-positions (40x magnification) from 9 fields from 4 slices spaced by 240 μm each were counted *per* animal.

4.3.20 Statistical analysis

The software used for cell counting and quantification of TH staining in the striatum was FIJI ImageJ (NIH Image, Bethesda, MD, USA). Data were expressed as mean ± SEM of at least three independent experiments performed in triplicate (*in vitro* experiments) or at least three different animals (*in vivo* experiments). The percentage of the number of PI-positive cells (Figure 4.4 B), Ki-67-positive cells (Figure 4.5 A) and NeuN-positive cells (Figure 4.5 D) was calculated relative to the number of total cells; the percentages of Nestin-positive cells (Figure 4.5 B) and of DCX-positive cells (Figure 4.5 C) were calculated relative to the total number Ki-67-positive cells. The controls (untreated cultures) were set to 100% in all analysis except for the evaluation of cell viability (PI, Figure 4.4 B). Statistical analysis was performed using GraphPad Prism 7 software (GraphPad, San Diego, CA, USA), by using one- or two-way ANOVA followed by Tukey's or Sidak's test, respectively, or by unpaired, two-tailed t-test. Values of $p < 0.05$ were considered significant.

4.4 Results

4.4.1 Characterization of hUCB-MNC-derived sEV

Native sEV were collected from hUCB-MNC by differential ultracentrifugation method [17]. NTA showed a canonical size distribution profile of the native sEV with an average size of 131 nm (Figure 4.1 A). Native sEV showed an average zeta potential of -25 mV, while sEV transfected with the Exo-Fect™ Exosome Transfection Reagent and a fluorescently labelled miR-124-3p-Cy5 had a zeta potential of -15 mV (Figure 4.1 B). The sEV structure was also characterized by TEM. Native sEV structure was found to be canonical, with the double membrane structure clearly observable around cup-shaped particles. The transfection of sEV with Exo-Fect™ and miR-124-3p-Cy5 preserved its morphological structure, but induced some aggregation (Figure 4.1 C), probably due to the Exo-Fect™ treatment, as recently reported by us [17]. To confirm that samples were enriched in sEV, we performed western blot analysis for common EV markers and potential contaminants in hUCB-MNC and native sEV samples. Figure 4.1 D shows that sEV derived from two donors expressed CD9, CD63 and heat shock protein 70 (HSP70), although their expression level seems to be donor-dependent. Calnexin, a marker of endoplasmic reticulum and ApoA-1, a component of high-density lipoproteins, were not detected in sEV samples (Figure 4.1 D) but as expected, detected in hUCB-MNC samples (Figure 4.1 E). Altogether, these results showed that our samples were enriched in sEV. Next, the loading efficiency of the sEV with miR-124-3p-Cy5 was assessed via fluorescence measurement. After the purification step, the sample was separated into a pellet (where sEV are localized) and a supernatant (where non-bound miR-124-3p-Cy5 is found). Note that only a residual signal was detected in the pellet and supernatant of samples of non-loaded sEV. When comparing the overall proportion of fluorescence in sEV + miR-124-3p-Cy5 pellet and sEV + miR-124-3p-Cy5 supernatant fractions, we found that the signal intensity present in the sEV pellet is higher than that of the supernatant (Figure 4.2 A). When comparing the overall proportion of fluorescence in each fraction, we found that 74% of the signal was present in the sEV fraction, whereas the remainder was in the supernatant (Figure 4.2 B). Therefore, most of the miR-124-3p was immobilized in sEV. Then, we quantified miR-124-3p in the loaded sEV by RT-qPCR (Figure 4.2 C). Relative to native sEV, there was a fold change increase in enriched sEV of over 1,000,000 times. Note that the amount of miR-124-3p in the native sEV is residual (Figure 4.2 C, D). To assess whether the loaded miR-124-3p was exposed or accessible to nucleases after Exo-Fect™ transfection, sEV loaded with miR-124-3p were treated with RNase. The RNase treatment did not change miR-124-3p levels in Exo-Fect™-modulated miR-124-3p sEV (Figure 4.2 D).

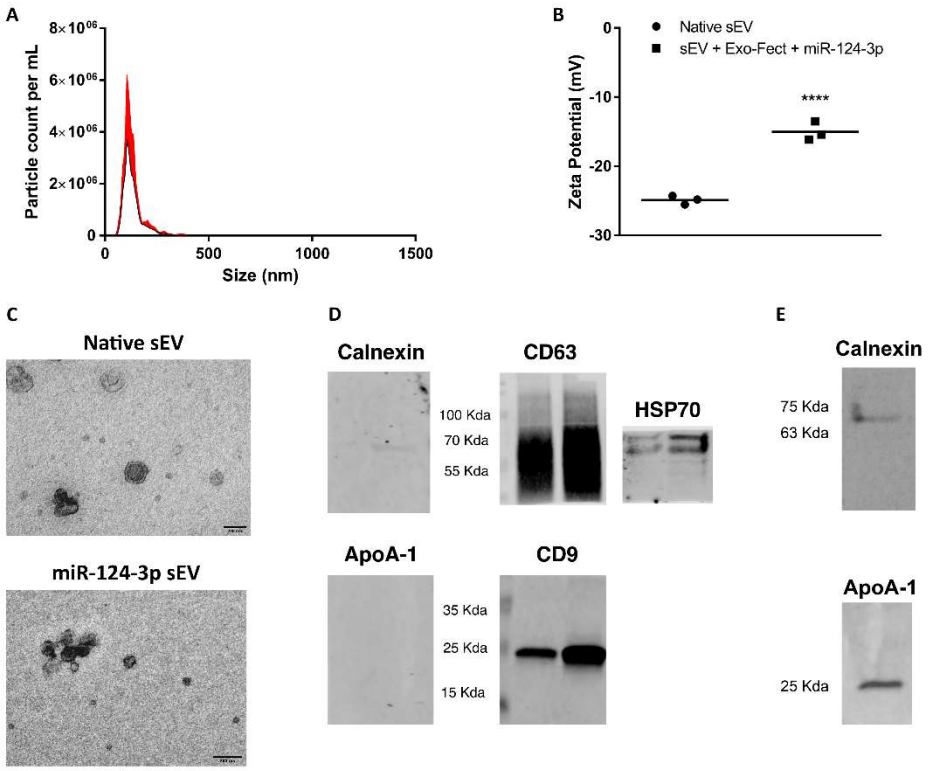

Figure 4.1. sEV characterization. (A) Size and particle concentration of sEV collected from human umbilical cord blood-derived mononuclear cells (hUCB-MNC), evaluated by NTA. **(B)** Zeta potential analysis of sEV before and after loading with miR-124-3p (miR-124-3p sEV). **(C)** Representative TEM images of native sEV and sEV enriched with miR-124. Scale bar: 200 nm **(D)** Common native sEV markers (CD63, CD9 and HSP70) and potential contaminants (calnexin and ApoA-1) were further analyzed by Western Blot, where each lane represents a different donor (n=2). **(E)** Non-EV markers were found in hUCB-MNC samples but not in (D) native sEV samples. One donor was used. For all other analyzes, n = 3 biological replicates. Statistical significance was calculated using two-way ANOVA with Sidak's correction, $p \leq 0.05$. Abbreviations: sEV: Small extracellular vesicles; NTA: Nanoparticle Tracking Analysis; miR-124-3p sEV: miR-124 enriched small extracellular vesicles; TEM: Transmission Electron Microscopy. [18]

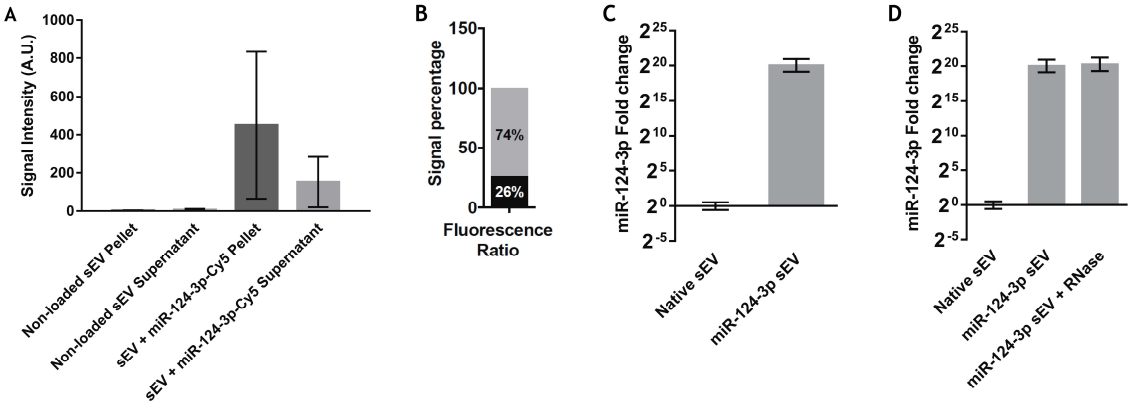

Figure 4.2. Modulation and loading of sEV with miR-124 by transfection with Exo-Fect™. (A) sEV (non-loaded or loaded with miR-124-3p-Cy5) were purified and the fluorescence of the pellet (sEV) and supernatant (leftover probe) were quantified. **(B)** After the loading protocol, the signal intensity in the sEV fraction (pellet) corresponded to over 74% of the total fluorescence observed in the sample. Loading efficiency in panel B was calculated using the formula: fluorescence intensity of the pellet/(fluorescence intensity of the pellet + fluorescence intensity of the supernatant). **(C)** qPCR against miR-124 in modified sEV showed an increase in miR-124 of over 1,000,000 times the control. **(D)** sEV loaded with Exo-Fect™ and miR-124 were treated with RNase, re-purified and miR-124 levels in the vesicles were quantified by qPCR. RNase treatment does not change miR-124 levels in sEV. For all the experiments, n = 3. For the qPCR analysis, U6 was used as housekeeping gene. Abbreviations: sEV: Small extracellular vesicles. Adapted from [18].

We also estimated that the number of miR-124-3p copies in 6.90 x 10^9 or 1.38 x 10^{10} sEV is 6.022 x 10^6 and 1.2 x 10^7 copies for native sEV (not transfected by Exo-Fect™) or 1.39 x 10^{11} and 2.78 x 10^{11} copies for miR-124-3p sEV, respectively (Figure 4.3). Thus, the number of miR-124-3p copies *per* native sEV is approximately 8.7 x 10^{-4}, i.e., 8.7 copies per 10 000 sEV while the number of miR-124-3p copies per miR-124-3p-transfected sEV is approximately 20 copies *per* sEV (Figure 4.3). These data suggest that miR-124-3p was either incorporated into the lumen or was entrapped in the membrane of sEV, therefore inaccessible to nucleases.

A

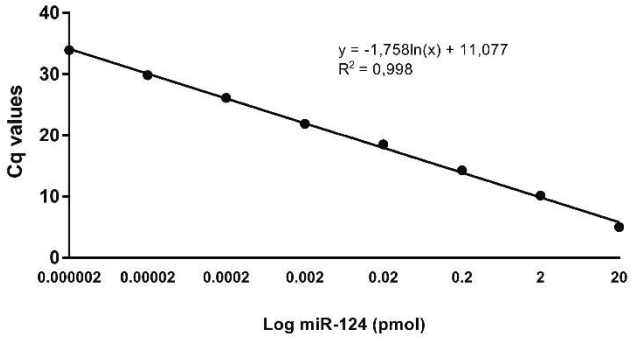

miR-124-3p (pmol)	Average Cq
0,000002	33,94
0,00002	29,85
0,0002	26,16
0,002	21,92
0,02	18,51
0,2	14,29
2	10,13
20	5,02

Sample	Average Cq (3 µg sEV)	Estimated miR-124 quantity (pmol)
Native sEV	31,97	0,00001
miR-124-3p sEV	13,69	0,23

B

Sample	Estimated miR-124 copies number		
	3 µg sEV (6.90 x 10^9 particles)	6 µg sEV (1.38 x 10^{10} particles)	10 µg sEV (2.30 x 10^{10} particles)
Native sEV	6.022 x 106	1.2 x 10^7	2 x 10^7
miR-124-3p sEV	1.39 x 10^{11}	2.78 x 10^{11}	4.6 x 10^{11}

Figure 4.3. Copies number extrapolation of miR-124 in sEV. (A) Calibration curve of miR-124-3p. Correlation analysis between Cq values and log amount of 10-fold serially diluted miR-124-3p (pmol). Each point represents the mean value of duplicate measurements. **(B)** miR-124 copy number extrapolation. Copies number of miR-124 endogenously present in native sEV or loaded into miR-124-3p sEV were extrapolated using (**A**) calibration curve of synthetic miR-124-3p. The resultant **(A)** value of miR-124 (pmol) was converted to miRNA molecules by multiplication through Avogadro's constant (≈ 6.022 x 10^{23} mol^{-1}). Abbreviations: pmol: picomol; miR-124-3p sEV: miR-124-3p-loaded small extracellular vesicles; Cq: quantification cycle. [18]

4.4.2 miR-124-3p sEV induced neuronal differentiation *in vitro*

Previously, we have shown that miR-124 loaded into polymeric NP was able to boost neurogenesis and the migration of new neurons into the 6-OHDA-lesioned striatum [9]. Based on these findings, we evaluated the ability of miR-124-3p sEV to induce neurogenesis *in vitro* by using primary SVZ NSC cell cultures. First, we showed that sEV efficiently deliver miR-124-3p-Cy5 (1.5x10^{10} particles (part)/mL) to SVZ cells, which localize preferentially as aggregates near cell nuclei (Figure 4.4 A). Then, based on preliminary studies, we tested the effects of two doses, 1.5x10^9 part/mL and 3x10^9 part/mL of native sEV (sEV), miR-124-3p sEV or scrambled (SCR) sEV in SVZ

neurogenesis *in vitro*. We have found that both sEV (3x10⁹ part/mL: $p < 0.05$; n = 6) and miR-124-3p sEV (1.5x10⁹ part/mL: $p < 0.05$; 3x10⁹ part/mL: $p < 0.01$; n = 7) significantly reduced basal cell death (Figure 4.4 B, C; mean absolute value in untreated control cultures: 22.4%, SEM: 1.1), as detected by the propidium iodide assay.

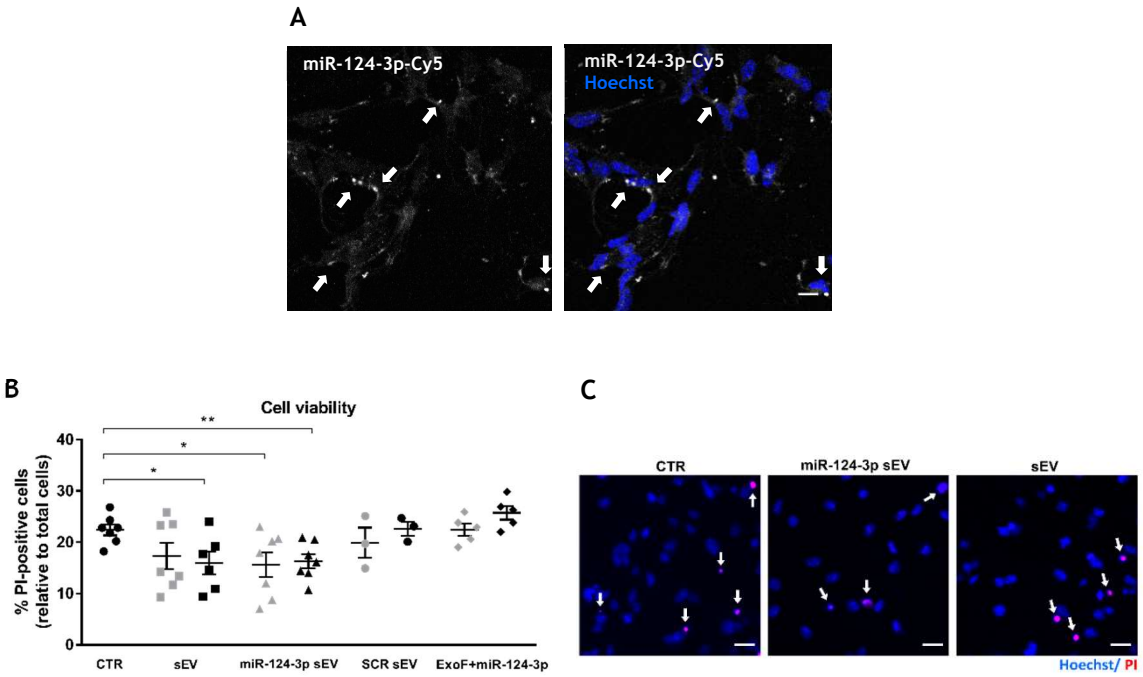

Figure 4.4. miR-124-3p-Cy5 are efficiently delivered by sEV into SVZ NSC and reduce NSC basal death. (A) Representative confocal images of SVZ NSC after treatment with 1.5x10¹⁰ particles/mL of miR-124-3p-Cy5 sEV for 4h (miR-124-3p-Cy5 is shown in gray and highlighted by white arrows). **(B)** Cell survival was evaluated in SVZ NSC treated with sEV transfected or not with miR-124 or scramble (SCR) using Exo-Fect™. Two doses of sEV were used: 1.5x10⁹ (gray symbols) or 3x10⁹ particles/mL (black symbols). An additional control was done by incubating cells with Exo-Fect™ and miR-124-3p in the absence of sEV (ExoF+miR-124). **(C)** Representative fluorescence photomicrographs of dead NSC (white arrows) in control (CTR) cultures and in 3x10⁹ particles/mL of sEV or miR-124-3p sEV-treated cultures. Nuclei are shown in blue, Ki-67 in green, Nestin in gray. Cell viability **(B, C)** was evaluated by PI incorporation. Cell nuclei were counterstained with Hoechst and shown in blue and PI in red. Scale bar: **(A)** 10 µm and **(C)** 20 µm. Data are expressed as mean ± SEM (n = 3–7). $^{**}p < 0.01$ and $^{*}p < 0.05$ vs control, using unpaired, two-tailed t-test. Abbreviations: SVZ NSC: subventricular zone neural stem cells; CTR: control; sEV: non-loaded small extracellular vesicles; miR-124-3p sEV: miR-124-3p-loaded small extracellular vesicles; SCR: Scramble miR; ExoF: Exo-Fect™; PI: propidium iodide; DCX: doublecortin. Adapted from [18].

The SVZ NSC culture is a mixed primary cell culture containing immature neural stem/progenitor cells (NSC/NPC) in distinct neuronal and glial lineages stages [9,19,20]. In the NSC untreated cultures used in this study (controls), proliferating cells labeled with Ki-67 represent about 16.6% (mean absolute value; Figure 4.5 A, SEM: 2.6) of the total number of cells. Among the Ki-67-positive cell pool, immature NSC/NPC labeled with Nestin represent about 53.2% (mean absolute value; Figure 4.5 B; SEM: 1.5), and immature neurons labeled with DCX represent about 34.3% (mean absolute value; Figure 4.5 C; SEM: 3.6). Moreover, control cultures showed about 20.6% NeuN-labeled mature neurons (mean absolute value; Figure 4.5 D; SEM: 1.5) of the total number of

cells. The mean absolute values of untreated cultures were then set to 100%. Next, we evaluated the effects of sEV on SVZ cell proliferation and neuronal differentiation. Overall, total cell proliferation, analyzed by the labeling against Ki-67, was not affected by sEV or miR-124-3p sEV as compared with control cultures (Figure 4.5 A). Then, we analyzed the effect of sEV in the proliferation of immature cells by performing co-labeling against Nestin or DCX a marker for newly born neurons, 48 h after treatments. As shown in Figure 4.5, miR-124-3p sEV reduced significantly the proliferation of NSC/NPC, at both doses ($Nestin^+/Ki\text{-}67^+$; Figure 4.5 B, F; $1.5x10^9$ part/mL; n = 6: $p < 0.05$ and $3x10^9$ part/mL; $p < 0.001$; n = 3), while native sEV significantly reduced the proliferation of NSC/NPC at the dose of $3x10^9$ part/mL ($Nestin^+/Ki\text{-}67^+$; Figure 4.5 B; $p < 0.001$; n = 3). Regarding the proliferation of newly born neurons, we found no significant effect in SVZ cells treated with miR-124-3p sEV ($DCX^+/Ki\text{-}67^+$; Figure 4.5 C, F; n = 5), comparing with control cultures (n = 6), while native sEV significantly reduced the proliferation at both doses ($DCX^+/Ki\text{-}67^+$; Figure 4.5 C, G; $1.5x10^9$ part/mL: $p < 0.01$ and $3x10^9$ part/mL: $p < 0.05$; n = 5). No significant effect was observed in the proliferation of NSC/NPC or newly born neurons in SVZ cells treated with SCR sEV (Figure 4.5 B and C respectively; n = 3), compared with control cultures. Then, to evaluate the effect on neuronal differentiation, SVZ cells were cultured in the presence of sEV for 7 days and processed for immunostaining against NeuN, a neuronal-specific nuclear protein. We have found that miR-124-3p sEV increased the percentage of NeuN-positive cells as compared with control cells (n = 7) (Figure 4.5 D, G; $1.5x10^9$ part/mL, n = 6, and $3x10^9$ part/mL, n = 5: $p < 0.0001$), SCR sEV- (Figure 4.5 D; $1.5x10^9$ part/mL, n = 3: $p < 0.01$ and $3x10^9$ part/mL, n = 3: $p < 0.05$) or sEV-treated cells (Figure 4.5 D; $1.5x10^9$ part/mL: $p < 0.001$, n = 3) by about 1.8-fold. This effect in neuronal differentiation was dependent on miR-124-3p because native sEV and SCR sEV did not alter the number of NeuN-positive cells (Figure 4.5 D). To exclude the effect of the transfection agent *per se*, SVZ cultures were also treated with Exo-Fect™ and miR-124-3p, in the absence of sEV. This treatment did not change cell survival (Figure 4.4 B), cell commitment (Figure 4.5 B, C) and neuronal differentiation (Figure 4.5 D) as compared to the control. Altogether, data suggest that miR-124-3p sEV induce neuronal differentiation of NSC *in vitro*.

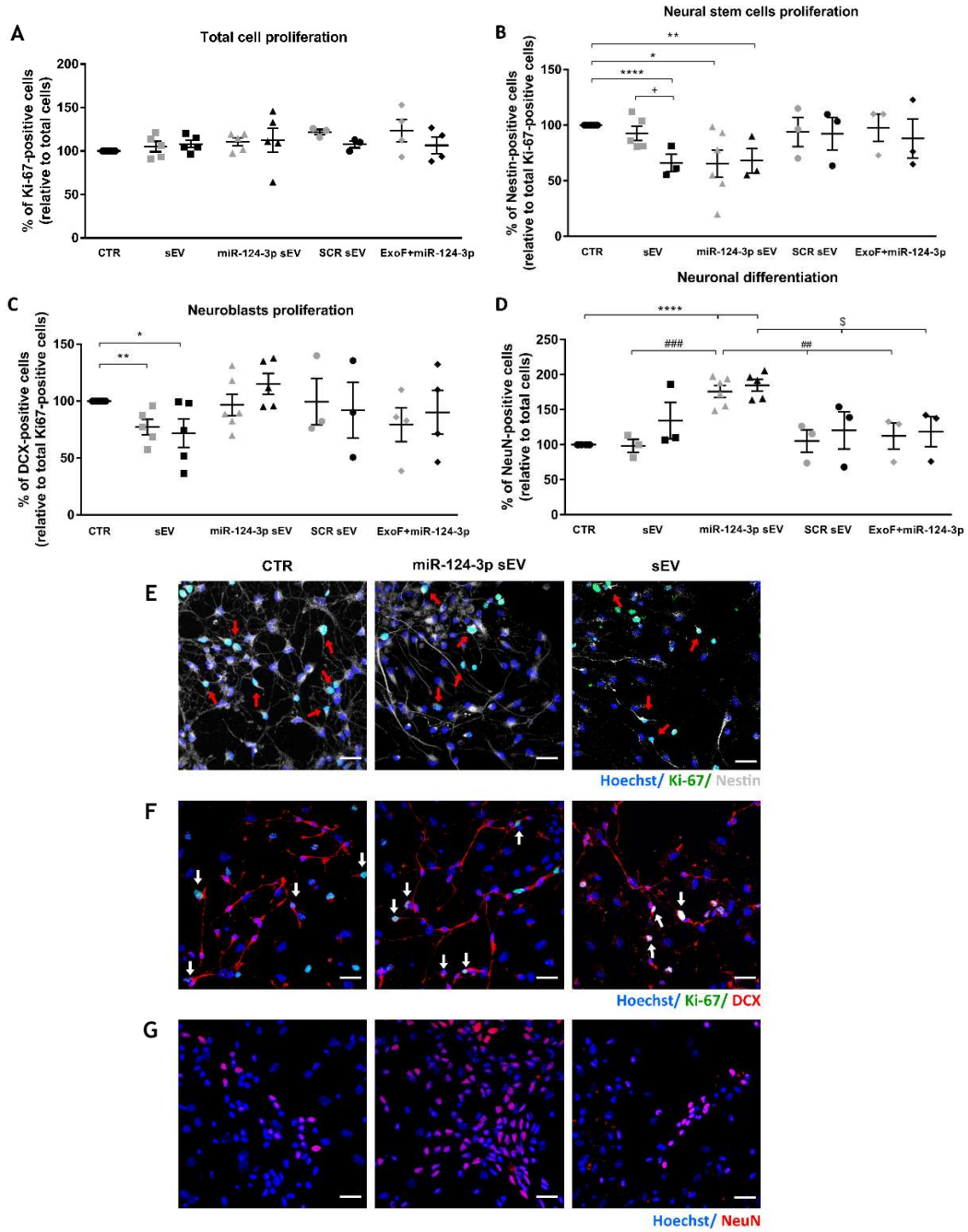

Figure 4.5. miR-124-3p sEV reduce immature cells proliferation while increase neuronal differentiation. Cell proliferation **(A)**, cell commitment **(B, C, E, F)** and neuronal differentiation **(D, G)** was evaluated in SVZ cells treated with sEV transfected or not with miR-124-3p or scramble (SCR) using Exo-Fect™. Two doses of sEV were used: 1.5x10^9 (gray symbols) or 3x10^9 particles/mL (black symbols). An additional control was done by incubating cells with Exo-Fect™ and miR-124-3p in the absence of sEV (ExoF+miR-124-3p). Representative fluorescence photomicrographs of proliferating NSC stained against Nestin/Ki-67 (**E**; red arrows), proliferating neuroblasts stained against DCX/Ki-67 (**F**; white arrows), and **(G)** mature neurons stained against NeuN in control (CTR) cultures and in 3x10^9 particles/mL of sEV or miR-124-3p sEV-treated cultures. Nuclei are shown in blue, Ki-67 in green, Nestin in gray, and DCX and NeuN in red. Scale bar: 20 µm. Proliferation of **(E)** NSC and **(F)** neuroblasts was evaluated by colocalization against Ki-67 and Nestin or DCX, respectively, 2 days after treatments. **(G)** Neuronal differentiation was evaluated by staining against NeuN, 7 days after treatments. Data are expressed as a percentage of control (mean ± SEM; n = 3–7). $^{****}p < 0.0001$, $^{**}p < 0.01$ and $^{*}p < 0.05$ vs control, $^{+}p < 0.05$ vs 1.5x10^9 particles/mL sEV, $^{###}p < 0.001$, and $^{##}p < 0.01$ vs 1.5x10^9 particles/mL miR-124-3p sEV and $^{\$}p < 0.05$ vs 3x10^9 particles/mL miR-124-3p sEV, using unpaired, two-tailed t-test. Abbreviations: SVZ NSC: subventricular zone neural stem cells; CTR: control; sEV: non-loaded small extracellular vesicles; miR-124-3p sEV: miR-124-3p-loaded small extracellular vesicles; SCR: Scramble miR; ExoF: Exo-Fect™; DCX: doublecortin. Adapted from [18].

4.4.3 miR-124-3p sEV do not increase the number of newly born neurons found in the 6-OHDA lesioned striatum *in vivo*

To evaluate the functional effects of miR-124-3p sEV *in vivo*, 20 pmol of miR-124-3p *per* $2.3x10^{10}$ particles (10 μg of sEV) were injected into the right lateral ventricles of adult C57BL/6 mice (Figure 4.6 A) as previously described by us [9]. In accordance with Figure 4.3 B, the number of miR-124-3p copies in $2.3x10^{10}$ sEV of native sEV or miR-124-3p sEV (10 μg sEV) is 2×10^7 and 4.6×10^{11} copies, respectively. First, we performed a qualitative evaluation of the biodistribution of sEV 24 h after the ICV injection of hUCB-MNC-derived sEV labeled with PKH67, a fluorescent membrane lipophilic dye commonly used to label sEV [17,21]. PKH67-labeled sEV were detected lining the SVZ (Figure 4.6 B.1) of both lateral ventricles and in the striatal parenchyma, at the vicinity of the intraventricular injection. Importantly, sEV were also detected in midbrain sections (Figure 4.6 B.2), mainly in the aqueduct, but also in the SN co-localizing with TH-positive dopaminergic neurons (Figure 4.6 B.3), the most susceptible neuronal population in PD. Then, we evaluated the ability of miR-124-3p sEV to trigger the migration of new neurons likely derived from SVZ into the 6-OHDA-lesioned striatum, the most likely regenerative response in PD [9]. Consistent with our previous study [9], the striatal administration of 6-OHDA increased the number of newly born neurons ($NeuN^+/BrdU^+$) found in the lesioned striatum, compared with saline-treated mice (Figure 4.6 C, D; mean absolute value in saline-treated mice: 9.37%, SEM: 1.2; $p < 0.05$, n = 3). A similar increase was observed in 6-OHDA-lesioned mice administered with scramble-loaded sEV (SCR sEV; $p < 0.01$, n = 3). However, the ICV administration of miR-124-3p sEV did not alter the number of newly born neurons in the lesioned striatum as compared with saline-treated mice (n = 3) (Figure 4.6 C, D). These results suggest that our formulation does not increase the number of newly born neurons in the lesioned striatum of 6-OHDA-treated mice.

4.4.4 miR-124-3p sEV promote neuroprotection against 6-OHDA-induced toxicity in PD models

Before proceeding to the *in vivo* studies, we first analyzed the internalization of hUCB-MNC-derived sEV labeled with PKH67 (sEV-PKH67; $1.5x10^{10}$ particles/mL), and sEV loaded with Cy5-labeled miR-124-3p (miR-124-3p-Cy5 sEV; $1.5x10^{10}$ particles/mL) in N27 DA cells by confocal analysis. We have found that after 4 h, sEV-PKH67 were efficiently internalized by cells (Figure 4.7 A) and miR-124-Cy5 were efficiently delivered by sEV to N27 DA cells being located preferentially in the vicinity of cell nuclei (Figure 4.7 B).

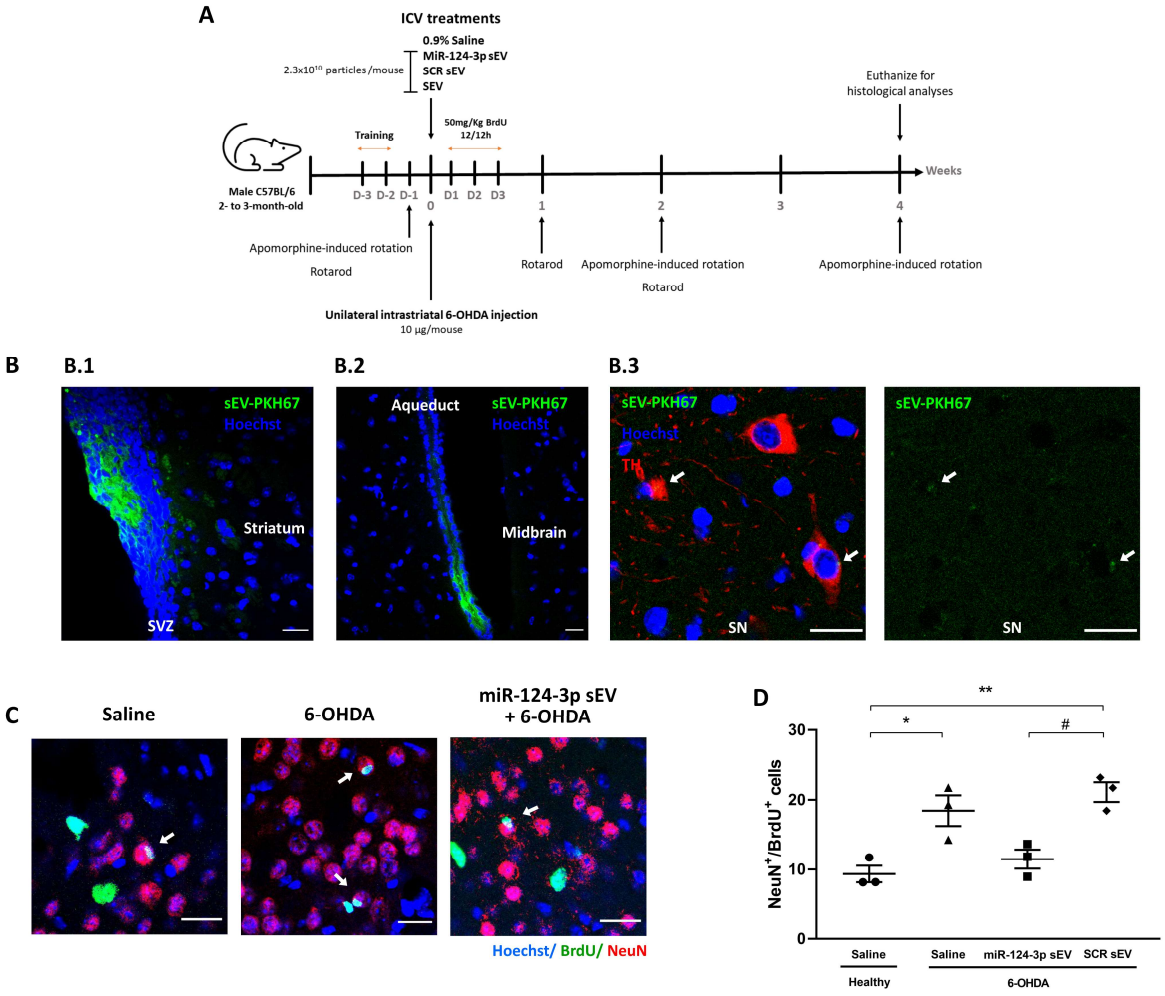

Figure 4.6. miR-124-3p sEV do not increase the number of SVZ-derived newly born neurons in the lesioned striatum of 6-OHDA-treated mice. (A) Design and timeline of the animal experimental procedure. Male C57Bl/6 mice were subjected to unilateral injection of 6-OHDA into the right striatum followed by an ICV injection with miR-124-3p sEV, SCR sEV, sEV, or saline. Then, mice received BrdU injections (every 12 h) during the following 3 day after surgery. Behavioral tests were performed on day -1, and on weeks 1, 2 and 4 after stereotaxic injections. After 4 weeks mice brains were collected for histological processing. **(B)** Representative confocal photomicrographs of **(B.1)** SVZ, striatal and **(B.2, B.3)** midbrain parenchyma 24 h after ICV injection of non-loaded sEV labeled with PKH67 (sEV-PKH67; shown in green). White arrows show sEV-PKH67 close to the cell nuclei. TH labeling (red) depicts dopaminergic neurons in the SN and nuclei are counterstained with Hoechst (blue). Scale bar: 20µm. **(C)** Representative confocal digital images of BrdU (green), NeuN (red), and Hoechst (blue) staining observed in the striatum of saline, 6-OHDA-treated mice or miR-124-3p sEV-treated 6-OHDA mice. Scale bar: 20 µm; white arrows highlight $NeuN^+/BrdU^+$ cells. **(D)** The bar graph depicts the total number of $NeuN^+BrdU^+$ cells found in the striatum of mice 4 weeks after treatments. Data are expressed as mean ± SEM, n = 3 mice. $^{**}p < 0.01$ and $^{*}p < 0.05$ vs. saline-treated mice (control); $^{\#}p < 0.05$ vs. miR-124-3p sEV-treated 6-OHDA-lesioned mice group using one-way ANOVA followed by Tukey's multiple comparison test. Abbreviations: 6-OHDA: 6-hydroxydopamine; SCR sEV: scramble-loaded small extracellular vesicles; sEV: non-loaded small extracellular vesicles; miR-124-3p sEV: miR-124-3p-loaded small extracellular vesicles; ICV: intracerebroventricular; BrdU: 5-bromo-2'-deoxyuridine; SN: substantia nigra; TH: tyrosine hydroxylase; SVZ: subventricular zone. [18]

Then, we evaluated the putative neuroprotective effect of miR-124-3p sEV in an *in vitro* model of PD using the CCK-8 assay. The viability of N27 DA cells decreased about 30% after exposure to 50 µM 6-OHDA for 24 h, while the concomitant treatment with $3x10^9$ part/mL miR-124-3p sEV was able to protect cells from 6-OHDA-induced toxicity

(Figure 4.7 C; $p < 0.05$, n = 3). Native sEV ($1.5x10^9$ part/mL: n = 3; $3x10^9$ part/mL: n = 2) did not promote neuroprotection, suggesting that the protective effect was due to miR-124-3p and not to the sEV itself. Moreover, none of the sEV formulations *per se* were toxic to DA cells (Figure 4.7 C).

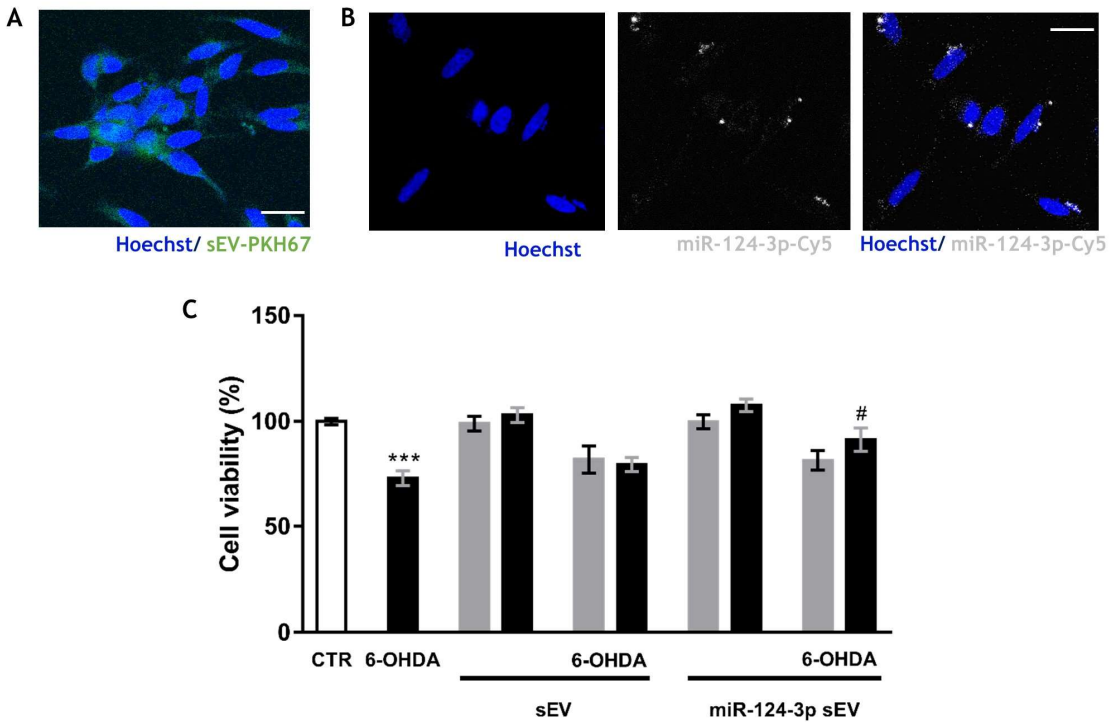

Figure 4.7. miR-124-3p sEV are internalized promoting neuroprotection against 6-OHDA-induced toxicity in N27 rat dopaminergic cells. (A) Representative photograph of N27 rat dopaminergic cell line after 4h treatment with $1.5x10^{10}$ particles/mL of **(A)** sEV-PKH67 (green) or **(B)** miR-124-3p-Cy5 sEV (miR-124-3p-Cy5 is shown in gray). Nuclei are shown in blue. Scale bar: 20 µm. **(C)** miR-124-3p sEV counteract dopaminergic cell death induced by 6-OHDA. Cell viability was assessed in N27 rat dopaminergic neural cell line exposed to 50 µM 6-OHDA and $1.5x10^9$ (gray bars) or $3x10^9$ particles/mL (black bars) of sEV or miR-124-3p SEV for 24h, by the CCK-8 kit assay. Data are expressed as a percentage of control (mean ± SEM; n=3 in all experimental conditions except for sEV + 6-OHDA at $3x10^9$ particles/mL: n = 2), from three independent experiments performed in triplicate. $^{***}p < 0.0001$ vs. control and $^{\#}p < 0.05$ vs. 6-OHDA-treated cells, using one-way ANOVA followed by Dunnett's multiple comparison test. Abbreviations: CTR: control; sEV: native small extracellular vesicles; miR-124-3p sEV: miR-124-3p-loaded small extracellular vesicles; 6-OHDA: 6-hydroxydopamine. Adapted from [18].

Next, we validated these results using the 6-OHDA-induced PD model *in vivo*. In accordance with *in vitro* studies, miR-124-3p sEV treatment fostered significant neuroprotection of dopaminergic neurons, as detected by the number of TH-positive neurons compared to the 6-OHDA-lesioned group (Figure 4.8 A, B; $p < 0.001$, n = 4). Also, the 6-OHDA injection caused a significant decrease in the intensity and percentage of area occupied by TH-positive fibers in the striatum as compared to saline-treated animals (set to 100%, n = 4) (Figure 4.8 A, C*;* $p < 0.0001$) while the exposure to miR-124-3p sEV significantly reduced the loss of TH staining in striatal fibers (Figure 4.8 A,

C; intensity and % area: $p < 0.01$, n = 4). As expected, the treatment with SCR sEV did not protect striatal TH-positive fibers and TH-positive neurons in SN from 6-OHDA-induced toxicity, suggesting that miR-124-3p is responsible for the neuroprotection of the nigrostriatal pathway in lesioned animals. Altogether, these results suggest that the administration of miR-124-3p sEV effectively protected dopaminergic neurons against the toxicity induced by 6-OHDA.

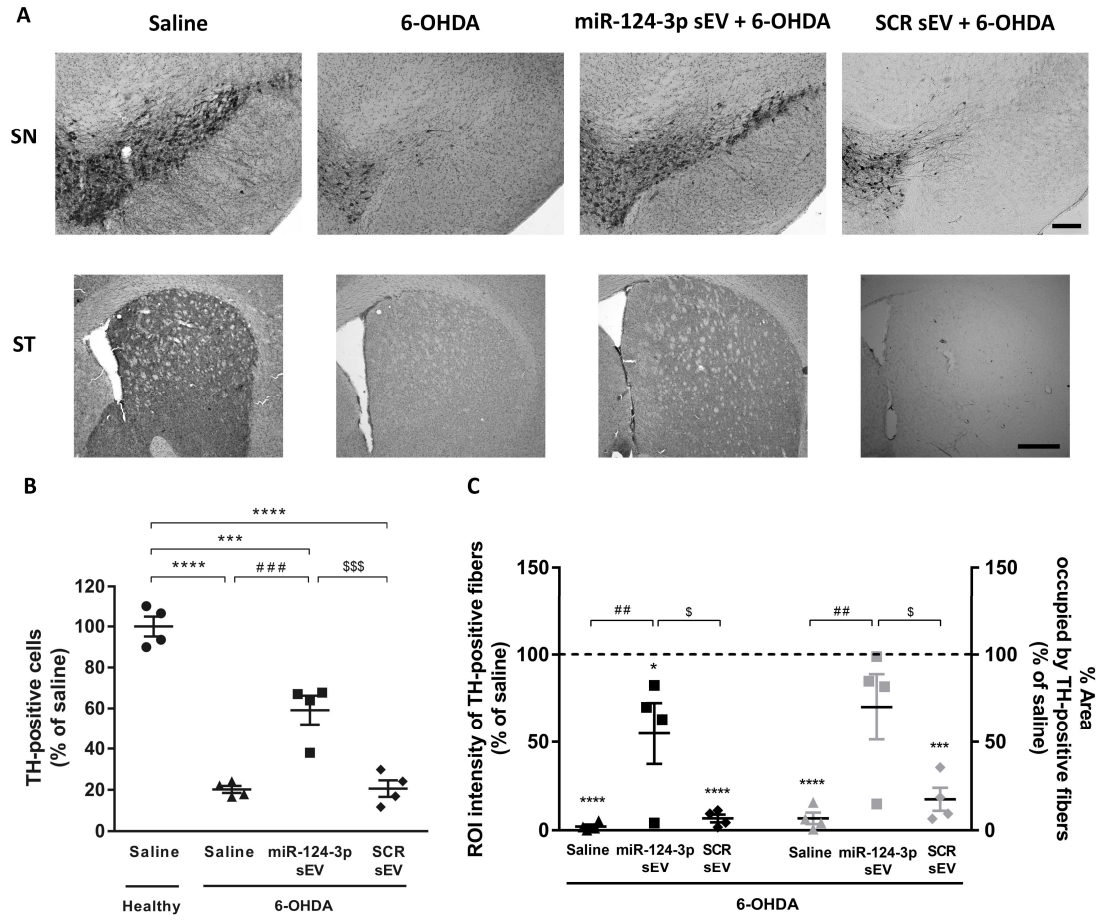

Figure 4.8. miR-124-3p sEV counteract dopaminergic degeneration induced by 6-OHDA. (A) Representative photomicrographs of SN and striatal sections immunostained for TH. Scale bar: 200 µm and 500 µm, respectively. **(B, C)** Quantitative analysis of **(B)** TH^+ cells in the SN and **(C)** intensity and area occupied by TH^+ fibers, 4 weeks after stereotaxic injections (Black symbols: Intensity; Gray symbols: % Area). Data are expressed as mean ± SEM, n = 4 mice. $^{****}p < 0.0001$, $^{***}p < 0.001$ vs. saline-treated mice (control; **(C)** set to 100%); $^{\#\#\#}p < 0.001$ and $^{\#\#}p < 0.01$ vs. 6-OHDA-lesioned mice group, $^{\$\$\$}p < 0.001$ and $^{\$}p < 0.05$ vs. miR-124-3p sEV + 6-OHDA-lesioned mice group using one-way ANOVA followed by Tukey's multiple comparison test. Abbreviations: 6-OHDA: 6-hydroxydopamine; SCR sEV: scramble-loaded small extracellular vesicles; sEV: non-loaded small extracellular vesicles; miR-124-3p sEV: miR-124-3p-loaded small extracellular vesicles; TH: tyrosine hydroxylase; SN: substantia nigra; PD: Parkinson's disease. [18]

4.4.5 miR-124-3p sEV counteracted PD-related motor deficits in the 6-OHDA mouse model

To unveil if our formulation counteracts the motor symptoms of 6-OHDA-lesioned mice, we performed the rotarod and apomorphine-induced rotation behavioral tests (Figure 4.6 A). These tests, widely used in PD models, evaluate motor function, balance, and grip strength (rotarod) and nigrostriatal dopamine depletion (apomorphine-induced rotation test). In the rotarod test, the latency time to fall off from the rod was reduced in 6-OHDA-lesioned mice (n = 5) compared to saline-treated mice (n = 4) (about 70% of saline) (Figure 4.9 A; $p < 0.0001$). Notably, the treatment with miR-124-3p sEV significantly increased the latency time to fall off from the rod by about 70% compared to 6-OHDA-lesioned animals ($p < 0.0001$, n = 5), resulting in no difference with saline-treated mice (Figure 4.9 A). These results indicate that miR-124-3p sEV fully counteracted 6-OHDA-induced motor performance and coordination deficits. We further evaluated motor behavior by the apomorphine-induced rotation test. Apomorphine is a dopamine receptor agonist that can uncover asymmetrical dopamine loss (occurring with the presently used unilateral 6-OHDA administration) through its induction of contralateral rotations. As expected, saline-treated mice exhibited a net rotation near zero, while 6-OHDA-lesioned mice showed a significant increase ($p < 0.0001$, n = 4 for saline and n = 5 for the 6-OHDA group) in the contralateral net rotations that was reverted by the miR-124-3p sEV treatment (Figure 4.9 B; Week 2: $p < 0.05$; Week 4: $p < 0.01$, n = 4). The treatment of lesioned animals with SCR sEV (n = 5) or sEV (n = 3) showed significant differences compared with miR-124-3p sEV treatment, however they did not reveal any differences when compared with 6-OHDA-injured animals in both rotarod (Figure 4.9 A) and apomorphine (Figure 4.9 B) tests. Overall, the behavior data attest to the therapeutic efficacy of miR-124-3p sEV in counteracting motor deficits in the PD mouse model.

4.5 Discussion

To the best of our knowledge, this is the first study using hUCB-MNC-derived sEV as a biological vehicle to deliver miR-124 in the context of PD. MiRNA are increasingly considered impactful molecular agents for the treatment of this neurodegenerative disease. miR-124 is particularly attractive, as it is downregulated in the SN of PD models and plasma of PD patients, and enhancing its expression boosts neuroprotection and neurogenesis in PD models [3,4,6,7,9,22,23].

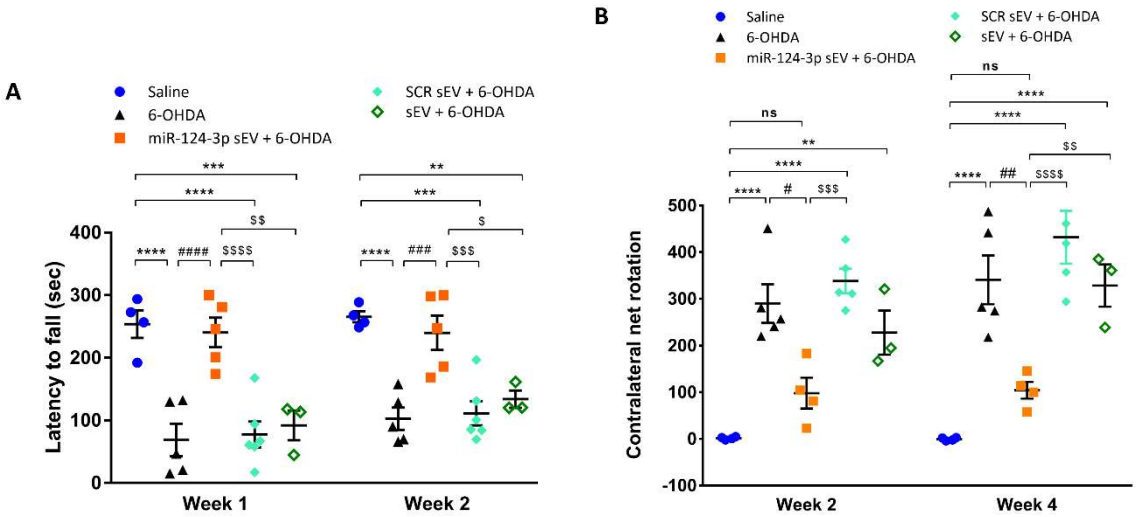

Figure 4.9. miR-124-3p sEV ameliorate motor symptoms in a mouse model of Parkinson's disease. (A, B) Behavioral data. **(A)** Latency remaining on the rotarod was tested in the first two weeks post 6-OHDA lesion. Data shown represent the four-trial average time on the rotarod. Data are expressed as mean of latency to fall from rod ± SEM; saline: n = 4; 6-OHDA and miR-124-3p sEV + 6-OHDA: n = 5; SCR sEV + 6-OHDA: n = 6 and sEV + 6-OHDA: n = 3. **(B)** Number of contralateral rotations induced by apomorphine were measured for 45 min, two and four weeks after 6-OHDA lesion. Data are expressed as mean of contralateral net turns ± SEM; saline and miR-124-3p sEV + 6-OHDA: n = 4; 6-OHDA and SCR sEV + 6-OHDA: n = 5 and sEV + 6-OHDA: n = 3. $^{****}p < 0.0001$, $^{***}p < 0.001$ and $^{**}p < 0.01$ vs. saline-treated mice (control); $^{\#\#\#\#}p < 0.0001$, $^{\#\#\#}p < 0.001$, $^{\#\#}p < 0.01$ and $^{\#}p < 0.05$ vs. 6-OHDA-lesioned mice group; $^{\$\$\$\$}p < 0.0001$, $^{\$\$\$}p < 0.001$, $^{\$\$}p < 0.01$ and $^{\$}p < 0.05$ vs miR-124-3p sEV + 6-OHDA-lesioned mice group using one-way ANOVA followed by Tukey's multiple comparison test. Abbreviations: 6-OHDA: 6-hydroxydopamine; SCR sEV: scramble-loaded small extracellular vesicles; sEV: non-loaded small extracellular vesicles; miR-124-3p sEV: miR-124-3p-loaded small extracellular vesicles. [18]

We have previously found that miR-124-loaded NP induce SVZ neurogenesis and counteract motor deficits in a 6-OHDA PD model *in vivo* [9]. miR-124 regulates several stages of neuronal differentiation, from early neuronal commitment to maturation by targeting Jagged Canonical Notch Ligand 1 (JAG1) [24,25], Ezh2 [26], STAT3 [27], and SRY-Box Transcription Factor 9 (Sox-9) [24]. Moreover, miR-124 enhances axonogenesis and neurite maturation by regulating cytoskeleton proteins and RhoG pathway, respectively [28,29]. In our mixed SVZ cell culture, containing distinct cell populations at different stages of development, miR-124 may regulate various steps during neuronal lineage differentiation and maturation. Interestingly, overexpression of miR-124 (among other factors) can also be involved in transforming human fibroblasts into functional mature neurons [30]. Some reports also suggest a synergistic role for miR-9 and miR-124 on the specification and survival of dopaminergic neurons in mice [31]. Additionally, several other studies have also reported the neuroprotective role of miR-124 in PD. MiR-124-3p was reported to attenuate dopaminergic degeneration found in *in vitro* and *in vivo* PD models by targeting several signaling pathways, including the ANXA5/ERK pathway [8], STAT3 [32], AMPK/mTOR pathway [7], the calpain

1/p25/cdk5 signaling [3], EDN2 [33], and Bim [34]. Altogether, these evidence highlight the relevance of increasing miR-124 levels as a novel therapeutic strategy for PD. However, miRNA are easily degraded by nucleases, and their delivery presents poor uptake efficiency due to their hydrophilic nature and negative charge [35]. To overcome these challenges, we previously developed polymeric NP able to release miR-124 [9]. Knowing the limitations of the previously developed NP-based delivery carriers, such as degradation, bioaccumulation, retention in the basal lamina, and toxicity, we developed a new and biological sEV-based carrier to deliver miR-124 in the brain. SEV have attracted considerable attention as drug delivery vehicles for treating several brain diseases. It has been previously reported that the administration of sEV loaded with anti-inflammatory or antioxidant drugs (curcumin and catalase, respectively) significantly decreased brain inflammation [36] and increased neuronal survival in a 6-OHDA PD mouse model [11]. Also, blood-derived sEV loaded with dopamine were shown to reach the striatum and SN, thus promoting the amelioration of the disease phenotype in the same model [14]. In this study, native sEV were obtained from hUCB-MNC and then loaded with miR-124-3p or SCR using the Exo-Fect™ Exosome Transfection Reagent [17]. The native sEV obtained had an average size of 131 nm and an average zeta potential of around -25 mV, while miR-124-loaded sEV had a zeta potential of -15 mV. This shift in zeta potential is likely due to the adsorption of some Exo-Fect™ molecules to the membrane of sEV. These results agree with our recent study showing that Exo-Fect™ interferes with sEV membrane structure, albeit not promoting the disruption of sEV membrane integrity [17], as well as other studies showing that Exo-Fect™ was an efficient strategy to load sEV with small nucleic acids [37]. Because residual non-absorbed Exo-Fect™ onto sEV may have the ability to transfect cells in a similar way as it does to EV, we have treated SVZ cultures with Exo-Fect™ and miR-124-3p in the absence of sEV. Our results showed that in contrast to Exo-Fect™-modulated miR-124-3p sEV, a mixture of Exo-Fect™ and miR-124-3p *per se* did not alter cell survival, cell commitment/proliferation, and neuronal differentiation compared to the control. Therefore, our data indicate that the miR-124-3p was delivered to cells via sEV. Using fluorescent-labeled miRNA, we found that 74% of the signal was present in the sEV fraction, suggesting most miR-124-Cy5 was immobilized in sEV. Other studies used a similar quantification strategy, showing that upon transfection of sEV with Exo-Fect™, around 80% of the fluorescent signal remained in the sEV fraction of the reaction [17,38]. Altogether, these data confirm that Exo-Fect™ treatment efficiently transfect sEV with miR-124-3p. However, the exact location of the miR-124-3p in the sEV remains unknown. Importantly, Exo-Fect™-modulated miR-124-3p sEV and treated with RNase had no change in miR-124-3p levels showing that the miR-124-3p was inaccessible to

nucleases. Further tests are needed to disclose whether miR-124-3p is entrapped in the sEV membrane or its lumen.

Then, we evaluated the effect of native sEV or sEV loaded with miR-124-3p or SCR in SVZ neurogenesis. We found that native sEV are able to counteract basal cell death and reduce the proliferation of NSC/NPC and neuroblasts in SVZ cultures. sEV cargo includes several bioactive molecules, namely proteins, mRNA, miRNA, lipids, among others. Several evidence suggests that the biological effects of sEV is mainly dependent on the intravesicular miRNA signature. We have previously characterized the cargo of the sEV used in this study in terms of miRNA by RNASeq [10]. Importantly, miR-124 was not found in the heatmap of miRNA in these sEV. Some of the enriched miRNA were reported to decrease proliferation in cancer cells, such as miR-let-7a [39]. Interestingly, Ohno and colleagues showed that intravenously injected GE11-targeted exosomes containing let-7a miR inhibit tumor growth in mice [40]. Other miRNA enriched in the sEV were reported to increase cell survival, such as miR-223 and miR-21 [41,42]. These putative miRNA feedback loops may be responsible for the bioactivity of sEV found in our study. In addition, these miRNA may have selectivity towards a specific cell phenotype. The SVZ culture is a mixed primary cell culture containing immature NSC/NPC, cells in distinct stages of the neuronal, oligodendroglial and astrocytic lineages. Therefore, differences in the dynamics on other cell populations, not studied in this work, could justify the proliferation data that we obtained. In the particular case of miR-124-3p sEV we found a reduction of the population of proliferative immature cells (Ki-67$^+$/Nestin$^+$) and an increase in the number of mature neurons (NeuN) without any significant effect on neuroblast proliferation (Ki-67$^+$/DCX$^+$). One possibility is that some NSC/NPC undergo direct neuronal differentiation without proliferating, as reported by others [43]. This process is accompanied by a decrease in the NSC pool. The loaded miR-124-3p may cooperate with intrinsic sEV miRNA cargo fostering neuronal differentiation [44]. For example, it was shown that miR-21-5p and miR-124-3p delivered by NP may cooperate to induced a pro-osteogenic differentiation effect which might impact in the regeneration of osteoporotic bone [45]. We may hypothesize that some feedback loops may also occur when loading sEV with miR-124-3p boosting neuronal differentiation. Moreover, we cannot exclude the involvement of other components in sEV in their biological activities (e.g., growth-factor-associated proteins, mRNA, lipids, etc.). Better knowledge about the cargo of these vesicles may help design more efficient bioengineering drug delivery platforms using sEV as a biological vehicle of therapeutic molecules. In terms of a gene or RNA delivery, an innovative approach would be to empty sEV of their cargo before loading with the therapeutic agent of interest. These innovative

drug delivery approaches should be explored in future studies. The *in vivo* data regarding neurogenesis disagrees with the *in vitro* data and our previous data using miR-124-loaded NP [9]. While in our previous report, we performed the overall analysis of neurogenesis in the SVZ, olfactory bulb, and striatum, in the current manuscript, our analysis focused on pathologically relevant brain regions only, namely the striatum. Therefore, we cannot exclude that miR-124-3p sEV may also impact OB neurogenesis *in vivo*. On the other side, we also showed that miR-124-loaded NP increase SVZ neurogenesis *in vitro* but not in the *in vivo* model of ischemic stroke [46]. The net effect in SVZ neurogenesis *in vivo* may depend on the pathology, experimental conditions, and the type of drug delivery system used. Regarding biodistribution *in vivo,* we found previously that polymeric NP were detected only in the SVZ, meaning they were easily trapped inside the basal lamina, thus limiting their diffusion across the brain parenchyma [47]. sEV were found in the SVZ, striatum, and SN, particularly dopaminergic neurons. Due to their biological nature, sEV have the exceptional ability to interact with recipient cells having a specific cell tropism that can target them to disease tissues, which contrasts to a relatively lower penetration efficiency of polymeric NP. For example, the intranasal administration of mesenchymal stem cell-derived sEV loaded with glucose-coated gold NP led to a higher brain accumulation/distribution than free gold NP [48]. Furthermore, the mesenchymal stem cell-derived sEV accumulated preferentially in injured brain regions, including the striatum of 6-OHDA PD rat model, and the large majority of the sEV was found in neurons [12]. Interestingly, Haney and collaborators developed macrophage-derived exosomes loaded with catalase, a potent antioxidant, to treat PD [11]. These exosomes showed superior intraneuronal accumulation (PC12 cells) compared with the considerably lower uptake of polymeric PLGA NP or liposomes. Ultimately, intranasal delivery of catalase-loaded exosomes exerted neuroprotective effects in *in vivo* 6-OHDA model of PD. Other studies suggest that membrane vesicles fused more effectively with the plasma membrane of cancer cells than polymeric NP and enabled the delivery of hydrophobic photosensitizers in spheroids and *in vivo* tumors more efficiently, thereby enhancing the therapeutic efficacy [49]. This superior uptake of sEV occurs mainly due to adhesion proteins, tetraspanins, and integrins, which are absent in synthetic NP. Moreover, sEV may comprise additional advantages over synthetic nanocarriers and cell-mediated drug delivery, avoiding the rapid clearance by phagocytosis and engulfment by lysosomes and toxicity [50]. sEV can also cross the blood-brain barrier and reach their targets. In fact, sEV loaded with catalase, dopamine or *GAPDH* siRNA were detected in PD mouse brain after intravenous administration [11,14,51]. Altogether these evidence suggest that sEV have a superior ability than polymeric NP to enhance the delivery of incorporated drugs

to target lesioned brain regions/cells ultimately increasing therapeutic drug efficacy. Future research should better investigate *in vivo* trafficking and biodistribution of sEV and their impact on pathological lesioned brain regions/cells for efficient and specific drug delivery. Importantly, our study shows that miR-124-3p sEV counteract dopaminergic degeneration and PD-related motor deficits in the 6-OHDA model of PD. Some have demonstrated the bioactivity of sEV themselves in the context of neurodegenerative diseases, including PD. For example, Chen and collaborators showed that sEV isolated from human umbilical cord mesenchymal stem cells promoted the proliferation of 6-OHDA-intoxicated SH-SY5Y cells while inhibiting apoptosis. *In vivo*, these sEV reduced dopaminergic neuronal loss in the SN while increasing dopamine levels in the striatum, alleviating the apomorphine-induced rotational behavior in a 6-OHDA rat model of PD [52]. In our study, native sEV and SCR sEV did not protect against 6-OHDA-induced lesion both *in vitro* and in *vivo*. Thus, the therapeutic neuroprotective effect promoted by miR-124-3p sEV in the *in vivo* PD model is likely mediated specifically by the miR-124. In our study, striatal injection of 6-OHDA caused ~80% cell death in SN and a strong dopaminergic denervation in the striatum. However, the 6-OHDA model does not fully mimic all the pathophysiologic mechanisms in PD. The toxin 6-OHDA induces mitochondrial impairment, proteasomal and lysosomal dysfunction, and neuroinflammation. Before moving into clinical trials, it is imperative to test the therapeutic effect of miR-124-3p sEV in other relevant preclinical models that address distinct but complementary aspects of PD pathophysiology. Toxin-induced models (e.g., MPTP, PQ, and rotenone) also induce oxidative stress and dopaminergic neurodegeneration but cause a severe and fast dopaminergic death, which does not resemble the disease's evolution in humans and fails to induce α-synuclein accumulation and aggregation. Alternatively, genetic models targeting PD-related genes, such as SNCA, LRRK2, and PINK1, could mimic other pathologic aspects of the disease [53]. While neurotoxins can be used to evaluate neuroprotective mechanisms, genetic models may be used to study mechanisms associated with alpha-synuclein aggregation and prodromal symptoms. Moreover, to approach the clinic translation, sEV should be administered ideally after the lesion and delivered using a non-invasive approach, such as the intranasal route [11,12,48].

4.6 Conclusions

Herein, we reported for the first time the therapeutic potential of microRNA-124-3p-enriched sEV for PD treatment. The delivery of miR-124-3p by sEV induced neuronal differentiation of SVZ NSC under physiological conditions *in vitro*. *In vivo*, we showed that ICV injection of miR-124-3p sEV protected the nigrostriatal pathway against 6-

OHDA-induced neurodegeneration and significantly improved motor performance of lesioned mice. Our findings support the use of miR-124-3p sEV as a new and efficient therapeutic approach to halt PD pathogenesis progression and open new perspectives for the treatment of other neurodegenerative diseases.

4.7 References

1. Dauer W, Przedborski S: Parkinson's disease: Mechanisms and models. *Neuron* 2003, 39:889–909.
2. Saraiva C, Esteves M, Bernardino L: MicroRNA: Basic concepts and implications for regeneration and repair of neurodegenerative diseases. *Biochem Pharmacol* 2017, 141:118–131.
3. Kanagaraj N, Beiping H, Dheen ST, Tay SSW: Downregulation of miR-124 in MPTP-treated mouse model of Parkinson's disease and MPP iodide-treated MN9D cells modulates the expression of the calpain/cdk5 pathway proteins. *Neuroscience* 2014, 272:167–79.
4. Li N, Pan X, Zhang J, Ma A, Yang S, Ma J, Xie A: Plasma levels of miR-137 and miR-124 are associated with Parkinson's disease but not with Parkinson's disease with depression. *Neurol Sci* 2017, 38:761–767.
5. Sonntag K-C: MicroRNAs and deregulated gene expression networks in neurodegeneration. *Brain Res* 2010, 1338:48–57.
6. Yao L, Zhu Z, Wu J, Zhang Y, Zhang H, Sun X, Qian C, Wang B, Xie L, Zhang S, et al.: MicroRNA-124 regulates the expression of p62/p38 and promotes autophagy in the inflammatory pathogenesis of Parkinson's disease. *FASEB J* 2019, 33:8648–8665.
7. Gong X, Wang H, Ye Y, Shu Y, Deng Y, He X, Lu G, Zhang S: miR-124 regulates cell apoptosis and autophagy in dopaminergic neurons and protects them by regulating AMPK/mTOR pathway in Parkinson's disease. *Am J Transl Res* 2016, 8:2127–37.
8. Dong RF, Zhang B, Tai LW, Liu HM, Shi FK, Liu NN: The Neuroprotective Role of MiR-124-3p in a 6-Hydroxydopamine-Induced Cell Model of Parkinson's Disease via the Regulation of ANAX5. *J Cell Biochem* 2018, 119:269–277.
9. Saraiva C, Paiva J, Santos T, Ferreira L, Bernardino L: MicroRNA-124 loaded nanoparticles enhance brain repair in Parkinson's disease. *J Control Release* 2016, 235:291–305.
10. Henriques-Antunes H, Cardoso RMS, Zonari A, Correia J, Leal EC, Jiménez-Balsa A, Lino MM, Barradas A, Kostic I, Gomes C, et al.: The Kinetics of Small Extracellular Vesicle Delivery Impacts Skin Tissue Regeneration. *ACS Nano* 2019,

13:8694–8707.

11. Haney MJ, Klyachko NL, Zhao Y, Gupta R, Plotnikova EG, He Z, Patel T, Piroyan A, Sokolsky M, Kabanov A V., et al.: Exosomes as drug delivery vehicles for Parkinson's disease therapy. *J Control Release* 2015, 207:18–30.
12. Perets N, Betzer O, Shapira R, Brenstein S, Angel A, Sadan T, Ashery U, Popovtzer R, Offen D: Golden Exosomes Selectively Target Brain Pathologies in Neurodegenerative and Neurodevelopmental Disorders. *Nano Lett* 2019, 19:3422–3431.
13. Guo S, Perets N, Betzer O, Ben-Shaul S, Sheinin A, Michaelevski I, Popovtzer R, Offen D, Levenberg S: Intranasal Delivery of Mesenchymal Stem Cell Derived Exosomes Loaded with Phosphatase and Tensin Homolog siRNA Repairs Complete Spinal Cord Injury. *ACS Nano* 2019, 13:10015–10028.
14. Qu M, Lin Q, Huang L, Fu Y, Wang L, He S, Fu Y, Yang S, Zhang Z, Zhang L, et al.: Dopamine-loaded blood exosomes targeted to brain for better treatment of Parkinson's disease. *J Control Release* 2018, 287:156–166.
15. Cooper JM, Wiklander PBO, Nordin JZ, Al-Shawi R, Wood MJ, Vithlani M, Schapira AH V., Simons JP, El-Andaloussi S, Alvarez-Erviti L: Systemic exosomal siRNA delivery reduced alpha-synuclein aggregates in brains of transgenic mice. *Mov Disord* 2014, 29:1476–1485.
16. Steel HC, Alessandrini M, Mellet J, Dessels C, Oloyo AK, Pepper MS: Cord Blood Stem Cell Banking. In *Stem Cell Processing*. *Stem Cells in Clinical Applications*. Edited by Van Pham P. Springer; 2016:163–180.
17. de Abreu RC, Ramos C V., Becher C, Lino M, Jesus C, da Costa Martins PA, Martins PAT, Moreno MJ, Fernandes H, Ferreira L: Exogenous loading of miRNAs into small extracellular vesicles. *J Extracell Vesicles* 2021, 10:e12111.
18. Esteves M, Abreu R, Fernandes H, Serra-Almeida C, Martins PAT, Barão M, Cristóvão AC, Saraiva C, Ferreira R, Ferreira L, et al.: MicroRNA-124-3p-enriched small extracellular vesicles as a therapeutic approach for Parkinson's disease. *Mol Ther* 2022, doi:10.1016/J.YMTHE.2022.06.003.
19. Agasse F, Bernardino L, Silva B, Ferreira R, Grade S, Malva JO: Response to Histamine Allows the Functional Identification of Neuronal Progenitors, Neurons, Astrocytes, and Immature Cells in Subventricular Zone Cell Cultures. *Rejuvenation Res* 2008, 11:187–200.
20. Agasse F, Bernardino L, Kristiansen H, Christiansen SH, Ferreira R, Silva B, Grade S, Woldbye DPD, Malva JO: Neuropeptide Y promotes neurogenesis in murine subventricular zone. *Stem Cells* 2008, 26:1636–45.
21. Maas SLN, De Vrij J, Van Der Vlist EJ, Geragousian B, Van Bloois L,

Mastrobattista E, Schiffelers RM, Wauben MHM, Broekman MLD, Nolte-'T Hoen ENM: Possibilities and limitations of current technologies for quantification of biological extracellular vesicles and synthetic mimics. *J Control Release* 2015, 200:87–96.

22. Yao L, Ye Y, Mao H, Lu F, He X, Lu G, Zhang S: MicroRNA-124 regulates the expression of MEKK3 in the inflammatory pathogenesis of Parkinson's disease. *J Neuroinflammation* 2018, 15:13.
23. Song Y, Li Z, He T, Qu M, Jiang L, Li W, Shi X, Pan J, Zhang L, Wang Y, et al.: M2 microglia-derived exosomes protect the mouse brain from ischemia-reperfusion injury via exosomal miR-124. *Theranostics* 2019, 9:2910–2923.
24. Cheng L-C, Pastrana E, Tavazoie M, Doetsch F: miR-124 regulates adult neurogenesis in the subventricular zone stem cell niche. *Nat Neurosci* 2009, 12:399–408.
25. Liu XS, Chopp M, Zhang RL, Tao T, Wang XL, Kassis H, Hozeska-Solgot A, Zhang L, Chen C, Zhang ZG: MicroRNA profiling in subventricular zone after stroke: MiR-124a regulates proliferation of neural progenitor cells through notch signaling pathway. *PLoS One* 2011, 6:1–11.
26. Neo WH, Yap K, Lee SH, Looi LS, Khandelia P, Neo SX, Makeyev E V., Su IH: MicroRNA miR-124 controls the choice between neuronal and astrocyte differentiation by fine-tuning Ezh2 expression. *J Biol Chem* 2014, 289:20788–20801.
27. Krichevsky AM, Sonntag K-C, Isacson O, Kosik KS: Specific MicroRNAs Modulate Embryonic Stem Cell–Derived Neurogenesis. *Stem Cells* 2006, 24:857–864.
28. Gu X, Meng S, Liu S, Jia C, Fang Y, Li S, Fu C, Song Q, Lin L, Wang X: MiR-124 Represses ROCK1 Expression to Promote Neurite Elongation Through Activation of the PI3K/Akt Signal Pathway. *J Mol Neurosci* 2014, 52:156–165.
29. Franke K, Otto W, Johannes S, Baumgart J, Nitsch R, Schumacher S: miR-124-regulated RhoG reduces neuronal process complexity via ELMO/Dock180/Rac1 and Cdc42 signalling. *EMBO J* 2012, 31:2908–2921.
30. Yoo AS, Sun AX, Li L, Shcheglovitov A, Portmann T, Li Y, Lee-Messer C, Dolmetsch RE, Tsien RW, Crabtree GR: MicroRNA-mediated conversion of human fibroblasts to neurons. *Nature* 2011, 476:228–231.
31. Huang T, Liu Y, Huang M, Zhao X, Cheng L: Wnt1-cre-mediated Conditional Loss of Dicer Results in Malformation of the Midbrain and Cerebellum and Failure of Neural Crest and Dopaminergic Differentiation in Mice. *J Mol Cell Biol* 2010, 2:152–163.
32. Geng L, Liu W, Chen Y: miR-124-3p attenuates MPP+-induced neuronal injury by

targeting STAT3 in SH-SY5Y cells. *Exp Biol Med* 2017, 242:1757–1764.

33. Wang J, Wang W, Zhai H: MicroRNA-124 Enhances Dopamine Receptor Expression and Neuronal Proliferation in Mouse Models of Parkinson's Disease via the Hedgehog Signaling Pathway by Targeting EDN2. *Neuroimmunomodulation* 2019, 26:174–187.
34. Wang H, Ye Y, Zhu Z, Mo L, Lin C, Wang Q, Wang H, Gong X, He X, Lu G, et al.: MiR-124 Regulates Apoptosis and Autophagy Process in MPTP Model of Parkinson's Disease by Targeting to Bim. *Brain Pathol* 2016, 26:167–176.
35. Chen Y, Zhao H, Tan Z, Zhang C, Fu X: Bottleneck limitations for microRNA-based therapeutics from bench to the bedside. *Pharmazie* 2015, 70:147–54.
36. Zhuang X, Xiang X, Grizzle W, Sun D, Zhang S, Axtell RC, Ju S, Mu J, Zhang L, Steinman L, et al.: Treatment of Brain Inflammatory Diseases by Delivering Exosome Encapsulated Anti-inflammatory Drugs From the Nasal Region to the Brain. *Mol Ther* 2011, 19:1769–1779.
37. Zeng Z, Li Y, Pan Y, Lan X, Song F, Sun J, Zhou K, Liu X, Ren X, Wang F, et al.: Cancer-derived exosomal miR-25-3p promotes pre-metastatic niche formation by inducing vascular permeability and angiogenesis. *Nat Commun* 2018, 9:1–14.
38. Pi F, Binzel DW, Lee TJ, Li Z, Sun M, Rychahou P, Li H, Haque F, Wang S, Croce CM, et al.: Nanoparticle orientation to control RNA loading and ligand display on extracellular vesicles for cancer regression. *Nat Nanotechnol* 2018, 13:82–89.
39. Luo C, Zhang J, Zhang Y, Zhang X, Chen Y, Fan W: Low expression of miR-let-7a promotes cell growth and invasion through the regulation of c-Myc in oral squamous cell carcinoma. *Cell Cycle* 2020, 19:1983–1993.
40. Ohno S, Takanashi M, Sudo K, Ueda S, Ishikawa A, Matsuyama N, Fujita K, Mizutani T, Ohgi T, Ochiya T, et al.: Systemically Injected Exosomes Targeted to EGFR Deliver Antitumor MicroRNA to Breast Cancer Cells. *Mol Ther* 2013, 21:185–191.
41. Huang B, Luo Q, Han Y, Huang D, Tang Q, Wu L: MiR-223/PAX6 Axis Regulates Glioblastoma Stem Cell Proliferation and the Chemo Resistance to TMZ via Regulating PI3K/Akt Pathway. *J Cell Biochem* 2017, 118:3452–3461.
42. Gao X, Xiong Y, Li Q, Han M, Shan D, Yang G, Zhang S, Xin D, Zhao R, Wang Z, et al.: Extracellular vesicle-mediated transfer of miR-21-5p from mesenchymal stromal cells to neurons alleviates early brain injury to improve cognitive function via the PTEN/Akt pathway after subarachnoid hemorrhage. *Cell Death Dis* 2020, 11:363.
43. Barbosa JS, Sanchez-Gonzalez R, Di Giaimo R, Baumgart E V., Theis FJ, Gotz M, Ninkovic J: Live imaging of adult neural stem cell behavior in the intact and

injured zebrafish brain. *Science (80-)* 2015, 348:789–793.

44. Lu Y-L, Liu Y, McCoy MJ, Yoo AS: MiR-124 synergism with ELAVL3 enhances target gene expression to promote neuronal maturity. *Proc Natl Acad Sci* 2021, 118:e2015454118.
45. Marycz K, Smieszek A, Marcinkowska K, Sikora M, Turlej E, Sobierajska P, Patej A, Bienko A, Wiglusz RJ: Nanohydroxyapatite (nHAp) Doped with Iron Oxide Nanoparticles (IO), miR-21 and miR-124 Under Magnetic Field Conditions Modulates Osteoblast Viability, Reduces Inflammation and Inhibits the Growth of Osteoclast – A Novel Concept for Osteoporosis Treatment: *Int J Nanomedicine* 2021, Volume 16:3429–3456.
46. Saraiva C, Talhada D, Rai A, Ferreira R, Ferreira L, Bernardino L, Ruscher K: MicroRNA-124-loaded nanoparticles increase survival and neuronal differentiation of neural stem cells in vitro but do not contribute to stroke outcome in vivo. *PLoS One* 2018, 13:e0193609.
47. Arends F, Lieleg O: Biophysical Properties of the Basal Lamina: A Highly Selective Extracellular Matrix. In *Composition and Function of the Extracellular Matrix in the Human Body*. Edited by Francesco Travascio. InTechOpen; 2016.
48. Betzer O, Perets N, Angel A, Motiei M, Sadan T, Yadid G, Offen D, Popovtzer R: In Vivo Neuroimaging of Exosomes Using Gold Nanoparticles. *ACS Nano* 2017, 11:10883–10893.
49. Lee J, Kim J, Jeong M, Lee H, Goh U, Kim H, Kim B, Park J-H: Liposome-Based Engineering of Cells To Package Hydrophobic Compounds in Membrane Vesicles for Tumor Penetration. *Nano Lett* 2015, 15:2938–2944.
50. Conlan RS, Pisano S, Oliveira MI, Ferrari M, Mendes Pinto I: Exosomes as Reconfigurable Therapeutic Systems. *Trends Mol Med* 2017, 23:636–650.
51. Alvarez-Erviti L, Seow Y, Yin H, Betts C, Lakhal S, Wood MJA: Delivery of siRNA to the mouse brain by systemic injection of targeted exosomes. *Nat Biotechnol 2011 294* 2011, 29:341–345.
52. Chen H, Liang F, Gu P, Xu B, Xu H, Wang W, Hou J: Exosomes derived from mesenchymal stem cells repair a Parkinson ' s disease model by inducing autophagy. *Cell Death Dis* 2020, 11.
53. Cenci MA, Björklund A: Animal models for preclinical Parkinson's research: An update and critical appraisal. *Prog Brain Res* 2020, 252:27–59.

Chapter 5

Concluding Remarks

5.1 Concluding Remarks and Future Perspectives

So far, there is no effective treatment for PD. The available treatments only alleviate the symptoms without halting or reversing the disease progression. Efforts to develop novel disease-modifying therapies for PD are challenging due to its multifactorial nature and difficulty in recapitulating all relevant pathophysiological hallmarks of the disease in pre-clinical studies, combined with the fact that diagnosis is made at an advanced stage. In the last decades, several studies have reported the dysregulation of various miRNA in brain diseases, highlighting its putative role as therapeutic targets. Particularly, the miR-124 is widely expressed in the healthy brain, but its levels are decreased in postmortem brains and plasma of PD patients as well in PD experimental models. Several reports showed that increasing intracellular levels of miR-124 in PD models counteract oxidative stress, autophagy dysregulation, neuroinflammation, and apoptosis of dopaminergic neurons. However, there is still no study analyzing the effect of miR-124 in the accumulation and aggregation of α-synuclein, which is considered a hallmark of PD pathology.

In Chapter 3, we investigated the effects of miR-124-3p in the expression levels of monomeric and phosphorylated (pS129) forms of α-synuclein in a PQ-induced model of PD. In this study, the intranigral administration of 250 nM miR-124-3p decreased the expression of monomeric α-synuclein in the striatum and SN and the expression of pS129-α-synuclein in the SN of the rats exposed to PQ. Regarding the potential role of Nox1-derived oxidative stress in α-synuclein pathology [1], Nox1/Rac1 signaling pathway was analyzed. The obtained data showed that miR-124-3p counteracted the increase in Nox1 and Rac1 protein levels induced by PQ in the SN. As reported [2], reduced levels of Pitx3 may be related with α-synuclein toxicity which leads to dopaminergic neurons death. In this work, the reduced levels of Pitx3 in the SN caused by the administration of PQ were found increase after the administration of miR-124-3p. However, neuroprotection of dopaminergic neurons was not observed in this model using this concentration of miR-124-3p. Additional studies using other miRNA concentrations or changing the exposure paradigm are of great importance. These results demonstrated a role of miR-124-3p in the modulation of α-synuclein behavior in a PD context, stressing the relevance of further studies to identify the molecular mechanisms and adjust experimental setups to boost dopaminergic survival.

Considering the limitations of naked miRNA delivery to the cells/tissues, in Chapter 4, we used sEV isolated from hUCB-MNC, as a biological vehicle to protect and effectively deliver miR-124 into the brain parenchyma. The main aim of this work was to evaluate

the therapeutic potential of sEV enriched with miR-124 in a PD pre-clinical animal model. miR-124-3p sEV treatment reduced the number of proliferative immature cells (Ki-67$^+$/Nestin$^+$) while increased the number of mature neurons (NeuN) in SVZ cultures *in vitro*. Additionally, native sEV showed to have bioactive molecules in their original cargos, which promoted the reduction of basal cell death, proliferation of immature cells and neuroblasts. To have a clear insight into the effects driven by miR-124 *per se*, eliminating the original cargos of sEV could be a promising strategy to be applied in future studies [3]. We showed that sEV were efficiently internalized by SVZ and N27 cells and able to deliver miR-124-3p, *in vitro*. *In vivo*, sEV were detected lining the SVZ of both ventricles and in the midbrain sections, mainly in the aqueduct but also in the SN co-localizing with TH-positive dopaminergic neurons. A single intracerebroventricular administration of miR-124-3p sEV induced significant protection of dopaminergic neurons in the SN and its striatal projections culminating in the amelioration of motor symptoms of 6-OHDA-challenged mice. Further studies are needed to address the miR-124 targets and mechanisms involved in protecting dopaminergic neurons. To strengthen the therapeutic potential of this formulation in PD, it remained to elucidate the effects of this formulation on other mechanisms involved in PD pathology, namely the α-synuclein toxicity, mitochondrial dysfunction, and oxidative stress, and neuroinflammation. Indeed, since none of the available preclinical models effectively recapitulate the PD, it is relevant to test the therapeutic effect of miR-124-3p sEV in other preclinical models to address distinct but complementary aspects of PD pathophysiology. Furthermore, to approach the clinic translation, sEV should be administered ideally after the lesion and delivered using a non-invasive approach, such as the intranasal route. Validation of the therapeutic efficacy of the miR-124-3p sEV formulation in PD models gives great hope to fulfill the unmet clinical need for effective and long-lasting neuroprotective strategies for PD. Thus, future clinical development of this strategy will undoubtedly be a groundbreaker in the field. Several concluded or ongoing clinical trials tested miRNA-based treatments, for example, miravirsen (produced by Roche/Santaris) and RG-101 (produced by Regulus Therapeutics), both antagomiRs targeting miR-122 to treat hepatitis C, are considered the flagship miRNA therapeutic products. Several other biopharmaceutical companies including miRagen Therapeutics (now Viridian Therapeutics), Abivax among others, are actively involved in the development of miRNA therapeutics, already considering the “next-generation” therapeutics for the cure of various diseases [4,5].

In conclusion, i) intranigral injection of miR-124 reduced the expression of monomeric α-synuclein and pS129-α-syn form, possibly via Nox1/Rac1 signaling pathway

modulation and Pitx3 expression regulation in a PQ-induced rat model of PD; ii) hUCB-MNC-derived sEV are easily internalized by cells and are efficient delivery vehicles for miR-124 and iii) ICV administration of miR-124-3p sEV protect nigrostriatal pathway against 6-OHDA-induced degeneration and significantly ameliorate motor deficits of lesioned mice. This study reinforces the neuroprotective role of miR-124 combined with the new reported effect in the modulation of α-synuclein pathology and opens new perspectives for the treatment of PD by using sEV as efficient biological vehicles of exogenous miRNA.

5.2 References

1. Choi DH, Cristóvão AC, Guhathakurta S, Lee J, Joh TH, Beal MF, Kim YS: NADPH oxidase 1-mediated oxidative stress leads to dopamine neuron death in Parkinson's disease. *Antioxidants Redox Signal* 2012, 16:1033–1045.
2. Wang Y, Chen X, Wang Y, Li S, Cai H, Le W: The essential role of transcription factor Pitx3 in preventing mesodiencephalic dopaminergic neurodegeneration and maintaining neuronal subtype identities during aging. *Cell Death Dis 2021 1211* 2021, 12:1–11.
3. Guo Y, Hu G, Xia Y, Li HY, Yuan J, Zhang J, Chen Y, Guo H, Yang Y, Wang Y, et al.: Eliminating the original cargos of glioblastoma cell-derived small extracellular vesicles for efficient drug delivery to glioblastoma with improved biosafety. *Bioact Mater* 2022, 16:204–217.
4. Bonneau E, Neveu B, Kostantin E, Tsongalis GJ, De Guire V: How close are miRNAs from clinical practice? A perspective on the diagnostic and therapeutic market. *EJIFCC* 2019, 30:114.
5. Chakraborty C, Sharma AR, Sharma G, Lee SS: Therapeutic advances of miRNAs: A preclinical and clinical update. *J Adv Res* 2021, 28:127–138.